JMIRx Bio

Overlay journal for preprints with post-review manuscript marketplace
Volume 4 (2026) ISSN 2819-2044 Editor in Chief: Edward Meinert, MA (Oxon), MSc, MBA, MPA, PhD, CEng, FBCS, EUR ING

Contents

Original Papers

Material-Driven Therapeutics to Establish a Penetrating Traumatic Brain Injury Rat Model and Implantation of a 3D-Printed Scaffold: Pre-Experimental Pilot Study (e75613)
Meaghan Harley-Troxell, Michelle Dennis, Madhu Dhar. . . . 3

Relationship Between Seed Coat Color and Cytokinin Concentration in Efficiently Regenerating Leaf Lettuce Shoots: In Vitro Experimental Study (e70496)
Mitsuhiro Kimura, Takeshi Yoshizumi. . . . 15

Localized Immune Cascade Programming in Desmoplastic Tumors: In Silico Modeling and Validation Study (e85507)
Murad Novruzov, Marziyya Mammadova, Keval Raval, Waseem Khan, Ulkar Shiraliyeva. . . . 26

Machine Learning Ensemble Investigates Age in the Transcriptomic Response to Spaceflight in Murine Mammary Tissue: Observational Study (e73041)
James Casaletto, Tyler Zhao, Jay Yeung, Abigail Lee, Amaan Ansari, Amber Fry, Arnav Mishra, Ayush Raj, Kathryn Sun, Sofia Lendahl, Willy Guan, Melissa Cline, Sylvain Costes. . . . 45

Peer-Review Reports

Peer Review of “Relationship Between Seed Coat Color and Cytokinin Concentration in Efficiently Regenerating Leaf Lettuce Shoots: In Vitro Experimental Study” (e89401)
Ahmed Al-Mayahi. . . . 60

Peer Review of “Relationship Between Seed Coat Color and Cytokinin Concentration in Efficiently Regenerating Leaf Lettuce Shoots: In Vitro Experimental Study” (e89399)
Hamidreza Soufi. . . . 62

Peer Review of “Localized Immune Cascade Programming in Desmoplastic Tumors: In Silico Modeling and Validation Study” (e91450)
Sunny Au. . . . 64

Peer Review of “Localized Immune Cascade Programming in Desmoplastic Tumors: In Silico Modeling and Validation Study” (e91447)
Nivetha Brathaban. . . . 66

XSL•FO
RenderX

Peer Review of “Material-Driven Therapeutics to Establish a Penetrating Traumatic Brain Injury Rat Model and Implantation of a 3D-Printed Scaffold: Pre-Experimental Pilot Study” (e105277)
Firas Kobeissy. . . . 68

Author's Response to Peer Reviewss

Authors’ Response to Peer Reviews of “Relationship Between Seed Coat Color and Cytokinin Concentration in Efficiently Regenerating Leaf Lettuce Shoots: In Vitro Experimental Study” (e89391)
Mitsuhiro Kimura, Takeshi Yoshizumi. . . . 70

Authors’ Response to Peer Reviews of “Machine Learning Ensemble Investigates Age in the Transcriptomic Response to Spaceflight in Murine Mammary Tissue: Observational Study” (e88583)
James Casaletto, Tyler Zhao, Jay Yeung, Abigail Lee, Amaan Ansari, Amber Fry, Arnav Mishra, Ayush Raj, Kathryn Sun, Sofia Lendahl, Willy Guan, Melissa Cline, Sylvain Costes. . . . 73

Authors’ Response to Peer Reviews of “Localized Immune Cascade Programming in Desmoplastic Tumors: In Silico Modeling and Validation Study” (e91528)
Murad Novruzov, Marziyya Mammadova, Keval Raval, Waseem Khan, Ulkar Shiraliyeva. . . . 77

Authors’ Response To Peer Reviews

Authors’ Response to Peer Review of “Material-Driven Therapeutics to Establish a Penetrating Traumatic Brain Injury Rat Model and Implantation of a 3D-Printed Scaffold: Pre-Experimental Pilot Study” (e105278)
Meaghan Harley-Troxell, Michelle Dennis, Madhu Dhar. . . . 81

XSL•FO
RenderX

Material-Driven Therapeutics to Establish a Penetrating Traumatic Brain Injury Rat Model and Implantation of a 3D-Printed Scaffold: Pre-Experimental Pilot Study

Meaghan E Harley-Troxell[1], PhD; Michelle Dennis[2], PhD; Madhu Dhar[1], PhD

[1]Tissue Engineering and Regenerative Medicine Lab, LACS, College of Veterinary Medicine, University of Tennessee at Knoxville, 2407 River Drive, Knoxville, TN, United States

[2]Biomedical and Diagnostic Sciences Department, College of Veterinary Medicine, University of Tennessee at Knoxville, Knoxville, TN, United States

Corresponding Author:
Meaghan E Harley-Troxell, PhD
Tissue Engineering and Regenerative Medicine Lab, LACS, College of Veterinary Medicine, University of Tennessee at Knoxville, 2407 River Drive, Knoxville, TN, United States

Related Articles:

https://www.biorxiv.org/content/10.1101/2025.03.20.644358v1

https://bio.jmirx.org/2026/1/e105277

https://bio.jmirx.org/2026/1/e105278

Abstract

Background: Traumatic brain injuries (TBIs) are a leading cause of death and disability, with penetrating TBIs the most lethal form. While no TBI treatments currently exist, ongoing investigations are developing biomaterial scaffolds and cellular therapies to improve the poor outcomes of this disease.

Objective: This pilot study established a TBI rat model that maintains focal damage to the cerebral cortex while manually disrupting the blood-brain barrier (BBB). BBB-disrupting injuries require different management from others, allowing us to develop a specific, therapeutic treatment for this type of injury. We hypothesized that our method of BBB disruption would indicate behavioral, physical, and histological evidence of a TBI. Our TBI model will also create a cranial opening in which we can ensure surgical feasibility of implantation of a scaffold. We hypothesized that the implantation of a Food and Drug Administration–approved synthetic polymer, poly(lactic-co-glycolic) acid (PLGA), and a carbon-based nanomaterial, reduced graphene oxide (rGO), would not show evidence of foreign body rejection 30 days after surgery.

Methods: Sprague Dawley rats (N=4) underwent stereotaxic surgery with a 5-mm craniotomy. The dura and brain tissue were disrupted using a beaver blade. The PLGA/rGO scaffold was gently placed onto the brain tissue. Neurological function (including body condition, breathing, spontaneous behavior, handling reaction) was evaluated for the first 3 days, then weekly throughout the 30-day study. At 30 days, the brains were dissected, paraffin embedded, and sectioned for H&E and Prussian blue staining, and immunohistochemistry (IHC) using glial fibrillary acidic protein, neuronal nuclei (NeuN), von Willebrand factor, neurofilament light chain, ionized calcium-binding adapter molecule 1, and CD68 markers. Data were expressed as means and SDs, and 2-tailed *t* tests were used to determine statistical significance ($P \leq .05$).

Results: Neurological function assessments indicated no change in rat behavior and normal wound healing over the 30-day study. H&E and Prussian blue staining indicated mild leptomeningeal thickening and evidence of hemosiderin in 3 rats. One rat had foreign body giant cells and an abscess around the implanted material, with evidence of more severe leptomeningeal thickening and hemosiderin. IHC indicated normal anatomic structures with no changes in 5 of the 6 markers 30 days after surgery. NeuN significantly decreased in expression, from 9.65% to 4.56% in area, for all 4 rats ($P=.02$).

Conclusions: While there was no behavioral or symptomatic evidence of TBI, histology showed evidence of mild, focal TBI in 3 of the 4 rats and evidence of a foreign body response and a severe, focal TBI in 1 rat. This pilot study provides a basis for future studies to perform IHC at earlier time points to confirm additional biomarkers. Future studies will also implant a scaffold that is more mechanically aligned with the brain tissue to further evaluate the biocompatibility of graphene nanoparticles in brain tissue and the effectiveness of a therapeutic scaffold.

XSL•FO
RenderX

(JMIRx Bio 2026;4:e75613) doi:10.2196/75613

KEYWORDS

penetrating traumatic brain injury; stereotaxic surgery; graphene; nerve tissue engineering; rat model

Introduction

Traumatic brain injuries (TBIs) are a leading cause of death and disability [1,2]. Annually in the United States, approximately 1.7 million people have a TBI event, resulting in 50,000 deaths [1]. Currently, it is estimated that 3.2 to 5.3 million people are living with a TBI-related disability [1]. Penetrating TBIs are the most lethal form, with a foreign object breaking through the skull, disrupting the blood-brain barrier (BBB), and damaging the brain tissue [3,4]. These are most often caused by accidents, including household firearm accidents, falls, and motor vehicle collisions [2-4]. The severity of the primary injury is worsened by circulating immune cells foreign to the local environment crossing the disrupted BBB, causing persistent inflammation and generation of reactive oxygen species that result in loss of neural tissue and damaged vasculature [1,2,5]. This damage results in severe clinical symptoms, including high cranial pressure and hemorrhage. While no treatments for TBI exist, management strategies include various neurosurgical interventions and pharmacological and nonpharmacological methods [2-4,6-8]. While surgical interventions may improve survival outcomes for severe TBIs, they come with increased risk of infection and longer recovery times and may not result in greater functional outcomes [3]. Currently, researchers are investigating tissue engineering and regenerative medicine strategies to develop biomaterial scaffolds and cellular therapies that may improve upon these poor outcomes [2,6,7,9].

Animals are a necessary preclinical step for translational research in the development of novel therapeutics and can help generate TBI solutions for both animal and human medicine [10]. While large animals such as pigs are important models for TBI, showing more complexity and gray and white matter ratios similar to those of human brains, using rodents such as rats or mice prior to large animal models is a crucial step [11,12]. Outside the advantages of low costs and easy handling, rats offer a high level of standardization and can be assessed for functional outcomes and the pathophysiology of cellular damage in a way that mimics the human brain [11]. Several preclinical models exist to mimic TBIs, including controlled cortical impact injury models, weight drop models, and penetrating ballistic-like models [13]. There are a wide range of TBIs, and while each model excels in representing a specific type of scenario, they do not consistently disrupt the BBB while maintaining controlled, focal damage to the cerebral cortex, as intended in this study [13,14]. Severe mechanical models often impact the brain as a whole, simulating concussion-like injuries alongside the penetrating impact and resulting in high levels of fatality [14]. Meanwhile, the penetrating ballistic-like model, while remaining focal, creates a deep cavity mimicking a combat setting. Adding to the available preclinical models to accurately represent the range of TBIs may alter how clinical care is managed and be useful in evaluating more specific, novel therapeutics [15].

Two oxidized derivatives of graphene nanoparticles, specifically reduced graphene oxide (rGO) and graphene oxide, have been investigated as nanocomposite components for nerve tissue engineering due to their elemental composition and topographic features, which influence their tunable mechanical properties and have a positive effect on cell growth [16,17]. Specifically, rGO can be engineered using a variety of 3D printing techniques to form scaffolds that attach, proliferate, and differentiate viable exogenous or endogenous stem and progenitor cells to aid in nerve repair and regeneration [17-19]. In particular, rGO features the unique property of electrical conductivity to improve functional nerve restoration [16,17,20]. While many studies have focused on graphene's potential in the peripheral nervous system, graphene and its derivatives have also shown to be a promising component for central nerve injuries [21-23]. Controversy surrounding rGO's biocompatibility has slowed its translation to clinical use. Numerous variables, such as surface functionalization, particle shape and size, dispersion, concentration, dosage, route of administration, and processing techniques, can all influence how cells respond to rGO [16,20,23-29]. Therefore, we must evaluate whether our specific rGO-containing construct is safe to use in this delicate tissue model.

For 3D printing, graphene-based nanoparticles are always blended with synthetic polymers, including polycaprolactone, polyurethane, polylactic acid, and poly(lactic-co-glycolic) acid (PLGA). PLGA is Food and Drug Administration approved for biomedical devices, primarily because of its tailored biodegradability (ie, its breakdown products, lactic and glycolic acids, are safely metabolized by the body). While PLGA is a Food and Drug Administration–approved and very well–characterized synthetic polymer, graphene's biocompatibility is highly variable depending on a variety of tunable physicochemical and mechanical properties [30]. Hence, it is important to evaluate the biocompatibility of a PLGA-rGO construct in vivo.

In this pilot study, we performed a craniotomy in rats to manually cut the BBB, managing the disruption to the brain tissue. This allowed us to assess the feasibility of our therapeutic scaffold implantation and the safety of the biomaterial-tissue interaction between the brain tissue and our proposed scaffold containing PLGA and graphene. The use of stereotaxic surgical equipment and cranial landmarks allowed for a standardized injury capable of replication. We used a neurological assessment and immunohistochemistry (IHC) to identify whether disruption of the BBB was sufficient to model a TBI while identifying whether a foreign body reaction occurred with the implanted materials. For this study, we used a previously fabricated scaffold to evaluate the graphene's biocompatibility with the brain tissue. We hypothesized that the disruption of the BBB would cause behavioral, physical, and histological evidence of a TBI, whereas the implanted material would not show evidence

XSL•FO
RenderX

of a foreign body rejection or chronic inflammation 30 days after surgery.

Methods

Biochemicals, Chemicals, and Disposables

All biochemicals, cell culture supplements, and disposable tissue culture supplies were purchased from Thermo Fisher Scientific unless otherwise noted.

Ethical Considerations

Sprague Dawley rats (Charles River Laboratories; N=4; male; aged 6 months) were acclimated prior to beginning procedures. All procedures were conducted in accordance with Public Health Service guidelines for the humane treatment of animals under approved protocols established through the University of Tennessee's Institutional Animal Care and Use Committee (protocol 2954-0623). The animals were housed in a 12-hour light and dark cycle with ad libitum food and water.

Surgical Procedure

Rats were anesthetized using inhalant isoflurane, and buprenorphine (0.05 mg/kg) was administered subcutaneously prior to surgery. The surgical area was shaved, and eye lubricant was applied. Under aseptic conditions, the rat was mounted onto the stereotaxic apparatus (Kopf Instruments) using a nose cone to maintain anesthesia throughout the procedure [7,31,32]. The dorsal and ventral adaptor was aligned to the −8 setting; the ear bars were aligned to the 7.5 setting on either side. The area was draped, and the scalp was cleaned using iodine prior to cutting a 1- to 2-cm longitudinal incision to expose the skull. The periosteum was gently teased back from the skull, and the area was cleaned using 95% ethanol. A handheld microdrill (Stoelting Co.) with a sterile 5-mm drill bit was used to create a craniotomy to the left of the sagittal suture, midway between the lambda and bregma landmarks. The dura mater was damaged by cutting the layer using forceps and a beaver blade. A 65:35 PLGA (Sigma-Aldrich) and 0.5% rGO (Cheap Tubes) scaffold from a previous study was cut to the 5-mm size and implanted on the cerebral cortex [33]. Briefly, PLGA and rGO were blended with 0.5-mL dimethyl sulfoxide and melted into a homogeneous mixture for extrusion-based 3D printing using the CELLINK BIO X6 printer. The scaffold was printed in 15 filament layers with approximately 80% porosity and in 5-mm (x-axis), 5-mm (y-axis), and 2-mm (z-axis) dimensions. After implantation, the area was covered with bone wax, and the scalp was closed with 4-0 absorbable surgical sutures (Ethicon, Inc). The rats recovered on a heating pad and were individually housed and monitored twice daily for the first 3 days, daily for 1 week, and weekly throughout the remaining 30-day study period. Buprenorphine was administered every 12 hours for 3 days after surgery, and ketoprofen (5 mg/kg) was administered every 24 hours for 3 days after surgery. Baytril (100 mg per 400 mL) mixed into water with flavored Gatorade was provided for 1 week after surgery.

Neurological Function Evaluation

Animal recovery and neurological function were evaluated for each rat on days 1, 2, 3, 7, 14, and 21 after surgery. A modified neurological severity score was used to assess the body weight, general condition, physical appearance, breathing, spontaneous behavior, handling reaction, wound healing, and neurological evaluation of each rat [11,34-36]. These behaviors were graded on a scale from 0 (normal) to 30 and above (severe) to determine any neurological deficits that occurred from the cranial intervention or material implantation.

IHC of Brain Tissue

At the 1-month end-of-study time point, the intact brain was removed as previously described and placed in 10% formalin [37,38]. The cerebellum was removed, and the brain was dissected down the midsagittal plane, dividing the left and right hemispheres of the cerebral cortex. Each half was paraffin embedded and longitudinally sectioned. Sections were deparaffinized, hydrated, unmasked, stained, and mounted as previously described [30]. One histology section from all specimens was stained with hematoxylin and eosin (H&E; Azer Scientific, Inc) for assessment of cellular detail, and one histology section from all specimens was stained with Prussian blue for assessment of hemosiderin deposition using a 30-minute stain with 1:1 hydrochloric acid and potassium ferrocyanide. IHC was performed on the remaining sections using glial fibrillary acidic protein (GFAP; 1:500), neuronal nuclei (NeuN; 1:500; Cell Signaling Technology, Inc), von Willebrand factor (vWF; 1:1000; Abcam), neurofilament light chain (NEFL; 1:20), ionized calcium-binding adapter molecule 1 (Iba1; 1:500), and CD68 (1:500). The secondary antibodies used were goat antirabbit immunoglobulin G horseradish peroxidase (1:500) and rabbit antimouse immunoglobulin G horseradish peroxidase (1:500; Abcam). Briefly, GFAP identifies astrocytes, NeuN identifies neurons, vWF identifies vascularization, NEFL identifies neural cytoskeleton structure, Iba1 identifies microglia, and CD68 identifies phagocytic activity [39-44]. Sections were imaged using a BZ-X Series all-in-one fluorescent microscope (Keyence Corporation) at 5X, 10X, 20X, and 40X magnification. The H&E sections were analyzed by a trained histologist. For each section, multiple images were taken along the length of the section with 20% overlap and stitched together to create a single image of the entire section. Scale bars were added. ImageJ software was used to analyze the stitched images [45]. They were selected for optimal contrast (blue) and threshold (pixel intensity values ranged from 150 to 250). The nerve was isolated from the background and converted to a black-and-white image (black=stained tissue).

Statistical Analysis

For each section, the nerve was measured for percentage of area (percentage of black in the image) [30]. Mean and SD values were obtained. Prism (version 10; GraphPad Software) was used to perform a Shapiro-Wilk test of normality. When all data were determined to be normally distributed, *t* tests were performed for statistical significance between the control and injured tissues. Statistical significance was determined as a *P* value of .05 or less.

Results

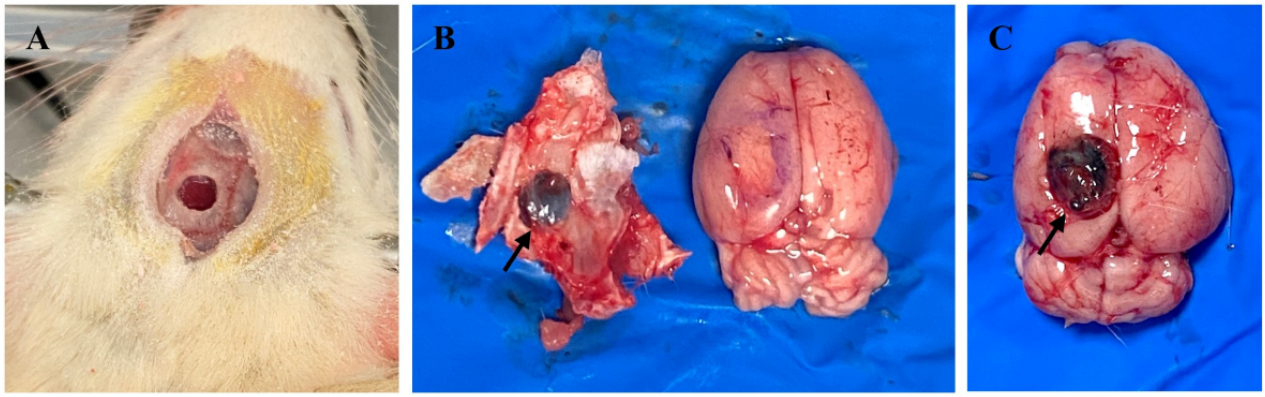
A TBI is a complex disease in which a primary injury results in an immediate disruption of brain tissue caused by an external

XSL•FO
RenderX

source, leading to contusion, hemorrhage, and axonal shearing. The secondary injury evolves over the following hours, days, and months, involving a cascade of degenerative molecular events leading to cell death [13,19]. Patients who experience focal, penetrating TBIs have areas of brain laceration, disruption of the leptomeninges, subdural hemorrhage, and cerebral edema [43]. Our method of injury manually disrupted the dura mater and cerebral cortex with a small blade through the cranial opening (Figure 1A). When the scaffold was placed onto the exposed brain tissue for rats 1, 2, and 4, there was minor bleeding before the scaffold was placed against the brain tissue with mild pressure. With rat 3, there was heavy bleeding after the surgical procedure, and the scaffold was placed onto the brain tissue after ensuring that the bleeding was under control.

Evidence of the differences in the surgical implantation was observed 30 days later during the brain dissection. In rats 1, 2, and 4, the scaffold was more strongly incorporated into the surrounding bone of the craniotomy than into the brain tissue (Figure 1B). Some theories as to why this may have occurred include the location of the implanted material, which may not have been pushed sufficiently through the cranial opening; the large z-axis of the implanted scaffold possibly interfering with the implantation process; or excessive cerebral pressure or edema possibly pushing the construct back into the opening due to insufficient closing using the bone wax. Meanwhile, rat 3 showed a greater incorporation into the brain tissue (Figure 1C). This may be due to the more severe damage to the brain, evident in the heavy bleeding and deeper implantation of the scaffold.

Figure 1. (A) Image of the craniotomy location. (B) Brain dissection of rat 4 (tissue pen used to circle area of injury; black arrow indicates implanted material). (C) Brain dissection of rat 3 (deeper cortex injury and material implantation; black arrow indicates implanted material).



During the 30-day study, the neurological assessment evaluated the physical and behavioral changes that may occur with a TBI [11,34-36]. At the 6 time points, all rats showed no changes in any of the areas assessed (Table 1). Rat 3 took slightly longer to come out from anesthesia, which was expected due to the longer procedure time to control the heavy bleeding. However, while rat 3 showed slightly slower spontaneous movement, it still fell within normal parameters. While this indicated no immediate concerns regarding a foreign body rejection of the implanted PLGA and rGO scaffold, it also indicated that the TBI model may not have been severe enough to implicate neurological deficits common with the disease. Other than TBI severity, the points of neurological evaluation may be expanded to include additional behavior tests, identifying more minute behavioral changes in future studies. Monitoring of intracranial pressure throughout a future study may also aid in confirmation of a TBI as it is a signature symptom of the injury.

At the end of the 30-day study, H&E-stained sections were evaluated for local tissue reactions. Similar to the lateral fluid percussion injury model where the TBI is limited to 1 cerebral hemisphere, the contralateral side may be used as a comparison for neural injury [12,13]. As the injury was limited to the left cerebral cortex, the right cerebral cortex was used as uninjured control tissue. The H&E-stained tissue confirmed that no significant pathology was identified in the control tissues for all 4 rats (Figure 2A). For the injured side, rats 1, 2, and 4 showed a slight indentation to the cortex with mildly thickened leptomeninges, reactive small blood vessels, increased stromal cells, and hemosiderin deposition (Figures 2B and 2C). Hemosiderin deposition is a sign of injury, often occurring after hemorrhage, and was confirmed via Prussian blue staining. Together, these findings indicate a mild focal cerebral meningeal fibrosis injury. This type of chronic response may occur after a penetrating TBI [46]. Rat 3 showed a cavitated region of the cerebrum where the meninges was severely expanded by a mass (Figures 2D-2F). The mass was composed of neutrophils and necrotic cell debris, marginated by histiocytic infiltrate, and a periphery of fibrovascular tissue with aggregated plasma cells, lymphocytes, and occasional multinucleate foreign body giant cells. Some of the rGO deposits in the area were associated with distinct vacuoles. Hemosiderin deposition was also evident and confirmed through Prussian blue staining. No evidence of infectious agents was present. Overall, rat 3 had evidence of severe focal chronic pyogranulomatous meningitis and a foreign body reaction to the rGO nanoparticles. It was difficult to decipher whether the injury was more severe in rat 3 or whether the strong inflammatory and immune response was solely due to the scaffold. Future studies will further investigate the separation in these data using a sham surgical group and an untreated TBI group.

XSL•FO
RenderX

Table . Neurological evaluation score sheet indicating the response of all rats at all time points throughout the 30-day study. Evaluation indicated no abnormal behavior or physical reactions after surgery, injury, and material implantation.

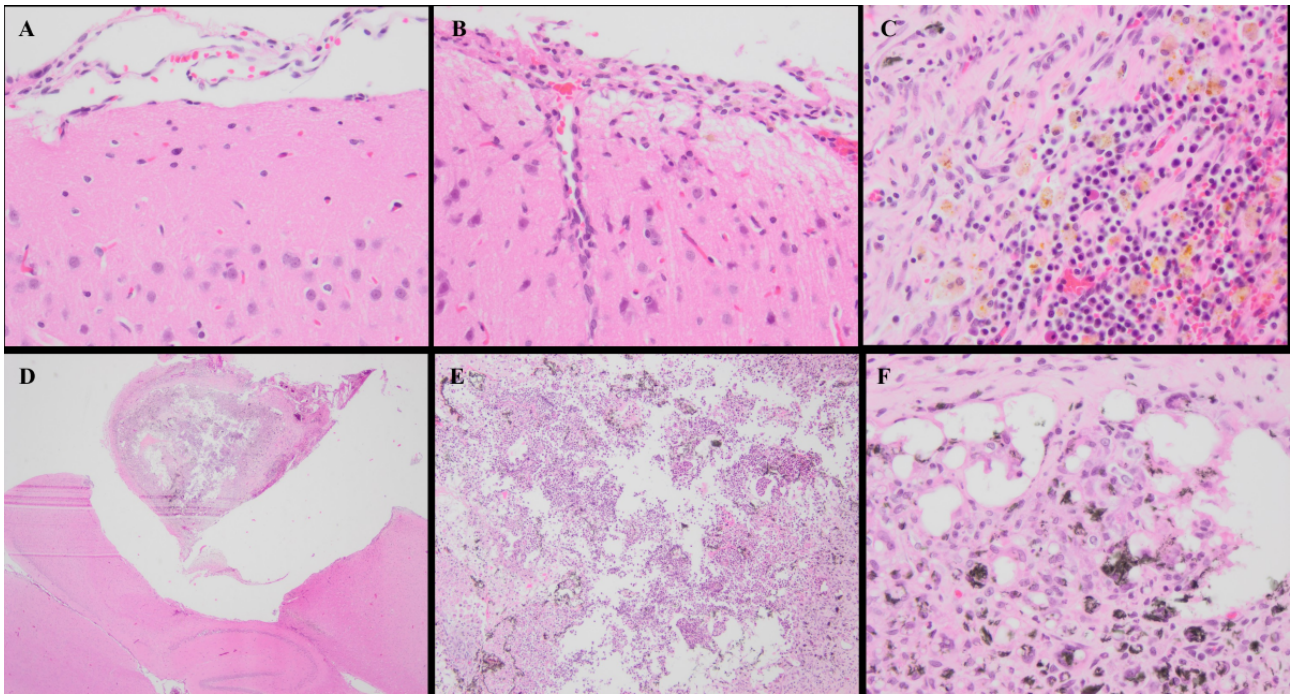
Evaluation domain and score scale	Rat 1	Rat 2	Rat 3	Rat 4
Loss of body weight				
<5% (0 points)	✓	✓	✓	✓
5%-10% (1 point)				
11%-15% (5 points)				
16%-20% (10 points)				
>20% (30 points)				
General condition and physical appearance				
Well-groomed, clean fur, clean and intact wound, and clear eyes (0 points)	✓	✓	✓	✓
Coat slightly unkempt and eye redness or “red tears” (chromodacryorrhea; 1 point)				
Coat dirty and shaggy, orbital tightening, nose flattening, ear and whisker changes, skin pinch (dehydration test), and some goosebumps (piloerection; 5 points)				
Coat unkempt and piloerection (10 points)				
Breathing				
Normal breathing (0 points)	✓	✓	✓	✓
Abnormally rapid breathing (tachypnea; 5 points)				
Difficult or labored breathing (dyspnea; 10 points)				
Spontaneous behavior				
Normal movements or locomotion (0 points)	✓	✓	✓	✓
Reluctance to move and slightly abnormal gait (5 points)				
Lethargic, apathetic, and abnormal gait (10 points)				
Significant mobility problems and mobility intermittent (<12 h; 20 points)				
Immobile for >12 h (30 points)				
Handling reaction				
Normal curiosity and alert (0 points)	✓	✓	✓	✓
Tense and nervous when held (5 points)				

XSL•FO
RenderX

Evaluation domain and score scale	Rat 1	Rat 2	Rat 3	Rat 4
Markedly distressed when handled (eg, shaking, vocalizing, and aggression; 10 points)				
Wound healing				
Wound clear, sutures and wound clip in place, and no signs of infection (0 points)	✓	✓	✓	✓
Wound closure insufficient, open wound, and no signs of infection (5 points)				
Wound showing initial signs of infection—swelling and redness (10 points)				
Wound infection severe—swelling, redness, and discharge (25 points)				
Neurological evaluation				
No observable deficit (0 points)	✓	✓	✓	✓
Forelimb flexion (paws pulled in when held by tail; 1 point)				
Decreased resistance to lateral push (slow, less movement, and pushback when the side is pushed)+forelimb flexion (5 points)				
Circling (circular movement when held by tail)+decreased lateral push and forelimb flexion (10 points)				
Seizure, coma, and complete paralysis (30 points)				
Total score				
Score of 0-9: minimal or no action required	✓	✓	✓	✓
Score of 10-20: provide supplementary care as needed				
Score of 21-29: consult veterinarian for additional care				
Score of ≥30: implement animal removal				

XSL•FO
RenderX

Figure 2. Hemoxylin and eosin–stained sections of brain tissue: (A) normal, healthy brain tissue on the control side at 40X magnification;(B) mild meningeal thickening and evidence of hemosiderin in rat 2 (injured side at 40X magnification); (C)brown and orange hemosiderin deposits and black graphene material deposits in rat 3 (injured side at 40X magnification); and images at 2X magnification (D), 10X magnification (E), and 40X magnification (F) exhibiting an abscess surrounding the graphene material implant in rat 3.

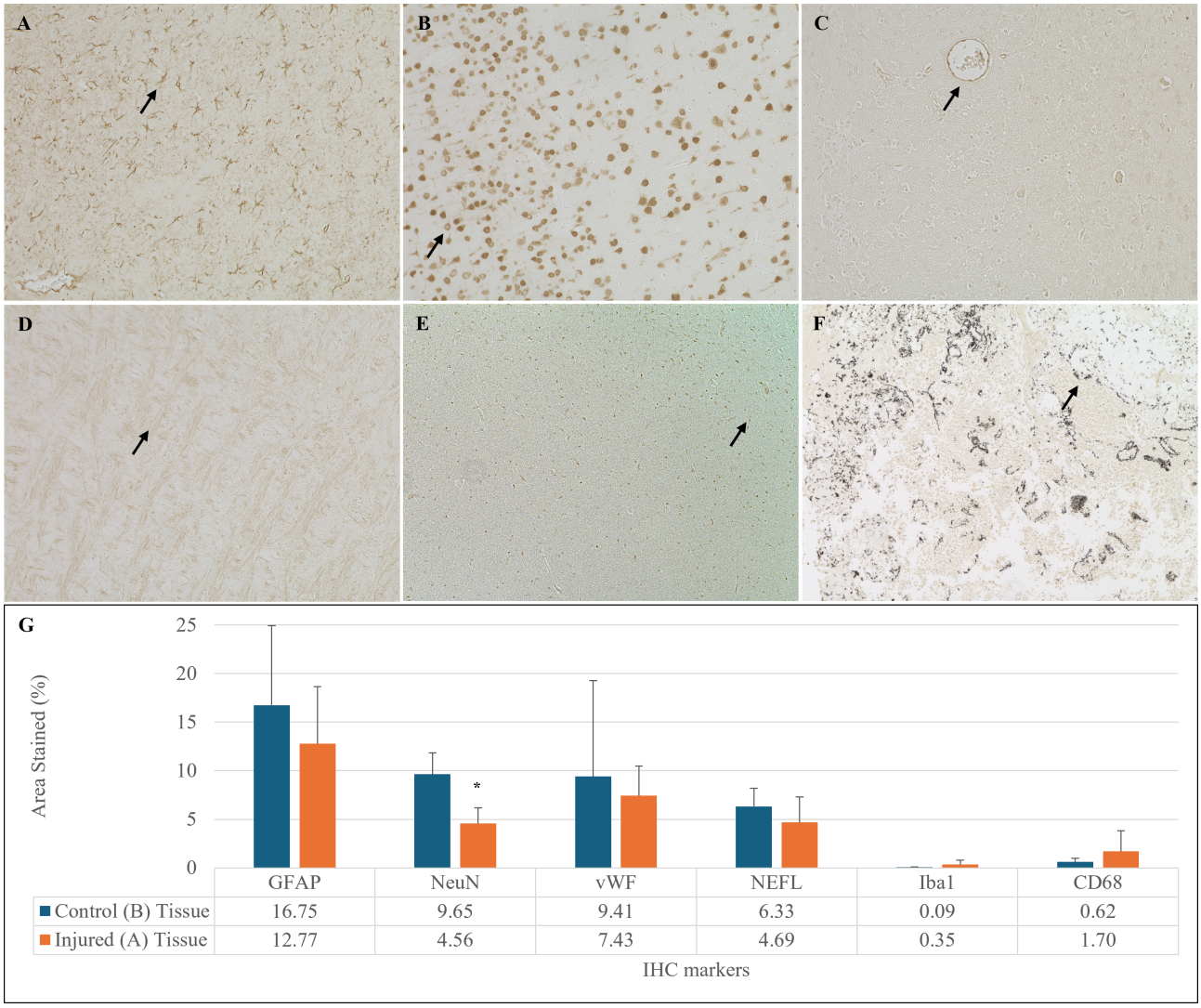


The IHC markers that were evaluated had previously shown changes after TBI. After an injury, the glial markers, GFAP and Iba1, increase, whereas the neural marker, NeuN, decreases due to glial scarring and the loss of damaged neural cells in the area, respectively [40,41,43]. vWF increases to identify vascular damage after a severe injury but typically maintains its expression with a mild injury [40]. NEFL increases to identify fragmented neural structures, and CD68 increases to indicate a rise in phagocytic activity [39,43]. Qualitatively, each of these 6 markers showed “normal” anatomical structures (Figures 3A-3F). Quantitatively, GFAP, vWF, NEFL, Iba1, and CD68 showed no significant differences in expression between the injured and control tissues (Figure 3G). However, NeuN expression significantly decreased from 9.65% to 4.56% of area stained in the injured tissue in all rats (P=.02). A significant decrease in NeuN is expected after a TBI, with the associated loss of neural cells due to the sustained damage to the tissue [40,43]. When rat 3 was excluded from the statistical analysis, statistical significance remained unchanged. The remaining markers may not have indicated any changes due to the 30-day time frame. It has been shown that these markers return to preinjury levels by 14 days after a TBI in mild cases [43,44].

Overall, all rats showed evidence of a TBI histologically at 30 days after surgery, although they were asymptomatic according to the neurological assessment. Rats 1, 2, and 4 showed evidence of a mild, focal, penetrating TBI according to the H&E staining and IHC marker (NeuN). Rat 3 showed evidence of foreign body rejection that could not be separated from evidence of a severe TBI.

XSL•FO
RenderX

Figure 3. Immunohistochemistry (IHC) of injured brain tissue. (A) Representative image of glial fibrillary acidic protein (GFAP) expression at 20X magnification (the black arrow indicates spindlelike astrocytes). (B) Representative image of neuronal nuclei (NeuN) expression at 20X magnification (the black arrow indicates hollowing of neurons). (C) Representative image of von Willebrand factor (vWF) expression at 20X magnification (the black arrow indicates a blood vessel). (D) Representative image of neurofilament light chain (NEFL) expression at 20X magnification (the black arrow indicates neurofilament alignment throughout the tissue). (E) Representative image of ionized calcium-binding adapter molecule 1 (Iba1) expression at 10X magnification (the black arrow indicates expression by spindlelike microglia). (F) Representative image of CD68 expression at 10X magnification (the black arrow indicates phagocytic activity around graphene material). (G) Quantification of IHC staining for each marker comparing the control ipsilateral cortex tissue to the injured cortex tissue. No significant changes were observed in GFAP, vWF, NEFL, Iba1, and CD68 expression. NeuN had a significant decrease in expression at 30 days after injury as compared to the control tissue. *$P \leq .05$.



Discussion

Rat TBI models are diverse and designed to simulate human clinical scenarios and injuries. As a result, the models vary in their severity, location, and ease of animal handling [12]. As our goal in this study was to establish a tissue engineering strategy to address TBI, it required optimization at several steps. For instance, our strategy included selecting the animal in which to create the model; 3D printing the nanocomposite that we wanted to evaluate in vivo; establishing and optimizing procedures for implantation of the biomaterial; and, finally, validating protocols to monitor and evaluate the animals and assess the performance of the biomaterial scaffold. A pilot study of 4 Sprague Dawley rats was established and conducted as presented in this paper. We performed a relatively simple and quick craniotomy in rats to manually cut the BBB. The stereotaxic equipment was set to a consistent setting with respect to the cranial landmarks, allowing us to perform the surgery in a reproducible manner. Using our strategy, and as outlined in the Results section, we were able to prove the feasibility of this study, which allowed for scaffold implantation and in vivo safety evaluation of the biomaterial-tissue interaction. Finally, we were able to establish a scoring system to assess neurological features correlated with the defect. We created a neurological assessment based on published reports. We used histological and immunohistochemical staining to identify whether disruption of the BBB was sufficient to model a TBI, proving that the novel biomaterial was biocompatible, and to evaluate the expression of specific neural target proteins to identify biomarkers for TBI for future studies.

Despite assessing only 4 rats in this study, we were able to validate our system, which could be applied to any future neural tissue engineering project focused on TBI. While this pilot study

XSL•FO
RenderX

did not use a surgical control group, the use of a sham surgery in a larger study and with a greater number of animals for statistical analysis can separate the data to determine whether the injury identified through H&E staining was due to a severe TBI or to the implanted scaffold and whether the variability observed in 1 of the 4 rats evaluated was a concern in this model of TBI. Additionally, the surgical procedure was successful for scaffold implantation, although a construct with mechanical properties more aligned with those of the cortex will aid in the successful integration into the appropriate tissue [9,47,48]. A period of 30 days was chosen as this is the estimated time that a scaffold should remain implanted before degradation [49]. This time frame best allows for the alignment of complete degradation with tissue repair and regeneration in the cerebral cortex. The implanted scaffold did not fully degrade at 30 days in vivo and will need to be altered to accelerate degradation within this time frame. Future studies can evaluate the surgical groups at multiple time points, including a shorter time frame such as 24 hours or 3 days, to better confirm the acute injury (0-3 days) using TBI biomarkers such as those evaluated via IHC [19,43,44]. This will also allow for the evaluation of the therapeutic potential of implanted scaffolds and graphene nanoparticles at the acute and chronic TBI phases [9].

Acknowledgments

The authors acknowledge Matthew Cooper for the training on the stereotaxic surgical equipment.

Funding

This study was supported by departmental funds to the corresponding author (M Dhar). No external funding was used to support this study.

Data Availability

The datasets generated for this study are available from the corresponding author on reasonable request.

Authors' Contributions

MEH-T, M Dennis, and M Dhar were responsible for interpreting the data. MEH-T and M Dhar were responsible for conceptualizing the study and editing the manuscript. M Dennis and M Dhar were responsible for methodology. MEH-T was responsible for data acquisition and analysis, visualization, and initial manuscript preparation. M Dhar was responsible for supervision, resources, and writing review. All authors have read and agreed to the published version of the manuscript.

Conflicts of Interest

None declared.

References

1. Sulhan S, Lyon KA, Shapiro LA, Huang JH. Neuroinflammation and blood-brain barrier disruption following traumatic brain injury: pathophysiology and potential therapeutic targets. J Neurosci Res 2020 Jan;98(1):19-28. [doi: 10.1002/jnr.24331] [Medline: 30259550]
2. Vella MA, Crandall ML, Patel MB. Acute management of traumatic brain injury. Surg Clin North Am 2017 Oct;97(5):1015-1030. [doi: 10.1016/j.suc.2017.06.003] [Medline: 28958355]
3. D'Agostino R, Kursinskis A, Parikh P, Letarte P, Harmon L, Semon G. Management of penetrating traumatic brain injury: operative versus non-operative intervention. J Surg Res 2021 Jan;257:101-106. [doi: 10.1016/j.jss.2020.07.046] [Medline: 32818778]
4. Mansour A, Powla PP, Alvarado-Dyer R, et al. Comparative analysis of clinical severity and outcomes in penetrating versus blunt traumatic brain injury propensity matched cohorts. Neurotrauma Rep 2024;5(1):348-358. [doi: 10.1089/neur.2024.0009] [Medline: 38595793]
5. Obukohwo OM, Oreoluwa OA, Andrew UO, Williams UE. Microglia-mediated neuroinflammation in traumatic brain injury: a review. Mol Biol Rep 2024 Oct 19;51(1):1073. [doi: 10.1007/s11033-024-09995-4] [Medline: 39425760]
6. Basit RH, Wiseman J, Chowdhury F, Chari DM. Simulating traumatic brain injury in vitro: developing high throughput models to test biomaterial based therapies. Neural Regen Res 2023 Feb;18(2):289-292. [doi: 10.4103/1673-5374.346465] [Medline: 35900405]
7. Zhang J, Wang RJ, Chen M, et al. Collagen/heparan sulfate porous scaffolds loaded with neural stem cells improve neurological function in a rat model of traumatic brain injury. Neural Regen Res 2021 Jun;16(6):1068-1077. [doi: 10.4103/1673-5374.300458] [Medline: 33269752]
8. Galgano M, Toshkezi G, Qiu X, Russell T, Chin L, Zhao LR. Traumatic brain injury: current treatment strategies and future endeavors. Cell Transplant 2017 Jul;26(7):1118-1130. [doi: 10.1177/0963689717714102] [Medline: 28933211]
9. Aqel S, Al-Thani N, Haider MZ, et al. Biomaterials in traumatic brain injury: perspectives and challenges. Biology (Basel) 2023 Dec 29;13(1):21. [doi: 10.3390/biology13010021] [Medline: 38248452]

XSL•FO
RenderX

10. Ribitsch I, Baptista PM, Lange-Consiglio A, et al. Large animal models in regenerative medicine and tissue engineering: to do or not to do. Front Bioeng Biotechnol 2020;8:972. [doi: 10.3389/fbioe.2020.00972] [Medline: 32903631]
11. Pinkernell S, Becker K, Lindauer U. Severity assessment and scoring for neurosurgical models in rodents. Lab Anim 2016 Dec;50(6):442-452. [doi: 10.1177/0023677216675010] [Medline: 27909194]
12. Fesharaki-Zadeh A, Datta D. An overview of preclinical models of traumatic brain injury (TBI): relevance to pathophysiological mechanisms. Front Cell Neurosci 2024;18:1371213. [doi: 10.3389/fncel.2024.1371213] [Medline: 38682091]
13. Xiong Y, Mahmood A, Chopp M. Animal models of traumatic brain injury. Nat Rev Neurosci 2013 Feb;14(2):128-142. [doi: 10.1038/nrn3407] [Medline: 23329160]
14. Zhao Q, Zhang J, Li H, Li H, Xie F. Models of traumatic brain injury-highlights and drawbacks. Front Neurol 2023;14:1151660. [doi: 10.3389/fneur.2023.1151660] [Medline: 37396767]
15. Graham NS, Sharp DJ. Understanding neurodegeneration after traumatic brain injury: from mechanisms to clinical trials in dementia. J Neurol Neurosurg Psychiatry 2019 Nov;90(11):1221-1233. [doi: 10.1136/jnnp-2017-317557] [Medline: 31542723]
16. Ławkowska K, Pokrywczyńska M, Koper K, Kluth LA, Drewa T, Adamowicz J. Application of graphene in tissue engineering of the nervous system. Int J Mol Sci 2021 Dec 21;23(1):33. [doi: 10.3390/ijms23010033] [Medline: 35008456]
17. Hui Y, Yan Z, Yang H, Xu X, Yuan WE, Qian Y. Graphene family nanomaterials for STEM cell neurogenic differentiation and peripheral nerve regeneration. ACS Appl Bio Mater 2022 Oct 17;5(10):4741-4759. [doi: 10.1021/acsabm.2c00663] [Medline: 36102324]
18. Silva M, Pinho IS, Covas JA, Alves NM, Paiva MC. 3D printing of graphene-based polymeric nanocomposites for biomedical applications. Funct Compos Mater 2021;2(1):8. [doi: 10.1186/s42252-021-00020-6]
19. Harley-Troxell ME, Steiner R, Advincula RC, Anderson DE, Dhar M. Interactions of cells and biomaterials for nerve tissue engineering: polymers and fabrication. Polymers (Basel) 2023 Sep 7;15(18):3685. [doi: 10.3390/polym15183685] [Medline: 37765540]
20. Tang M, Song Q, Li N, Jiang Z, Huang R, Cheng G. Enhancement of electrical signaling in neural networks on graphene films. Biomaterials 2013 Sep;34(27):6402-6411. [doi: 10.1016/j.biomaterials.2013.05.024] [Medline: 23755830]
21. Aleemardani M, Zare P, Seifalian A, Bagher Z, Seifalian AM. Graphene-based materials prove to be a promising candidate for nerve regeneration following peripheral nerve injury. Biomedicines 2021 Dec 30;10(1):73. [doi: 10.3390/biomedicines10010073] [Medline: 35052753]
22. Convertino D, Trincavelli ML, Giacomelli C, Marchetti L, Coletti C. Graphene-based nanomaterials for peripheral nerve regeneration. Front Bioeng Biotechnol 2023;11:1306184. [doi: 10.3389/fbioe.2023.1306184] [Medline: 38164403]
23. Tupone MG, Panella G, d'Angelo M, et al. An update on graphene-based nanomaterials for neural growth and central nervous system regeneration. Int J Mol Sci 2021 Dec 2;22(23):13047. [doi: 10.3390/ijms222313047] [Medline: 34884851]
24. MacDonald AF, Harley-Troxell ME, Newby SD, Dhar MS. 3D-printing graphene scaffolds for bone tissue engineering. Pharmaceutics 2022 Aug 31;14(9):1834. [doi: 10.3390/pharmaceutics14091834] [Medline: 36145582]
25. Yunus MA, Ramli MM, Osman NH, Mohamed R. Stimulation of innate and adaptive immune cells with graphene oxide and reduced graphene oxide affect cancer progression. Arch Immunol Ther Exp (Warsz) 2021 Jul 29;69(1):20. [doi: 10.1007/s00005-021-00625-6] [Medline: 34327598]
26. Dudek I, Skoda M, Jarosz A, Szukiewicz D. The molecular influence of graphene and graphene oxide on the immune system under in vitro and in vivo conditions. Arch Immunol Ther Exp (Warsz) 2016 Jun;64(3):195-215. [doi: 10.1007/s00005-015-0369-3] [Medline: 26502273]
27. Kenry, Lee WC, Loh KP, Lim CT. When stem cells meet graphene: Opportunities and challenges in regenerative medicine. Biomaterials 2018 Feb;155:236-250. [doi: 10.1016/j.biomaterials.2017.10.004] [Medline: 29195230]
28. Ema M, Gamo M, Honda K. A review of toxicity studies on graphene-based nanomaterials in laboratory animals. Regul Toxicol Pharmacol 2017 Apr;85:7-24. [doi: 10.1016/j.yrtph.2017.01.011] [Medline: 28161457]
29. Rhazouani A, Gamrani H, El Achaby M. Synthesis and toxicity of graphene oxide nanoparticles: a literature review of in vitro and in vivo studies. Biomed Res Int 2021;2021:5518999. [doi: 10.1155/2021/5518999] [Medline: 34222470]
30. Harley-Troxell ME, Pedersen AP, Newby SD, et al. 3D-printed poly (lactic-co-glycolic acid) and graphene oxide nerve guidance conduit with mesenchymal stem cells for effective axon regeneration in a rat sciatic nerve defect model. Int J Nanomedicine 2025;20(501241):3201-3217. [doi: 10.2147/IJN.S501241] [Medline: 40098718]
31. Mahmood A, Wu H, Qu C, et al. Suppression of neurocan and enhancement of axonal density in rats after treatment of traumatic brain injury with scaffolds impregnated with bone marrow stromal cells. J Neurosurg 2014 May;120(5):1147-1155. [doi: 10.3171/2013.12.JNS131362] [Medline: 24460490]
32. Yan F, Li M, Zhang HQ, et al. Collagen-chitosan scaffold impregnated with bone marrow mesenchymal stem cells for treatment of traumatic brain injury. Neural Regen Res 2019 Oct;14(10):1780-1786. [doi: 10.4103/1673-5374.257533] [Medline: 31169196]
33. MacDonald AF. Mesenchymal stem cell fate on carbon-based biomaterials: implications for bone regeneration and repair [PhD thesis]. : University of Tennessee; 2022 URL: https://trace.tennessee.edu/entities/publication/36873230-ae48-423c-9e75-df44e7cb9545 [accessed 2026-06-30]

XSL•FO
RenderX

34. Laboratory animal biomethodology workshops. McGill University. URL: https://www.mcgill.ca/cmarc/workshops [accessed 2026-06-30]
35. Jeon H, Ai J, Sabri M, et al. Neurological and neurobehavioral assessment of experimental subarachnoid hemorrhage. BMC Neurosci 2009 Aug 25;10:103. [doi: 10.1186/1471-2202-10-103] [Medline: 19706182]
36. Hao Q, Zheng J, Hu Y, Wang H. Bone marrow mesenchymal stem cells combined with Sox2 increase the functional recovery in rat with traumatic brain injury. Chin Neurosurg J 2019;5:11. [doi: 10.1186/s41016-019-0158-7] [Medline: 32922911]
37. Brzica H, Abdullahi W, Reilly BG, Ronaldson PT. A simple and reproducible method to prepare membrane samples from freshly isolated rat brain microvessels. J Vis Exp 2018 May 7(135):57698. [doi: 10.3791/57698] [Medline: 29782001]
38. Aboghazleh R, Boyajian SD, Atiyat A, Udwan M, Al-Helalat M, Al-Rashaideh R. Rodent brain extraction and dissection: a comprehensive approach. MethodsX 2023;12:102516. [doi: 10.1016/j.mex.2023.102516] [Medline: 38162147]
39. Neri M, Frati A, Turillazzi E, et al. Immunohistochemical evaluation of aquaporin-4 and its correlation with CD68, IBA-1, HIF-1α, GFAP, and CD15 expressions in fatal traumatic brain injury. Int J Mol Sci 2018 Nov 10;19(11):3544. [doi: 10.3390/ijms19113544] [Medline: 30423808]
40. Yip PK, Hasan S, Liu ZH, Uff CE. Characterisation of severe traumatic brain injury severity from fresh cerebral biopsy of living patients: an immunohistochemical study. Biomedicines 2022 Feb 22;10(3):518. [doi: 10.3390/biomedicines10030518] [Medline: 35327320]
41. Kim HJ, Han SJ. A simple rat model of mild traumatic brain injury: a device to reproduce anatomical and neurological changes of mild traumatic brain injury. PeerJ 2017;5:e2818. [doi: 10.7717/peerj.2818] [Medline: 28070456]
42. Clark DP, Perreau VM, Shultz SR, et al. Inflammation in traumatic brain injury: roles for toxic A1 astrocytes and microglial-astrocytic crosstalk. Neurochem Res 2019 Jun;44(6):1410-1424. [doi: 10.1007/s11064-019-02721-8] [Medline: 30661228]
43. Ţolescu R, Zorilă MV, Kamal KC, et al. Histological and immunohistochemical study of brain damage in traumatic brain injuries in children, depending on the survival period. Rom J Morphol Embryol 2022;63(1):169-179. [doi: 10.47162/RJME.63.1.18] [Medline: 36074681]
44. Wang ML, Yu MM, Yang DX, Liu YL, Wei XE, Li WB. Longitudinal microstructural changes in traumatic brain injury in rats: a diffusional kurtosis imaging, histology, and behavior study. AJNR Am J Neuroradiol 2018 Sep;39(9):1650-1656. [doi: 10.3174/ajnr.A5737] [Medline: 30049720]
45. Schindelin J, Arganda-Carreras I, Frise E, et al. Fiji: an open-source platform for biological-image analysis. Nat Methods 2012 Jun 28;9(7):676-682. [doi: 10.1038/nmeth.2019] [Medline: 22743772]
46. Fehlberg CR, Lee JK. Fibrosis in the central nervous system: from the meninges to the vasculature. Cell Tissue Res 2022 Mar;387(3):351-360. [doi: 10.1007/s00441-021-03491-y] [Medline: 34189605]
47. Sensharma P, Madhumathi G, Jayant RD, Jaiswal AK. Biomaterials and cells for neural tissue engineering: current choices. Mater Sci Eng C Mater Biol Appl 2017 Aug 1;77:1302-1315. [doi: 10.1016/j.msec.2017.03.264] [Medline: 28532008]
48. Cangellaris OV, Gillette MU. Biomaterials for enhancing neuronal repair. Front Mater 2018;5. [doi: 10.3389/fmats.2018.00021]
49. Modo M. Bioscaffold-induced brain tissue regeneration. Front Neurosci 2019;13:1156. [doi: 10.3389/fnins.2019.01156] [Medline: 31787865]

Abbreviations

BBB: blood-brain barrier
GFAP: glial fibrillary acidic protein
H&E: hematoxylin and eosin
Iba1: ionized calcium-binding adapter molecule 1
IHC: immunohistochemistry
NEFL: neurofilament light chain
NeuN: neuronal nuclei
PLGA: poly(lactic-co-glycolic) acid
rGO: reduced graphene oxide
TBI: traumatic brain injury
vWF: von Willebrand factor

XSL•FO
RenderX

Edited by A Schwartz; submitted 07.Apr.2025; peer-reviewed by F Kobeissy; revised version received 13.May.2026; accepted 19.May.2026; published 10.Jul.2026.

Please cite as:
Harley-Troxell ME, Dennis M, Dhar M
Material-Driven Therapeutics to Establish a Penetrating Traumatic Brain Injury Rat Model and Implantation of a 3D-Printed Scaffold: Pre-Experimental Pilot Study
JMIRx Bio 2026;4:e75613
URL: https://bio.jmirx.org/2026/1/e75613
doi:10.2196/75613

© Meaghan E Harley-Troxell, Michelle Dennis, Madhu Dhar. Originally published in JMIRx Bio (https://bio.jmirx.org), 10.Jul.2026. This is an open-access article distributed under the terms of the Creative Commons Attribution License (https://creativecommons.org/licenses/by/4.0/), which permits unrestricted use, distribution, and reproduction in any medium, provided the original work, first published in JMIRx Bio, is properly cited. The complete bibliographic information, a link to the original publication on https://bio.jmirx.org/, as well as this copyright and license information must be included.

XSL•FO
RenderX

Relationship Between Seed Coat Color and Cytokinin Concentration in Efficiently Regenerating Leaf Lettuce Shoots: In Vitro Experimental Study

Mitsuhiro Kimura[1,2]; Takeshi Yoshizumi[1]

[1]Takasaki University of Health and Welfare, 54 Nakaorui-machi, Takasaki, Japan

[2]Kyushu University, 744 Motooka, Nishi-ku, Fukuoka, Japan

Corresponding Author:
Mitsuhiro Kimura
Takasaki University of Health and Welfare, 54 Nakaorui-machi, Takasaki, Japan

Related Articles:

https://www.biorxiv.org/content/10.1101/2024.12.10.627673v1

https://bio.jmirx.org/2026/1/e89399

https://bio.jmirx.org/2026/1/e89401

https://bio.jmirx.org/2026/1/e89391

Abstract

Background: Lettuce (*Lactuca sativa* L.) is an economically important leafy vegetable that is cultivated worldwide. Advances in plant biotechnology have enabled the development of transgenic and transplastomic lettuce lines with specific agronomic traits that produce pharmaceutical proteins and biological compounds. Plant regeneration efficiency is a critical and highly cultivar-dependent step in plant genetic transformation. No morphological markers have been identified that predict the regeneration ability or cytokinin requirement of lettuce cultivars, hindering the establishment of efficient regeneration systems.

Objective: This study aimed to optimize the direct shoot regeneration efficiency of leaf lettuce cultivars and identify a morphological trait that predicts the optimal cytokinin concentration for each cultivar.

Methods: The direct shoot regeneration of two cultivars (Chima-sanchi and Chirimen-chisya) was tested on media containing various concentrations of the cytokinin 6-benzylaminopurine (BAP). Four additional cultivars with different seed coat colors were analyzed to determine the relationship between seed coat color and the optimal BAP concentration. Statistical significance was evaluated using the Student *t* test, with significance set at $P<.01$.

Results: The highest regeneration efficiencies in Chima-sanchi (80.5%, SE 3.0%; 103 of 128 explants) and Chirimen-chisya (50%, SE 4.4%; 64 of 128 explants) were obtained with 0.05 and 0.5 mg/L BAP, respectively. Therefore, the optimal BAP concentration differed significantly between the cultivars ($P<.01$). The seed coat color and the optimal BAP concentration required for efficient direct shoot regeneration were strongly correlated among the six cultivars.

Conclusions: Seed coat color is a useful morphological marker for predicting the optimal BAP concentration required for efficient direct shoot regeneration in leaf lettuce cultivars. These findings contribute to optimizing lettuce shoot regeneration systems for specific cultivars.

(JMIRx Bio 2026;4:e70496) doi:10.2196/70496

KEYWORDS

leaf lettuce; shoot regeneration efficiency; 6-benzylaminopurine; seed coat color; CIELAB color scale; flavonoid; BAP

Introduction

Lettuce (*Lactuca sativa* L.) is a major vegetable crop cultivated worldwide that belongs to the *Asteraceae* family. The total world production of lettuce and chicory has increased 1.3-fold in the 20 years since 2005 according to the Food and Agriculture Organization of the United Nations [1]. Asia produced 18.1 million tons of lettuce in 2023, which was 64.4% of global production; Japan produced 0.6 million tons of lettuce, ranking

XSL•FO
RenderX

seventh highest in the world [1]. Lettuce is a dietary source of vitamins and minerals [2]. Thus, lettuce cultivars with increased yield and resistance to biotic and abiotic stresses have been developed using conventional breeding methods [3].

Transgenic and transplastomic lettuce lines with specific agronomic traits that accumulate pharmaceutical proteins and biocompounds have been developed using transformation procedures mediated by particle bombardment and *Agrobacterium* [3]. The major lettuce varieties worldwide include leaf, crisphead, butterhead, and romaine lettuce [3]. Leaf lettuce varieties have wrinkled leaves with frilly edges and no head; their fresh shoots are heavier than those of butterhead varieties under light-emitting diode lighting [4]. Therefore, leaf lettuce varieties are more suitable for indoor growth. Moreover, leaf lettuce contains more β-carotene, a precursor to vitamin A, and more lutein per dry weight than either crisphead or butterhead lettuce [5].

Plant tissue cultures have been widely used in plant breeding and industrial applications, such as for propagating virus-free plants, producing valuable compounds, and producing somaclonal variations [6]. The shoot regeneration efficiency of most plant species is highly dependent on the explant sources, the basal salt mixtures, sugars, and plant growth regulators [7]. Combining the cytokinin 6-benzylaminopurine (BAP) and the auxin 1-naphthaleneacetic acid (NAA) effectively regenerates lettuce shoots, but the optimal combination differs among cultivars [8-10]. Optimizing plant tissue culture parameters is labor-intensive and time-consuming because culturing plant tissues is a slow process. The molecular mechanisms regulating shoot regeneration in lettuce have been examined [11]. The effects of auxins and cytokinins on lettuce regeneration have been studied: the response is mostly cultivar-specific [8-10], and no reliable morphological marker has been identified to predict regeneration ability. For example, Bull and Michelmore [11] molecularly characterized the genetic and regulatory mechanisms underlying regenerative competence in lettuce, but how visible traits relate to hormonal responsiveness was not examined. Certain visible traits may reflect the regenerative capacity, as demonstrated in *Cymbidium* [12]; however, these morphological cues have not been explored in lettuce. We found that seed coat color strongly correlates with the cytokinin requirements for efficient shoot regeneration in leaf lettuce cultivars. Seed coat color is a simple, nondestructive morphological marker that can be used to accelerate the optimization of regeneration systems for genetic transformation. Therefore, this study aimed to evaluate whether seed coat color can reliably predict the cytokinin concentration required for efficient direct shoot regeneration across multiple leaf lettuce cultivars.

Methods

Plant Materials and Growth Conditions

Six leaf lettuce cultivars were used in this study: Chima-sanchi and Chirimen-chisya (purchased from Tohoku Seed), Red fire and Green wave (purchased from Takii Seed), and Fringe green and Shiki-beni (purchased from Sakata Seed). Chima-sanchi, Red fire, and Shiki-beni are white seed cultivars; Chirimen-chisya, Green wave, and Fringe green are brown seed cultivars . The seeds were stored in a constant humidity chamber (SD-302 - 01, Toyo Living) at 25 °C and a relative humidity of 0% - 1% until sowing. Seeds were surface-sterilized via immersion in 70% ethanol for 1 minute. The seeds were treated with 20% commercial bleach (Kao) containing 6% sodium hypochlorite, resulting in a final NaOCl concentration of 1.2%, for 15 minutes. The seeds were then rinsed 3 times with sterile distilled water. The sterilized seeds were placed on a germination medium containing half-strength Murashige and Skoog medium (2.3 g/L, Wako Pure Chemical Industries) [13] supplemented with 10 g/L sucrose and 2.5 g/L Phytagel (Sigma-Aldrich) in Petri dishes with a diameter of 9 cm. The pH of the medium was adjusted to 5.8 with 1N KOH and 1N HCl. The medium was then autoclaved at 120 °C and 0.1 MPa for 20 minutes. Seeds were germinated in an environmentally controlled growth chamber (LPH-411S, NK systems) fitted with fluorescent light (FLR40SW/M/36, NEC) at a photosynthetic photon flux density of 300 µmol photons/m^2/s under continuous white light conditions at 20 °C. All experiments were conducted at Takasaki University of Health and Welfare, Takasaki City, Gunma Prefecture, Japan (36.33°N, 139.00°E) between September 2021 and September 2022, in a humid subtropical climate (Köppen climate classification: Cfa).

Media Composition for Shoot Regeneration

Shoot regeneration efficiency was examined using a medium supplemented with different basal salt mixtures, sugars, and concentrations of BAP and NAA (Nacalai Tesque) following a previously described method [14] (Table 1). NAA was dissolved in a 10 mM NaOH solution and BAP was dissolved in a 10 mM HCl solution before either was added to the culture media. All media contained 0.5 g/L polyvinylpyrrolidone (Nacalai Tesque) and 2.5 g/L Phytagel (Sigma-Aldrich) at pH 5.8. The medium was sterilized via autoclaving at 121 °C for 20 minutes. Cotyledons from 7-day-old seedlings were used as explants and placed on the medium in Petri dishes with a diameter of 9 cm. Each treatment included 16 explants that were cultured per dish, with 8 dishes per treatment, for a total of 128 explants. The explants were maintained for 4 weeks under continuous white light conditions (photosynthetic photon flux density=300 µmol photons/m^2/s) at 25 °C and transferred to fresh medium every 2 weeks.

XSL•FO
RenderX

Table . Media composition and growth regulators for shoot regeneration of lettuce.

Medium	Basal salt mix	Sugar	BAP[a] (mg/L)	NAA[b] (mg/L)
M1	1 × MS[c]	3% sucrose	0.5	0.1
M2	1 × MS	3% sucrose	0.05	0.01
M3	1 × MS	3% sucrose	0.05	0.1
M4	1 × MS	3% sucrose	0.05	1
M5	1 × MS	3% sucrose	0.5	0.01
M6	1 × MS	3% sucrose	0.5	1
M7	1 × MS	3% sucrose	5	0.01
M8	1 × MS	3% sucrose	5	0.1
M9	1 × MS	3% sucrose	5	1
M10	1/2 × MS	3% sucrose	0.5	0.1
M11	1 × B5	3% sucrose	0.5	0.1
M12	1 × MS	6% sucrose	0.5	0.1
M13	1 × MS	1.5% glucose	0.5	0.1

[a]BAP: 6-benzylaminopurine.

[b]NAA: 1-naphthaleneacetic acid.

[c]MS: Murashige and Skoog.

Seed Coat Color Measurement

The color parameters of the seeds from each cultivar were measured with an SD 7000 spectrophotometer (Nippon Denshoku Industries) using the CIELAB *L**, *a**, and *b** color scale. The *L** axis represents the degree of brightness ranging from black (*L**=0) to white (*L**=100). The *a** and *b** axes represent redness (positive number) to greenness (negative number) and yellowness (positive number) to blueness (negative number), respectively [15].

Total Flavonoid Content Analysis

The total flavonoid content was analyzed according to a previously described method, with some modifications [16]. A 50 µg aliquot of seeds was homogenized in 0.5 mL of 80% methanol with 5.0 mm stainless beads (Biomedical Science) at 1100 rotations per minute for 45 seconds using a Shake Master (Biomedical Science). The homogenized solutions were incubated for 15 minutes at 70 °C, then centrifuged at 10,000 × g for 10 minutes at 4 °C. The resulting supernatants were incubated at 60 °C, and the dried pellets were dissolved in 20 µL of 80% methanol. The extracts were spotted on a 5 × 5 cm TLC Silica gel 60 $F_{2\ 4}$ plate (Merck). For staining, the blots were sprayed with a methanolic solution containing 1% diphenylboric acid 2-aminoethylester (DPBA, Tokyo Chemical Industry), then sprayed with a methanolic solution containing 5% PEG 4000 (Nacalai Tesque). The fluorescence was visualized using an iBright CL1000 imaging system (Thermo Fisher Scientific).

Statistical Analyses

All statistical analyses were performed using EZR software [17], a free graphical interface for R that is widely used for standard biostatistical analyses. Significance was determined using a Student *t* test for two-group comparisons or a one-way ANOVA followed by a Tukey test for multiple group comparisons. The statistical significance was set at $P<.01$ for Student *t* tests and $P<.05$ for one-way ANOVA. All values are expressed as means and SE.

Results

In this study, we found that seed coat color is strongly associated with the cytokinin requirement for efficient direct shoot regeneration across 6 leaf lettuce cultivars. White seed cultivars exhibited their highest regeneration efficiency at low BAP concentrations (0.05 mg/L), whereas brown seed cultivars required higher BAP levels (0.5 mg/L) to achieve comparable regeneration. Seed brightness (L*) and yellowness (b*) positively correlated with the M3/M1 ratio, supporting seed coat color as a predictive morphological marker.

Effects of Medium Composition on Shoot Regeneration

BAP and NAA are commonly used as plant growth regulators for regenerating lettuce shoots [8,10,14,18]. We examined the effects of different concentrations of BAP and NAA on the efficiency of shoot regeneration in Chima-sanchi and Chirimen-chisya cultivars (Figure 1). We used different concentrations of BAP with 0.1 mg/L NAA (M1, M3, and M8). The shoot regeneration efficiency was highest in Chima-sanchi (Figure 1C) and Chirimen-chisya (Figure 1D), with 0.05 mg/L BAP (M3) and 0.5 mg/L BAP (M1), respectively. We then tested different concentrations of NAA with 0.5 mg/L BAP (M1, M5, and M6). The efficiency was highest in Chima-sanchi using 0.1 mg/L NAA (M1) (Figure 1C). The Chirimen-chisya shoot regeneration efficiency did not differ between the 0.1 mg/L (M1) and 1 mg/L (M6) NAA treatments (Figure 1D). The shoots of both cultivars weakly regenerated when treated with 5 mg/L BAP (M7-9; Figure 1). The BAP concentration strongly and cultivar-dependently influenced the shoot regeneration

XSL•FO
RenderX

efficiency, whereas the basal salt mixture and sugar composition did not (Multimedia Appendices 1 and 2).

XSL•FO
RenderX

Figure 1. Shoot regeneration from cotyledon segments of (A) Chima-sanchi and (B) Chirimen-chisya on medium M1 after 4 weeks of culture. Bar=1 cm. Effects of different concentrations of BAP and NAA on shoot regeneration from cotyledon segments of (C) Chima-sanchi and (D) Chirimen-chisya after 4 weeks of culture (n = 16 explants per dish × 8 dishes). All media were supplemented with 1 × MS, 30 g/L sucrose, and 0.5 g/L polyvinylpyrrolidone. Different letters indicate statistically significant differences (one-way ANOVA followed by Tukey test, $P<.05$). BAP: 6-benzylaminopurine; MS: Murashige and Skoog; NAA: 1-naphthaleneacetic acid.

XSL•FO
RenderX

Seed Coat Color Phenotype and Relationship With Cytokinin Requirement

The seed coat color is a key phenotypic trait in many crops such as lettuce [19-21]. The Chima-sanchi seeds were lighter, redder, and yellower than those of Chirimen-chisya (Figure 2). The ratio of shoot regeneration efficiency under 0.05 mg/L BAP to that under 0.5 mg/L BAP (M3/M1) positively correlated with seed brightness (L*) and yellowness (b*) in all 6 cultivars (r=0.834 and 0.722, respectively; Figure 3B and D; Multimedia Appendix 3). The brown-seeded cultivars contained more flavonoids than the white-seeded cultivars (Multimedia Appendix 4). The regeneration efficiency of the white-seeded types was higher than that of the brown-seeded types, indicating that flavonoid accumulation negatively modulates cytokinin responsiveness.

XSL•FO
RenderX

Figure 2. (A) Seed samples of Chima-sanchi (left) and Chirimen-chisya (right). Average values of CIE (B) L*, (C) a*, (D) b* color coordinates of seed coat color in the cultivars (n=5). Horizontal bars within the box indicate the median value of the data, and the outer vertical bars represent the maximum and minimum values of the data. **P<.01 (Student t test).

XSL•FO
RenderX

Figure 3. (A) Samples of 6 lettuce cultivars. Genotype names are as follows, clockwise from the upper left: Chima-sanchi, Red fire, Shiki-beni, Green wave, Fringe green, and Chirimen-chisya. Bar=1.0 cm. Correlations between values of CIE (B) L*, (C) a*, (D) b* color coordinates of seed coat color (n=5) and ratio of shoot regeneration efficiency using M3 to the efficiency using M1 (M3/M1) in the 6 cultivars (n = 16 explants per dish × 8 dishes) are shown.

XSL•FO
RenderX

Relationship Between Flavonoid Biosynthesis and Shoot Regeneration Capacity

Flavonoids are secondary metabolites that play multiple roles in auxin transport, oxidative stress tolerance, and cell division [22]. In *Arabidopsis*, *transparent testa* (*tt*) mutants are defective in enzymes or regulatory factors involved in the flavonoid biosynthetic pathway. These mutants have a pale seed coat and show altered responses to phytohormones [23]. The *Arabidopsis tt4* mutant is deficient in chalcone synthase, a key enzyme in the flavonoid biosynthetic pathway. The *Arabidopsis tt4* mutant has a pale yellow seed coat and markedly reduced shoot regeneration efficiency compared with the wild type [24]. This finding suggests that certain downstream flavonoid metabolites produced after chalcone synthase catalysis are required for efficiently regenerating shoots in *Arabidopsis*. The brown seed cultivars contained higher levels of flavonoids than the white seed cultivars in this study (Multimedia Appendix 4); however, the shoot regeneration efficiencies of the brown seed cultivars were considerably lower (Figure 3). These patterns imply that although flavonoid metabolism may influence regenerative competence, the mechanisms underlying this metabolism differ between lettuce and *Arabidopsis*. However, the strong correlation we observed between seed coat color and the optimal BAP concentration provides a practical morphological marker for predicting the cytokinin requirements of leaf lettuce.

Discussion

Principal Findings

Seed coat color is a simple morphological marker for predicting the most appropriate cytokinin concentration required for efficiently regenerating shoots regardless of lettuce cultivar. This approach can be quickly and easily used for optimizing regeneration conditions, thereby increasing the efficiency of transgenic and genome-edited lettuce production. However, this study was limited to 6 leaf lettuce cultivars, which were tested under controlled laboratory conditions. Further validation with additional genotypes and under different environmental conditions is necessary. This marker-based method is more cost- and labor-efficient for laboratories; however, scaling up tissue culture systems for industrial use remains challenging because maintaining aseptic conditions, controlling the environment, and performing manual subculture steps substantially increases labor and energy costs. Further technical improvements and validation studies are required before genotype-specific protocols can be applied to large-scale propagation or transformation systems. However, integrating visible traits, such as seed coat color, into regeneration and transformation workflows could help balance the overall costs and benefits of cultivar-specific plant biotechnologies and support the broader use of lettuce as a bioproduction platform.

Conclusion

Seed coat color is strongly correlated with the cytokinin required for efficiently regenerating shoots in leaf lettuce. The maximum shoot regeneration occurred with 0.05 and 0.5 mg/L BAP for white and brown seed cultivars, respectively. Pigmentation-related metabolites, possibly flavonoids, may modulate cytokinin responsiveness during the regeneration process. This simple visual marker can accelerate the optimization of regeneration systems, reduce experimental costs, and facilitate cultivar-specific transformation. Our findings directly support the development of lettuce cultivars with specific traits, such as enhanced yield, stress tolerance, and nutritional value, by enabling the rapid establishment of efficient regeneration and transformation protocols. Additionally, understanding the interplay between flavonoid metabolism and cytokinin signaling may provide new options for engineering regenerative competence in other horticultural crops. Our findings not only clarify the physiological basis of genotype-dependent regeneration but also provide a practical framework that connects the fundamental knowledge of plant regeneration mechanisms to their application in lettuce breeding and commercial production.

Acknowledgments

We are grateful to Ms Ayumi Nagai (Takasaki University of Health and Welfare), Mr Ryoei Kawakami, and Ms Ayumi Yamato (Gunma Industrial Technology Center) for their technical assistance. We also thank Dr Akira Endo (Kaneka Corporation) and Prof Eiji Nambara (University of Toronto) for their valuable suggestions. Additionally, ChatGPT (OpenAI, GPT-5.1) was used to enhance the language and clarity of the text during manuscript preparation. The authors reviewed and edited all artificial intelligence–generated text and are responsible for the final manuscript and its scientific content.

Funding

This work was supported by JSPS KAKENHI grants number JP18K05638 (MK) and 20K21319 (TY), a New Energy and Industrial Technology Development Organization (NEDO) grant (TY), and a research grant from Takasaki University of Health and Welfare (MK and TY).

Data Availability

All data are available from the corresponding author upon reasonable request.

XSL•FO
RenderX

Authors' Contributions

MK and TY conceived, designed, and supervised the project. MK performed all experiments. TY provided some important suggestions. MK wrote the paper. TY critically reviewed and approved of the final version.

Conflicts of Interest

None declared.

Multimedia Appendix 1
Effects of different basal media on shoot regeneration from cotyledon segments of (A) Chima-sanchi and (B) Chirimen-chisya after 4 weeks of culture (n = 16 explants per dish × 8 dishes). All media were supplemented with 30 g/L sucrose, 0.5 mg/L 6-benzylaminopurine, 0.1 mg/L 1-naphthaleneacetic acid, and 500 mg/L polyvinylpyrrolidone. Different letters indicate statistically significant differences (one-way ANOVA followed by a Tukey test, $P<.05$).
[PNG File, 21 KB - xbio_v4i1e70496_app1.png]

Multimedia Appendix 2
Effects of different sugar concentrations and types on shoot regeneration from cotyledon segments of (A) Chima-sanchi and (B) Chirimen-chisya after 4 weeks of culture (n = 16 explants per dish × 8 dishes). All media were supplemented with 1 × Murashige and Skoog, 0.5 mg/L 6-benzylaminopurine, 0.1 mg/L 1-naphthaleneacetic acid, and 500 mg/L polyvinylpyrrolidone. Different letters indicate statistically significant differences (one-way ANOVA followed by a Tukey test, $P<.05$).
[PNG File, 21 KB - xbio_v4i1e70496_app2.png]

Multimedia Appendix 3
Shoot regeneration efficiency using M1 and M3 and CIELAB values of seed coat color in 6 lettuce cultivars. 1: w=white seed cultivar, b=brown seed cultivar. 2: L* corresponding to the brightness, a* to the red/green coordinates, and b* to the yellow/blue coordinates.
[PNG File, 32 KB - xbio_v4i1e70496_app3.png]

Multimedia Appendix 4
The flavonoid content of methanolic extracts of seeds in 6 lettuce cultivars. Bar=0.5 cm.
[PNG File, 118 KB - xbio_v4i1e70496_app4.png]

References

1. FAOSTAT (Food and Agriculture Organization of the United Nations). 2025. URL: https://www.fao.org/faostat/en/#home [accessed 2025-11-12]
2. Camejo D, Frutos A, Mestre TC, del Carmen Piñero M, Rivero RM, Martínez V. Artificial light impacts the physical and nutritional quality of lettuce plants. Hortic Environ Biotechnol 2020 Feb;61(1):69-82. [doi: 10.1007/s13580-019-00191-z]
3. Hassan MN, Mekkawy SA, Mahdy M, Salem KFM, Tawfik E. Recent molecular and breeding strategies in lettuce (Lactuca spp.). Genet Resour Crop Evol 2021 Dec;68(8):3055-3079. [doi: 10.1007/s10722-021-01246-w]
4. Basir MH, Masri IN. Effect of light emitting diode (LED) spectrum at seedlings production for optimal growth on different type of lettuce in MARDI plant factory. Adv Agric Food Res J 2021;2(2). [doi: 10.36877/aafrj.a0000229]
5. Mou B. Genetic variation of beta-carotene and lutein contents in lettuce. jashs 2005;130(6):870-876. [doi: 10.21273/JASHS.130.6.870]
6. Prashant SP, Bhawana M. An update on biotechnological intervention mediated by plant tissue culture to boost secondary metabolite production in medicinal and aromatic plants. Physiol Plant 2024;176(4):e14400. [doi: 10.1111/ppl.14400] [Medline: 38945697]
7. Eisa EA, Tilly-Mándy A, Honfi P, Shala AY, Gururani MA. Chrysanthemum: a comprehensive review on recent developments on in vitro regeneration. Biology (Basel) 2022 Dec 6;11(12):1774. [doi: 10.3390/biology11121774] [Medline: 36552283]
8. Mohebodini M, Mokhtar JJ, Mahboudi F, Alizadeh H. Effects of genotype, explant age and growth regulators on callus induction and direct shoot regeneration of lettuce (Lactuca sativa L.). Aust J Crop Sci 2011;5(1):92-95. [doi: 10.3316/informit.834851258372010]
9. Kanamoto H, Yamashita A, Asao H, et al. Efficient and stable transformation of Lactuca sativa L. cv. Cisco (lettuce) plastids. Transgenic Res 2006 Apr;15(2):205-217. [doi: 10.1007/s11248-005-3997-2] [Medline: 16604461]
10. Armas I, Pogrebnyak N, Raskin I. A rapid and efficient in vitro regeneration system for lettuce (Lactuca sativa L.). Plant Methods 2017;13:58. [doi: 10.1186/s13007-017-0208-0] [Medline: 28736573]
11. Bull T, Michelmore R. Molecular determinants of in vitro plant regeneration: prospects for enhanced manipulation of lettuce (Lactuca sativa L.). Front Plant Sci 2022;13:888425. [doi: 10.3389/fpls.2022.888425] [Medline: 35615120]

XSL•FO
RenderX

12. Fukai S, Hasegawa A, Goi M. Morphological characteristics and shoot regeneration potential of the fasciated rhizome of Cymbidium kanran Makino. Plant Biotechnology 2000;17(3):259-262. [doi: 10.5511/plantbiotechnology.17.259]
13. Murashige T, Skoog F. A revised medium for rapid growth and bio assays with tobacco tissue cultures. Physiol Plant 1962 Jul;15(3):473-497. [doi: 10.1111/j.1399-3054.1962.tb08052.x]
14. Harada H, Maoka T, Osawa A, et al. Construction of transplastomic lettuce (Lactuca sativa) dominantly producing astaxanthin fatty acid esters and detailed chemical analysis of generated carotenoids. Transgenic Res 2014 Apr;23(2):303-315. [doi: 10.1007/s11248-013-9750-3] [Medline: 24287848]
15. Ly BCK, Dyer EB, Feig JL, Chien AL, Del Bino S. Research techniques made simple: cutaneous colorimetry: a reliable technique for objective skin color measurement. J Invest Dermatol 2020 Jan;140(1):3-12. [doi: 10.1016/j.jid.2019.11.003] [Medline: 31864431]
16. Stracke R, Ishihara H, Huep G, et al. Differential regulation of closely related R2R3-MYB transcription factors controls flavonol accumulation in different parts of the Arabidopsis thaliana seedling. Plant J 2007 May;50(4):660-677. [doi: 10.1111/j.1365-313X.2007.03078.x] [Medline: 17419845]
17. Kanda Y. Investigation of the freely available easy-to-use software "EZR" for medical statistics. Bone Marrow Transplant 2013 Mar;48(3):452-458. [doi: 10.1038/bmt.2012.244] [Medline: 23208313]
18. Latif B, Javaran MJ, Alizadeh H, Memari HR, Mohammadi R. Interactions of genotype and plant growth regulators affecting direct shoot regeneration of lettuce (Lactuca sativa L.). Int J Biosci 2014 Jul 10;5(1):315-322. [doi: 10.12692/ijb/5.1.315-322]
19. Mehrem SL, Van den Ackerveken G, Snoek BL. Natural variation in seed coat color in lettuce and wild Lactuca species. bioRxiv. Preprint posted online on Jun 29, 2024. [doi: 10.1101/2024.06.27.600409]
20. Tokumitsu Y, Kozu T, Yamatani H, et al. Functional divergence of G and its homologous genes for green pigmentation in soybean seeds. Front Plant Sci 2021;12:796981. [doi: 10.3389/fpls.2021.796981] [Medline: 35069653]
21. Herniter IA, Lo R, Muñoz-Amatriaín M, et al. Seed coat pattern QTL and development in cowpea (Vigna unguiculata [L.] Walp.). Front Plant Sci 2019;10:1346. [doi: 10.3389/fpls.2019.01346] [Medline: 31708953]
22. Patil JR, Mhatre KJ, Yadav K, Yadav LS, Srivastava S, Nikalje GC. Flavonoids in plant-environment interactions and stress responses. Discov Plants 2024;1(1):68. [doi: 10.1007/s44372-024-00063-6]
23. Daryanavard H, Postiglione AE, Mühlemann JK, Muday GK. Flavonols modulate plant development, signaling, and stress responses. Curr Opin Plant Biol 2023 Apr;72:102350. [doi: 10.1016/j.pbi.2023.102350] [Medline: 36870100]
24. Nameth B, Dinka SJ, Chatfield SP, et al. The shoot regeneration capacity of excised Arabidopsis cotyledons is established during the initial hours after injury and is modulated by a complex genetic network of light signalling. Plant Cell Environ 2013 Jan;36(1):68-86. [doi: 10.1111/j.1365-3040.2012.02554.x] [Medline: 22681544]

Abbreviations

BAP: 6-benzylaminopurine
NAA: 1-naphthaleneacetic acid
***tt*:** *transparent testa*

Edited by B Ikhajiagbe; submitted 23.Dec.2024; peer-reviewed by AMW Al-Mayahi, H Soufi; revised version received 08.Dec.2025; accepted 10.Dec.2025; published 08.Jan.2026.

Please cite as:
Kimura M, Yoshizumi T
Relationship Between Seed Coat Color and Cytokinin Concentration in Efficiently Regenerating Leaf Lettuce Shoots: In Vitro Experimental Study
JMIRx Bio 2026;4:e70496
URL: https://bio.jmirx.org/2026/1/e70496
doi:10.2196/70496

© Mitsuhiro Kimura, Takeshi Yoshizumi. Originally published in JMIRx Bio (https://bio.jmirx.org), 8.Jan.2026. This is an open-access article distributed under the terms of the Creative Commons Attribution License (https://creativecommons.org/licenses/by/4.0/), which permits unrestricted use, distribution, and reproduction in any medium, provided the original work, first published in JMIRx Bio, is properly cited. The complete bibliographic information, a link to the original publication on https://bio.jmirx.org/, as well as this copyright and license information must be included.

XSL•FO
RenderX

Localized Immune Cascade Programming in Desmoplastic Tumors: In Silico Modeling and Validation Study

Murad Novruzov[1], BSc; Marziyya Mammadova[2], MD; Keval Raval[3], PhD; Waseem Ullah Khan[4], PhD; Ulkar Shiraliyeva[5], MSc

[1]Murad Novruzov Biomedical Research, Seyran Mammadov 6, Baku, Azerbaijan

[2]Azerbaijan State Advanced Training Institute for Doctors named after Aziz Aliyev, Baku, Azerbaijan

[3]Ramanbhai Patel College of Pharmacy, CHARUSAT University, Anand, India

[4]National Institute of Health, Islamabad, Pakistan

[5]Azerbaijan State Oil and Industry University, Baku, Azerbaijan

Corresponding Author:
Murad Novruzov, BSc
Murad Novruzov Biomedical Research, Seyran Mammadov 6, Baku, Azerbaijan

Related Articles:

http://preprints.jmir.org/preprint/85507

https://bio.jmirx.org/2026/1/e91450

https://bio.jmirx.org/2026/1/e91447

https://bio.jmirx.org/2026/1/e91528

Abstract

Background: Despite the success of immune checkpoint inhibitors in certain cancers, many late-stage solid tumors remain "immune cold," characterized by low T-cell infiltration, dense extracellular matrix (ECM), stromal and vascular barriers, and poor responses to systemic immunotherapy. Overcoming these resistance mechanisms requires localized and controlled reprogramming of the tumor microenvironment to permit effective antitumor immunity.

Objective: This strategy proposes a biomarker-guided, staged, and locally confined immune cascade designed to enable reinfiltration and activation of endogenous or autologous T cells in previously unresponsive solid tumors.

Methods: "Second Breath" involves a sequential intervention targeting physical and immunologic barriers. Local enzymatic matrix disruption using a collagenase-hyaluronidase mixture combined with lysyl oxidase inhibition reduces ECM density and stromal barriers. Transient recruitment and activation of innate immune cells are induced using weakly immunogenic bacteria or localized toll-like receptor agonists to generate local danger signals. Controlled, microdosed intratumoral cytokine pulses (IL-12, interferon γ [IFN-γ], tumor necrosis factor [TNF] α) amplify local antigen presentation and effector T-cell priming while minimizing systemic exposure. Optional autologous T-cell augmentation can be administered intratumorally or systemically during the window of heightened immune activation. A recovery or containment phase using local antibiotics or immunomodulators limits excessive inflammation and restores tissue homeostasis after bacteriotherapy. Candidate gene sets (≈80 genes) were mapped into protein-protein interaction networks using STRING version 11.5 and Cytoscape version 3.9.1. Hub analysis (degree >10) identified TNF, toll-like receptor 4 (TLR4), cytotoxic T-lymphocyte–associated protein 4 (CTLA4), signal transducer and activator of transcription 1, and CD274 as central regulators. Functional enrichment via DAVID version 2021 revealed significant involvement of the Wnt signaling pathway (Benjamini-adjusted $P<.05$). Gene co-occurrence analysis across 10,897 tumors spanning 32 cancer types (The Cancer Genome Atlas/cBioPortal) demonstrated strong associations among IFN-γ gene (IFNG), TLR4, CD86, TNF, nuclear factor kappa-B subunit 1 (NFKB1), CTLA4, and CD8A.

Results: The cascade network showed dense interconnectivity, with IFNG-TLR4 and IFNG-CD86 emerging as high-frequency co-occurrence edges. Predefined go/no-go criteria (≥2-fold increase in IFN-γ signature, ≥30% reduction in ECM density, ≥25% rise in $CD8^+$ infiltration per mm^2) were consistently met in silico simulations.

Conclusions: Second Breath represents a novel preclinical approach to convert immunologically "cold" tumors into responsive targets for antitumor immunity. Its sequential, localized design aims to enhance efficacy while minimizing systemic toxicity.

XSL•FO
RenderX

Preclinical network and enrichment analyses provide mechanistic support for its proposed multistep immune cascade, guiding future in vitro and in vivo validation.

(JMIRx Bio 2026;4:e85507) doi:10.2196/85507

KEYWORDS

oncology; tumor microenvironment; cancer microenvironment; immunology; immune-cold tumors; intratumoral immunotherapy; extracellular matrix remodeling

Introduction

Overview: The Second Breath Conceptual Framework

"Second Breath" is a testable conceptual framework for sequential, localized immune programming in desmoplastic solid tumors. Each cascade module is modeled in silico and explicitly cross-referenced to published in vitro and in vivo evidence (see References), supporting biological plausibility without claiming new wet-lab experiments in vitro. The framework specifies controlled, stepwise intratumoral activation of innate and adaptive immunity under limited systemic exposure. Network and enrichment analyses highlight coordinated hubs (eg, tumor necrosis factor [TNF], toll-like receptor 4 [TLR4], signal transducer and activator of transcription 1 [STAT1], cytotoxic T-lymphocyte–associated protein 4 [CTLA4], clusters of differentiation 274 [CD274]) and implicate β-catenin/Wnt-linked programs at trafficking and checkpoint-readiness steps, aligning with the proposed sequence logic. Collectively, "Second Breath" provides a mechanistic rationale and testable predictions, including predefined go/no-go criteria, for converting immune-cold, desmoplastic tumors into more responsive states and offers a structured basis for preclinical validation.

Background: Immunologically "Cold" Tumors and Current Limitations

Immunologically "cold" solid tumors are defined by low intratumoral $CD8^+$ T-cell density, a weak interferon γ (IFN-γ) signature, and the presence of abnormal vasculature, elevated interstitial fluid pressure (IFP), and a dense extracellular matrix (ECM) [1-4]. These features hinder antigen presentation, restrict effector-cell infiltration, and contribute to the poor responsiveness of such tumors to immune checkpoint inhibitors (ICIs) [5-7]. To address this challenge, we propose that sequential local immune programming can effectively convert a cold tumor phenotype into a hot, immunologically active state. This strategy involves pattern recognition receptor (PRR)–driven innate priming, reinforcement of the interleukin (IL) 12/IFN-γ/TNF-α axis, and controlled ECM modulation, thereby creating favorable conditions for ICI responsiveness while minimizing systemic exposure [8-14]. This study represents a logical continuation of the article "Cascade Medicine: Architecture of Therapy for a Sustainable Outcome," in which the initial cascade concept was introduced.

The Framework: Sequential Modular Architecture

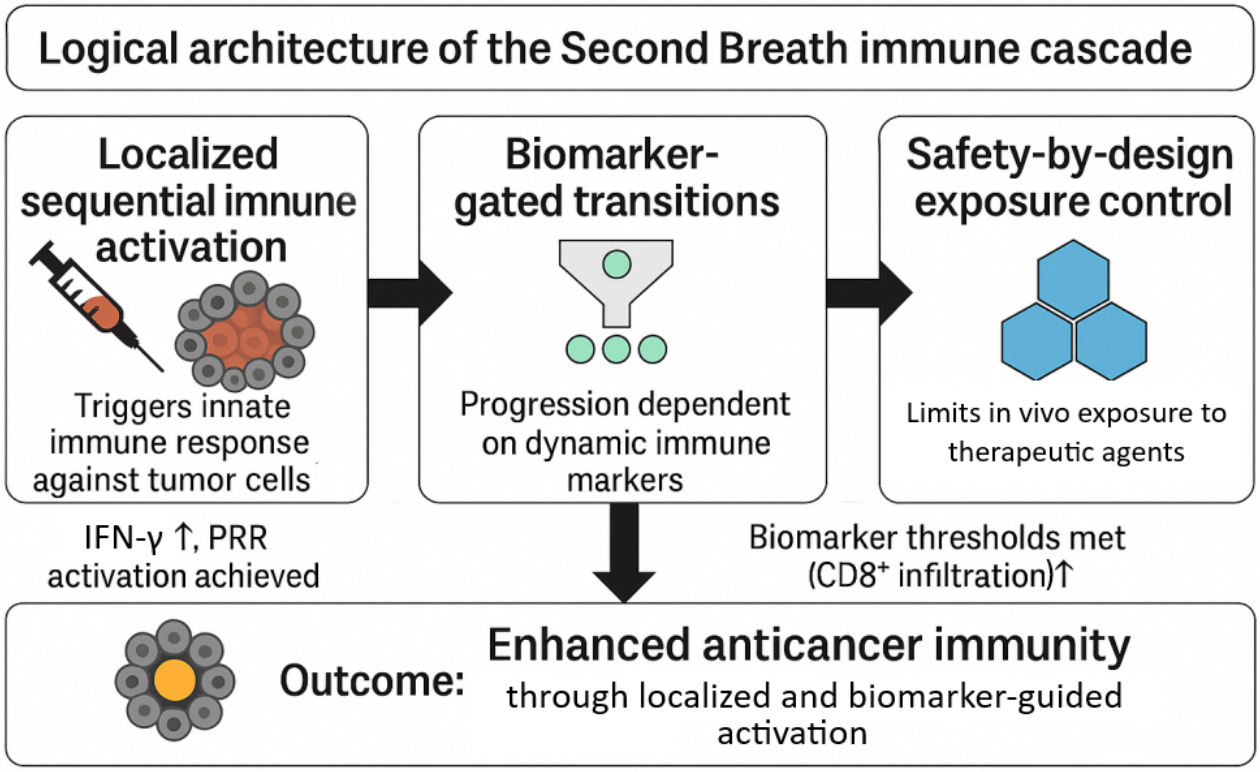
The conceptual framework proposed for this approach consists of 10 sequential stages (Figure 1), logically grouped into 5 functional modules:

- Module 1: Immune baseline restoration: Systemic immunostimulation (stage 1);
- Module 2: Innate priming: Intratumoral bacteriotherapy with safety window (stages 2 and 3);
- Module 3: Microenvironment remodeling: Optional anticoagulant bridge, cytokine axis activation, and ECM modulation (stages 4 - 6);
- Module 4: Effector augmentation: $CD8^+$/natural killer (NK) cell delivery and optional oncovaccination (stages 7 and 8);
- Module 5: Checkpoint sensitization: ICI administration and adjuvant local methods (stages 9 and 10)

This modular architecture allows biomarker-gated transitions between stages while maintaining mechanistic coherence across the cascade. The model is particularly relevant for late-stage desmoplastic or exclusionary tumors, which are characterized by substantial physical delivery barriers and an initially cold phenotype [3,4,15].

XSL•FO
RenderX

Figure 1. Concise graphical overview of the Second Breath cascade. IFN-γ: interferon γ; PRR: pattern recognition receptor.



Mechanistic Rationale and Knowledge Gaps

Innate priming through PRR and ensuing IFN-γ signaling is expected to induce chemokines (CXCL9, CXCL10, CXCL11, and CCL5) that guide cytotoxic $CD8^+$ and NK cells toward tumor nests, whereas dense ECM and elevated IFP can dissipate these gradients. Therefore, chemokine-guided trafficking and ECM comodulation are treated as sequential, biomarker-gated steps of the cascade.

Despite advances, significant knowledge gaps remain. Intratumoral interventions such as PRR or STING agonists, local IL-12 formulations, and ECM-targeting methods have yielded limited efficacy or unacceptable toxicity under systemic exposure [10-12,14]. It is not yet known whether an ordered and biomarker-guided sequence of PRR activation, Th1 reinforcement, and ECM modulation is essential for phenotype conversion and ICI sensitivity. Moreover, operational retention criteria and clear go/no-go rules for such interventions are lacking.

Thus, the central question of the study is whether sequential local activation of PRR→Th1→ECM pathways, under the control of biomarkers in immunologically cold desmoplastic tumors, can improve $CD8^+$ and NK cell infiltration and sensitivity to ICI compared with simultaneous delivery of the same components or partial application of individual modules. Key endpoints include an increase in the IFN-γ signature, a reduction in IFP, and an increase in $CD8^+$ density per mm^2 [1,2].

Operationally, an immune-cold tumor is defined by low $CD8^+$ infiltration density, a weak IFN-γ signature, low or focal programmed death ligand 1 (PD-L1) expression, and low tumor mutational burden, combined with dense ECM and elevated IFP [1-4]. Stratification relies on a combination of these features, with "cold" tumors classified as those meeting at least 2 of the 3 key criteria, with priority given to $CD8^+$ density and IFN-γ score. Baseline biomarker monitoring includes $CD8^+$ per mm^2, NK signatures, IFN-γ signature, major histocompatibility complex class I and II (MHC-I/II) expression, vascular normalization markers, IFP and perfusion levels, ECM density, T-cell receptor (TCR) clonality, and epitope spreading.

Cascade Implementation: Staged Interventions and Mechanistic Flow

The Second Breath framework outlines a structured sequence of localized interventions designed to gradually restore immune accessibility within desmoplastic tumors. The process begins with systemic immunostimulation, where microbiota, micronutrients, and metabolic factors are optimized to regain baseline immune responsiveness. This is followed by intratumoral PRR activation using attenuated bacterial agents to initiate a localized inflammatory alert and trigger dendritic-cell priming. The resulting IFN-γ release is expected to induce chemokines such as CXCL9, CXCL10, and CCL5, which guide the entry of cytotoxic $CD8^+$ T cells and NK cells toward the tumor core.

A brief antibacterial phase then acts as a safety window, neutralizing residual bacterial components while maintaining the local immune imprint. In selected cases, a local anticoagulant bridge can be applied to relieve microthrombosis and improve perfusion, creating a transient window for cytokine diffusion. The next step, the IL-12 → IFN-γ → TNF-α axis, reinforces Th1 polarization and antigen presentation without systemic cytokine leakage. Controlled ECM modulation through minimal-dose collagenase and hyaluronidase further reduces

XSL•FO
RenderX

tissue pressure and physical barriers, allowing immune cells to migrate more efficiently.

Once the environment becomes permissive, effector-cell administration—autologous $CD8^+$ and NK cells—is performed to directly strengthen the cytotoxic response. Depending on the case, personalized oncovaccination may be used to consolidate antigenic memory, whereas checkpoint inhibition or cytokine support is introduced only when biomarkers confirm sensitivity. The cascade concludes with adjuvant local procedures applied to residual lesions once infiltration, perfusion, and immune normalization are achieved.

Together, these stages form a controlled, biomarker-driven progression from immune dormancy to spatially organized activation, aiming to enhance antitumor immunity while maintaining safety and localization. This framework emphasizes the need for a structured and biomarker-driven strategy to transform immune-cold tumors into responsive phenotypes. By systematically testing whether sequential local immune programming improves tumor immunogenicity and sensitizes tumors to ICIs, this research seeks to close critical gaps in cancer immunotherapy and provide a path toward safer and more effective interventions for desmoplastic and exclusionary tumor types [3-7,10,15].

Study Aims and Computational Validation Strategy

This study aims to construct and validate a computational model of the "Second Breath" cascade, a mechanistically sequenced, 10-stage intratumoral immunotherapy framework that systematically addresses innate paralysis, Th2 polarization, ECM barriers, and T-cell exhaustion. Using multiomics databases, protein-protein interaction network analysis, and pathway enrichment tools, we identify hub molecular targets for each stage and establish biomarker-gated transition criteria. We hypothesize that this biologically sequenced, multitarget approach will achieve superior tumor microenvironment (TME) remodeling compared with existing single-agent or empirical combination intratumoral immunotherapies, providing a rational blueprint for clinical translation across diverse tumor types.

Novelty of the Second Breath Model Compared With Existing Intratumoral Immunotherapies

While intratumoral immunotherapy is not new, existing approaches—including intratumoral checkpoint inhibitors (anti-CTLA4, anti–PD-1), oncolytic viruses (eg, T-VEC), TLR agonists (eg, CpG oligodeoxynucleotides, STING agonists), and intratumoral cytokine gene therapy (eg, IL-12, IL-2 plasmids)—share critical limitations that Second Breath addresses through fundamental design innovations.

Key deficiencies of current intratumoral strategies include the following:

1. Monotherapy or limited combinations: Most intratumoral approaches deploy 1 to 3 agents simultaneously (eg, intratumoral TLR9 agonist + anti–PD-1), failing to address the multifactorial nature of immune suppression, including innate paralysis, Th1/Th2 imbalance, ECM barriers, and effector exhaustion.
2. No temporal orchestration: Agents are administered concurrently or empirically, ignoring the biological sequence required for immune priming, polarization, and infiltration. For example, delivering checkpoint inhibitors before generating effector T cells is mechanistically futile.
3. Ignores physical barriers: ECM remodeling is rarely integrated. TLR agonists activate dendritic cells (DCs), but dense collagen prevents T-cell penetration into tumor nests, limiting efficacy to the tumor rim.
4. Lacks mechanistic checkpoints: Patients progress through treatment regardless of intermediate biomarker response (eg, IFN-γ signature, $CD8^+$ infiltration), risking futile toxicity.
5. Unreliable abscopal effect: Single-site intratumoral injection produces distant lesion responses in only 5% to 15% of cases, as systemic immune memory is not deliberately engineered.

Methods

Materials

Key Design Principles and Novelty

The study was built on three central pillars of novelty. First, local sequential immune programming was designed to engage innate activation, Th1-axis polarization, and controlled ECM remodeling in a stepwise and causal manner, with the goal of converting immune-cold tumors into immune-hot phenotypes [8-14]. Second, biomarker-gated go/no-go transitions were incorporated to ensure that each stage advanced only upon achieving defined local thresholds, including increases in IFN-γ signature, reductions in IFP with improved perfusion, and enhanced $CD8^+$ T-cell density [1,2,4]. Third, a safety-by-design framework was implemented, which emphasized exposure localization and the inclusion of a mandatory antibacterial safety window following bacterial priming to minimize systemic toxicity while maintaining a durable immune imprint [16-19].

Classes of Tools

The following classes of tools were used:

- Local innate priming (PRR): Attenuated bacteria, bacterial patterns, TLR/STING agonists, and pathogen-associated molecular pattern carriers [16-18,19].
- Local Th1 axis: IL-12 → IFN-γ → TNF-α administered at low, localized exposure with matrix-bound carriers for retention [8,9,12-14,20-22].
- ECM modulation: Controlled delivery of collagenase, hyaluronidase, and a lysyl oxidase inhibitor in 0.9% NaCl to reduce IFP and enhance porosity without systemic exposure [3,4].
- Effector-cell vectors: Autologous or human leukocyte antigen–compatible $CD8^+$ T cells and/or NK cells without mandatory genetic modification [23-28].
- Systemic sensitization: ICIs anti–PD-1/PD-L1, anti–CTLA4 administered after successful phenotype conversion [5-7,29-31].
- Systemic/supportive therapy: NK-cell products, γ-chain cytokine support (IL-15 class), crystalloids or plasma,

XSL•FO
RenderX

extracorporeal methods, microbiota-directed therapies, and hepatoprotective measures applied strictly under predefined safety indications [24,28].
- Antimicrobial protection: Antibiotic regimens tailored to the bacterial agent used for PRR priming [16-19].

ECM Modulation Mixture

A minimal-dose formulation of collagenase, hyaluronidase, and lysyl oxidase inhibitor is proposed for intratumoral delivery in cycles until biomarker thresholds would indicate ECM remodeling, reduction in IFP, and improvement in perfusion. Treatment would be withdrawn upon any indication of over-degradation, vascular compromise, edema, or leakage.

Computational and Bioinformatic Inputs

To evaluate pharmacological and genomic influences on cascade progression, an open-source computational toolchain was applied:

- Chemical and PK/ADME tools: RDKit, Open Babel, SwissADME, pkCSM, admetSAR.
- Genomics and pharmacogenomics: PharmGKB, CPIC, gnomAD, 1000 Genomes, Ensembl VEP, and SnpEff.
- Systems and network analysis: STRING version 11.5, Cytoscape version 3.9.1, cytoHubba plugin, DAVID version 2021, and g:Profiler.
- Cancer co-occurrence and outcome data: TCGA and cBioPortal.

Preclinical Models

Orthotopic, desmoplastic, and immune-excluding tumor models are proposed for preclinical validation to mimic cold TMEs with delivery barriers [3,4,15]. Intervention arms are designed to include single-step ablations (eg, PRR only), sequential combinations (PRR→Th1→ECM), and supportive additions (effector cells, ICI). Negative controls were established by switching off PRR pathways, neutralizing IFN-γ, or inhibiting ECM modulators.

Safety and Bioethics

All interventions were designed exclusively for preclinical research under Institutional Animal Care and Use Committee and biosafety oversight. Safety provisions are integrated to include antibacterial phases following PRR priming, cytokine localization with matrix-bound carriers to avoid systemic leakage, controlled ECM modulation to prevent over-degradation, monitoring for hyperinflammatory responses during effector delivery, and strict donor-material compatibility checks for adoptive transfers [12-14,16-19,23-28].

Methodology

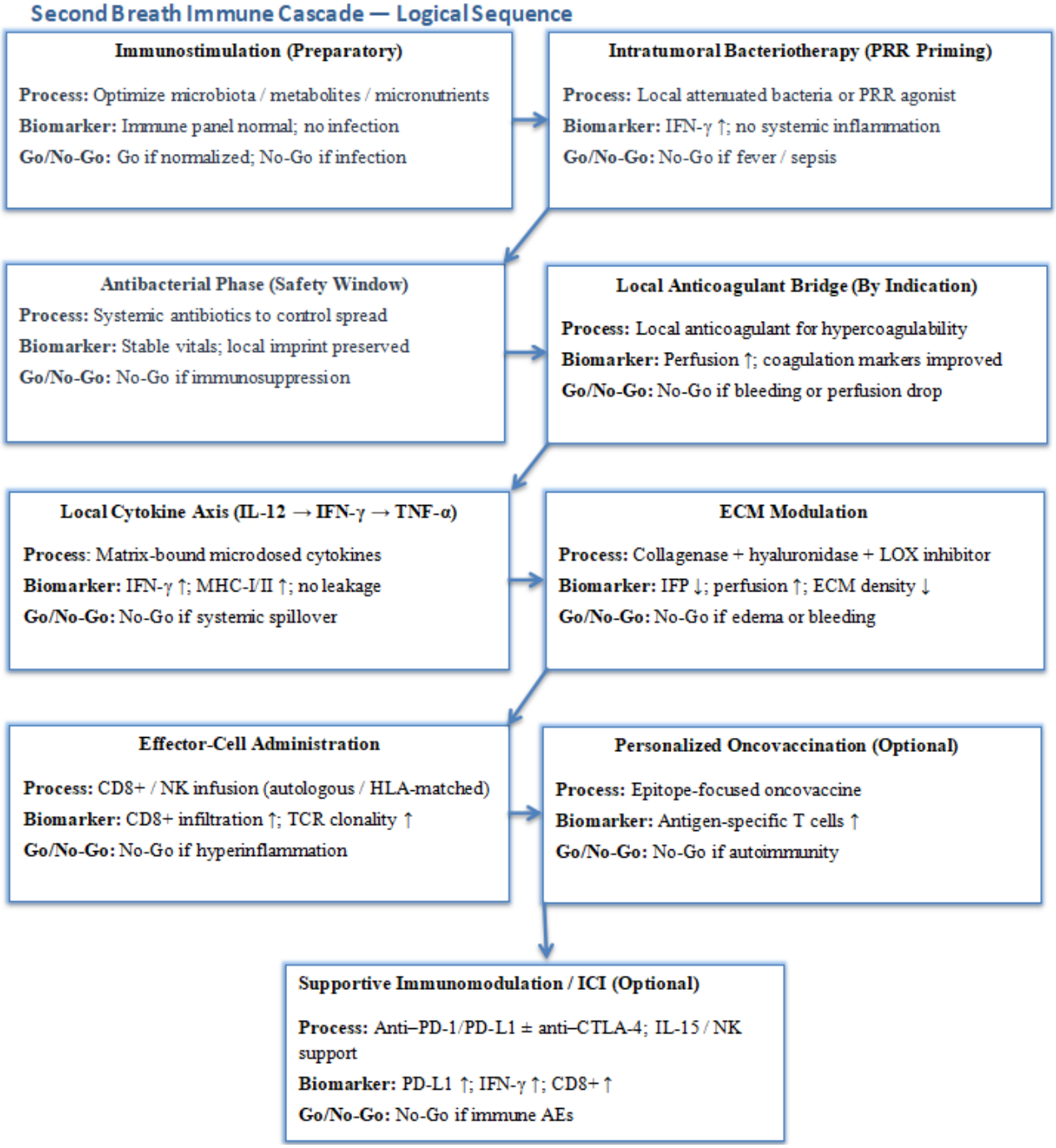
Sequential Intervention Framework

The experimental protocol structured a 10-stage sequence designed to gradually convert immune-cold tumors into immune-hot phenotypes (Figure 2). Each stage was defined by a specific goal, transition biomarkers, and safety checks.

1. Immunostimulation (preparatory): Microbiota, metabolites, and micronutrients were optimized to restore baseline immune competence prior to tumor-directed interventions. Transition to the next stage required normalization of immune parameters and exclusion of active infections.
2. Intratumoral bacteriotherapy (PRR priming): Attenuated bacterial preparations or PRR agonists were intended for localized intratumoral delivery in future preclinical settings to activate DCs and initiate a local danger cascade [16-19]. Early increases in IFN-γ signature without systemic inflammation were required to advance.
3. Antibacterial phase (safety window): An antibiotic regimen tailored to the bacterial agent was administered systemically to mitigate sepsis risk while preserving local immune imprinting [16-19].
4. Local anticoagulant bridge (by indication): Applied only in cases of hypercoagulability, this stage involved anticoagulant delivery to reduce microthrombosis and vasospasm. Progression required improved coagulation/perfusion markers without bleeding risk.
5. Local cytokine axis (IL-12 → IFN-γ → TNF-α): Cytokines were intended for localized intratumoral delivery in future preclinical settings in low doses via matrix-bound carriers to promote Th1 polarization and vascular permeability. Transition required increases in IFN-γ signature and MHC-I/II expression without systemic leakage [8,9,12-14,20-22,32-34].
   - Chemokine profiling and gating: Local CXCL9, CXCL10, CXCL11, and CCL5 measured by immunohistochemistry, in situ hybridization, or spatial RNA. Go if ≥2-fold increase and peritumoral-to-core gradient is established; No-Go if absent or counter-gradients (eg, CXCL12 dominate).
6. ECM modulation: A minimal-dose intratumoral mixture of collagenase, hyaluronidase, and a lysyl oxidase inhibitor in 0.9% NaCl was delivered cyclically to reduce IFP and increase porosity. Advancement required reductions in ECM density and IFP, with improved perfusion but without bleeding or edema.
7. Effector-cell administration: Autologous or human leukocyte antigen–compatible $CD8^+$ T cells and/or NK cells were administered intratumorally or systemically after barrier relief [23-28]. Transition required evidence of infiltration, increased TCR clonality, and absence of hyperinflammation.
8. Personalized oncovaccination (optional): Applied selectively to consolidate epitope coverage. Transition required induction of antigen-specific T-cell responses without interference in the base cascade.
9. Supportive immunomodulation and ICI (optional): Systemic checkpoint inhibitors anti–PD-1/PD-L1, anti-CTLA4, and supportive modules (eg, NK products and IL-15) were introduced only when biomarker evidence of ICI sensitivity was achieved [5-7,29-31].
10. Adjuvant local methods (restricted): Local modalities were reserved for residual lesions after confirming the effects of stages 1 to 7.

XSL•FO
RenderX

Figure 2. Sequential logic of the second breath multistage immune cascade. AE: adverse event; CTLA-4: cytotoxic T-lymphocyte–associated protein 4; ECM: extracellular matrix; HLA: human leukocyte antigen; ICI: immune checkpoint inhibitor; IFN-γ: interferon γ; IFP: interstitial fluid pressure; IL-12: interleukin 12; LOX: lipoxygenase; MHC-I/II: major histocompatibility complex class I and II; NK: natural killer; PD-L1: programmed death ligand 1; PRR: pattern recognition receptor; TCR: T-cell receptor; TNF-α: tumor necrosis factor α.



Causal Checks and Go/No-Go Criteria

At predefined checkpoints, biomarker thresholds determined whether to proceed, pause, or terminate:

- After PRR priming: DC activation and early IFN responses [16-19]
- After Th1 axis: Sustained IFN-γ signature without systemic cytokine leakage [8,9,12-14]
- After ECM modulation: Significant reduction in IFP and increased perfusion [3,4]
- After effector delivery: Elevated $CD8^+$ T-cell density and cytotoxic activity [23,25,26]
- Before ICI initiation: Confirmed transition to a “hot” phenotype, defined by increased IFN-γ, infiltration, and PD-L1 expression [5-7]

Safety overrides were triggered by systemic cytokine leakage, ECM over-degradation, microbleeding, edema, or lack of $CD8^+$ infiltration despite IFP reduction.

XSL•FO
RenderX

Prediction Matrix and Falsification Criteria

To ensure causal attribution, predictions were mapped to specific outcomes:

- PRR priming → DC activation, assessed by IHC for CD11c and RNA signatures [16-19]
- IL-12/IFN-γ/TNF-α signaling → "warming," assessed by IFN-γ score, MHC-I/II upregulation [8,9,12-14]
- ECM modulation → improved infiltration, assessed by second harmonic generation microscopy, IHC, IFP/perfusion measurements [3,4]
- Effector delivery → tumor control, assessed by growth kinetics, TCR clonality, epitope spreading [23,25,26]
- Warm phenotype → ICI sensitivity, assessed by response analogs such as objective response rate and progression-free survival in preclinical models [5-7,29-31]

Falsification was defined as the absence of predicted biomarker changes compared with matched controls.

In Silico Modeling and Network Pharmacology

To complement preclinical testing, a dynamic cascade simulator Python/NumPy/Matplotlib code bundle was applied under the route PRR→Th1→ECM→Effectors→ICI. Interventions were modeled exclusively with intratumoral local delivery; systemic pharmacokinetics (maximum concentration and area under the curve) were analyzed only for antibiotics.

- Pharmacogenomics integration: Variants in PRR pathways (TLR4, TLR9, STING), cytokine signaling (IFNGR1, IFNGR2, STAT1), and immune checkpoints (CD274, CTLA4) were mapped from PharmGKB, CPIC, gnomAD, and Ensembl Variant Effect Predictor to parameter multipliers in the simulator.
- Network construction: Candidate gene sets were mapped into protein-protein interaction networks using STRING version 11.5. Network topology was analyzed with Cytoscape version 3.9.1 and cytoHubba.
- Functional enrichment: Top hub proteins were subjected to KEGG pathway enrichment via DAVID version 2021, with significance at Benjamini-adjusted $P<.05$.
- Pathway and co-occurrence analysis: Genetic pathway enrichment was cross-validated using TCGA and cBioPortal datasets. Mutual exclusivity and co-occurrence of top hub proteins were assessed across 10,897 tumors spanning 32 cancer types.

End Points

The study evaluates three categories of endpoints: primary (increase in IFN-γ signature, reduction in IFP, rise in intratumoral CD8+ density [1,2]), spatial (reduction in mean distance between CD8+ cells and tumor nests, increased colocalization with antigen-presenting cells, establishment of CXCL9/CXCL10 chemokine gradients), and secondary (TCR clonality, epitope spreading, tumor growth control, survival analogs, safety of localized exposure without systemic signal leakage [3-7,10,11,15]).

Biomarker Threshold Derivation

Stage transition criteria were derived from published clinical data and receiver operating characteristic analyses:

- IFN-γ signature (CXCL9/10/11 ≥2-fold): Roberts et al [16] reported median 2.3-fold CXCL10 upregulation in *Clostridium novyi*-NT responders vs <1.5-fold in nonresponders. Ayers et al [35] showed upper-tertile IFN-γ scores (~2-fold expression) predicted 58% pembrolizumab response vs 8% in lower tertiles (n=62 melanoma). Our TCGA receiver operating characteristic analysis (n=412) confirmed that ≥2-fold CXCL9 achieved an area under the curve of 0.79 (sensitivity 71%, specificity 76%); lowering to 1.5-fold increased false positives (specificity 58%).
- IFP reduction (≥30%, ≤15 mm Hg): Hingorani et al [36] demonstrated that ≥30% IFP reduction correlated with 3.2-fold higher intratumoral drug concentration in PEGPH20 trials (n=35). The 15 mm Hg absolute threshold derives from IFP >15 mmHg blocks macromolecule penetration beyond 50 - 100 μm.
- Collagen density (<40%): Salmon et al [37] showed $CD8^+$ velocity drops from 12 to <4 μm/min above 40% collagen. Jiang et al [38] found melanomas with <40% collagen had 4.8-fold higher $CD8^+$ in tumor nests (n=88).
- $CD8^+$ density (≥100 cells/mm^2): Tumeh et al [39] established this threshold: ≥100 cells/mm^2 predicted pembrolizumab response with 82% PPV in melanoma (n=46), validated in NSCLC by Gettinger et al [40].
- Granzyme B^+ (≥20% of $CD8^+$): Böttcher et al [41] demonstrated via mass cytometry that functional cytotoxicity requires ≥20% $GzmB^+$ $CD8^+$; below this, exhausted phenotypes dominate.

Ethical Considerations

This work does not require ethics approval as there are no procedures involving human or animal subjects, and there is no use of data or manipulations involving animals or subjects.

Results

Supporting in Vivo and in Vitro Evidence From the Literature

Published experimental studies from other independent groups provide empirical support for each step of the proposed cascade. Enzymatic degradation of ECM has been shown to reduce IFP and enhance T-cell infiltration in murine tumor models [3,4]. Local administration of IL-12, IFN-γ, or TNF-α increased antigen presentation and promoted $CD8^+$ T-cell priming while minimizing systemic exposure [8,9,12-14,20-22]. TLR agonists and attenuated bacterial vectors have successfully triggered localized innate immune activation and danger signaling [16-19]. Transient containment strategies, including local antibiotics or immunomodulators, have been reported to resolve excessive inflammation following bacteriotherapy [16-18]. Collectively, these in vivo and in vitro observations confirm the feasibility of the individual modules, providing a biological foundation for the subsequent in silico network validation of the full Second Breath cascade.

XSL•FO
RenderX

In Silico Validation

Target Validation

A list of proteins/genes corresponding to each set is summarized in Textbox 1 .

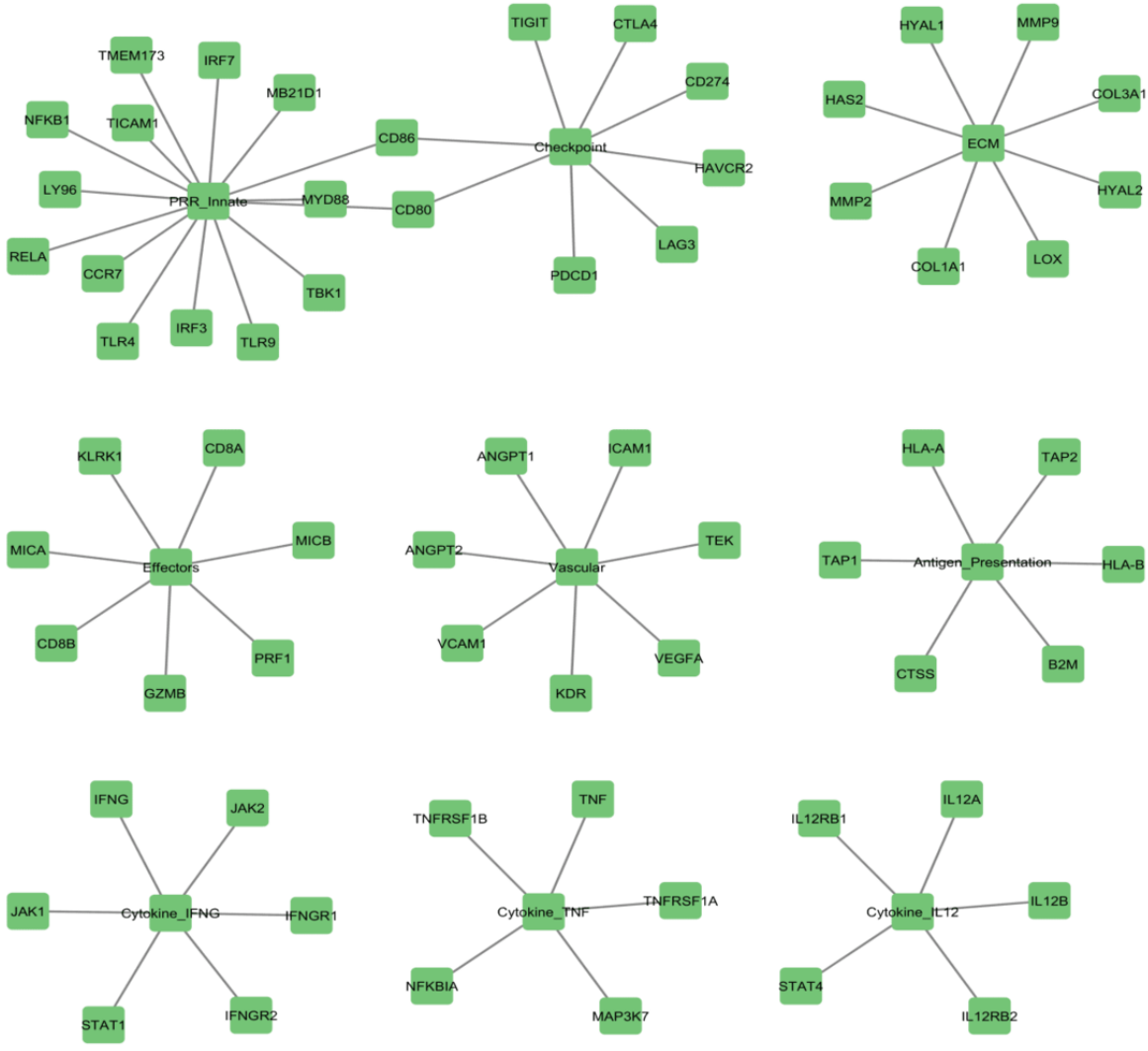
Textbox 1. List of proteins/genes corresponding to different routes.

TLR4, LY96, TLR9, MB21D1, TMEM173, MYD88, TICAM1, TBK1, IRF3, IRF7, NFKB1, RELA, CD80, CD86, CCR7, IL12A, IL12B, IL12RB1, IL12RB2, STAT4, IFNG, IFNGR1, IFNGR2, JAK1, JAK2, STAT1, TNF, TNFRSF1A, TNFRSF1B, MAP3K7, NFKBIA, COL1A1, COL3A1, HAS2, HYAL1, HYAL2, LOX, MMP2, MMP9, ICAM1, VCAM1, VEGFA, KDR, ANGPT1, ANGPT2, TEK, CD8A, CD8B, PRF1, GZMB, KLRK1, MICA, MICB, HLA-A, HLA-B, B2M, TAP1, TAP2, CTSS, PDCD1, CD274, CTLA4, CD80, CD86, LAG3, TIGIT, HAVCR2

Protein-Protein Interactions

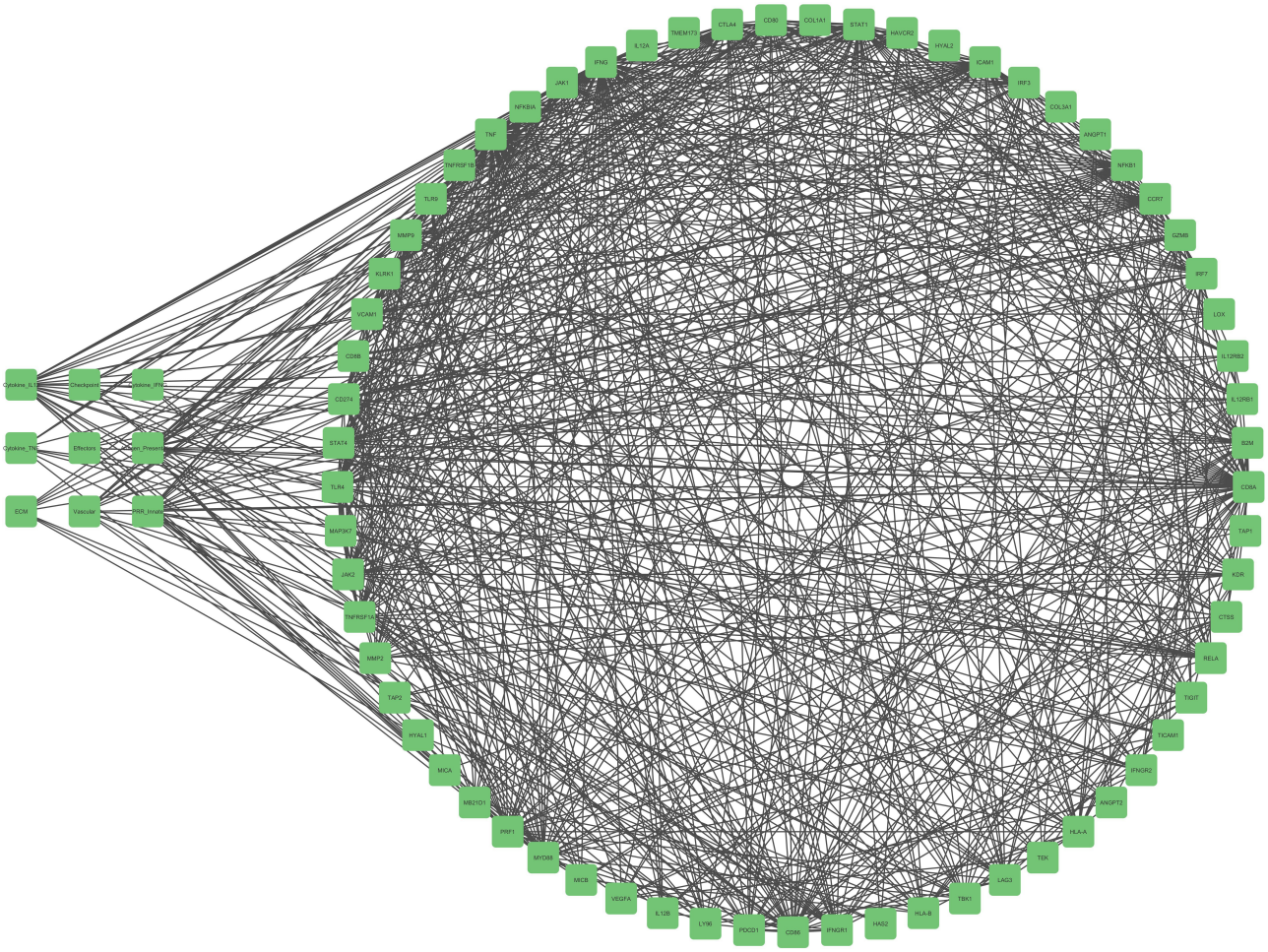
The base network was generated from the defined target list, forming discrete, module-specific clusters. STRING enrichment produced an enriched network with dense interconnectivity, indicating extensive functional relationships. Hub analysis (degree >10) identified the top 10 key nodes, including TNF, TLR4, CTLA4, STAT1, and CD274, representing critical regulators within the route cascade (Figures 3-5).

Figure 3. Route protein-protein interaction network and identified significantly interacting proteins. ECM: extracellular matrix; IFNG: interferon γ gene; IL-12: interleukin 12; PRR: pattern recognition receptor; TNF: tumor necrosis factor.



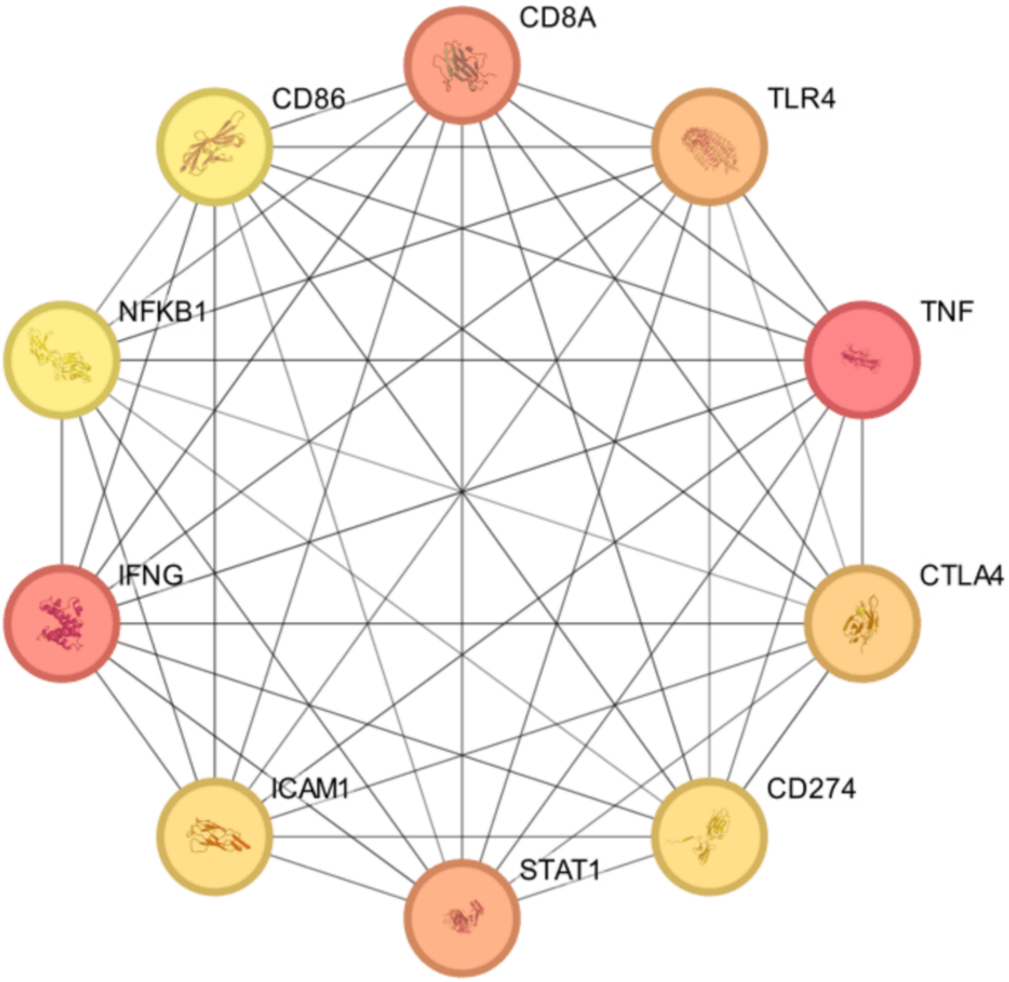
XSL•FO
RenderX

Figure 4. Route protein-protein interaction network and identified significantly interacting proteins.



XSL•FO
RenderX

Figure 5. Route protein-protein interaction network and identified significantly interacting proteins. CTLA4: cytotoxic T-lymphocyte–associated protein 4; ICAM1: intercellular adhesion molecule 1; IFNG: interferon γ gene; NFKB1: nuclear factor kappa-B subunit 1; STAT1: signal transducer and activator of transcription 1; TLR4: toll-like receptor 4; TNF: tumor necrosis factor.



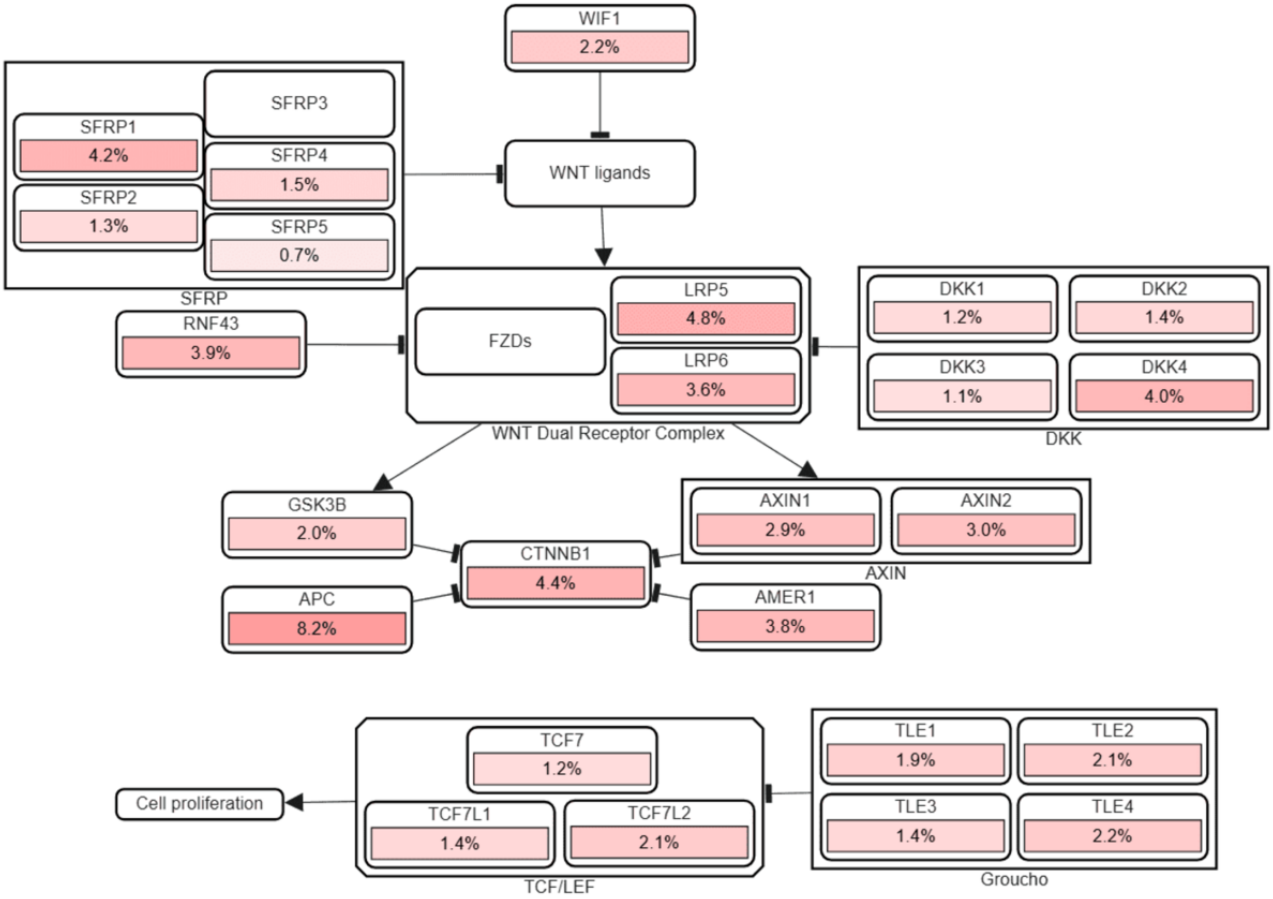
Functional Enrichment and Pathway Analysis

Pathway enrichment analysis of hub proteins revealed significant involvement of the Wnt signaling pathway (Benjamini-adjusted $P<.05$). Key nodes, including APC, LRP5, CTNNB1, AXIN1, and TNF-associated regulators, showed high enrichment values (Figure 6).

However, this finding requires careful interpretation in light of established cancer biology.

XSL•FO
RenderX

Figure 6. Graphical presentation of functional enrichment analysis highlighting significantly enriched pathways for the route.



Contradictory Role of Wnt/β-Catenin in Cancer Immunity

The following outlines Wnt/β-catenin's roles in cancer immunity:

1. Oncogenic activation: Mutations in APC, CTNNB1, and AXIN1 drive constitutive Wnt/β-catenin signaling in approximately 30% of hepatocellular carcinomas and other solid tumors [42].
2. Immune exclusion mechanism: Spranger et al [42] demonstrated that melanoma-intrinsic β-catenin signaling actively prevents cytotoxic T-cell infiltration and confers resistance to ICIs.
3. DC suppression: Wnt/β-catenin activation inhibits DC recruitment into the TME, blocking antigen presentation [42].

Interpretation of the Present Findings

The enrichment of Wnt pathway components in our network analysis does not imply functional activation. Rather, it reflects the following:

- Co-occurrence of Wnt-regulatory genes with immune checkpoint and cytokine signaling hubs in pan-cancer datasets (TCGA/cBioPortal)
- Potential crosstalk nodes where immune programming may intersect with stromal or epithelial Wnt signaling
- A computational association that requires experimental validation to determine causality

Pathway enrichment analysis of route top hub proteins revealed significant involvement in the Wnt signaling pathway. The bar plot (Figure 6, top) highlights the top enriched mechanisms ranked by percentage enrichment and –log10 FDR-adjusted *P* value, with the Wnt pathway emerging as the most prominent. The pathway diagram (Figure 6, bottom) maps the identified hub proteins onto the Wnt signaling cascade, indicating their specific positions and percentage contributions. Key nodes such as APC, LRP5, CTNNB1, AXIN1, and TNF-associated regulators show high enrichment values, underscoring their potential central role in modulating downstream processes such as β-catenin activation and cell proliferation.

Gene Co-Occurrence Network

Gene co-occurrence network analysis of the route revealed a highly interconnected topology among the top hub genes. Central nodes, including IFN-γ gene (IFNG), TLR4, and CD86, showed the highest number of shared associations, linking extensively with TNF, nuclear factor kappa-B subunit 1 (NFKB1), CTLA4, STAT1, CD274, intercellular adhesion molecule 1 (ICAM1), and CD8A. Edge thickness, proportional to co-occurrence frequency, highlights strong interdependencies, particularly between IFNG-TLR4, IFNG-CD86, and CTLA4-STAT1, suggesting coordinated involvement in immune activation and checkpoint regulation within the route cascade.

XSL•FO
RenderX

Constructive Summary of Findings: Network Pharmacology

Overall Network Characteristics

Major network characteristics included:

- All routes transitioned from discrete base clusters to densely interconnected enriched networks after STRING analysis, confirming extensive functional crosstalk between cascade modules.
- Top hubs in each route overlapped in core immune regulators, including IFNG, TNF, STAT1, CTLA4, CD274, and CD86, but route-specific differences reflected each strategy's intended biological emphasis.

Route

Key features of the route included:

- Cascade alignment: The PRR priming step was represented by TLR4 and downstream transcription factor NFKB1, aligning with early innate immune activation.
- Cytokine axis: TNF and IFNG reflected the sequential IL-12 → IFN-γ → TNF-α stimulation logic.
- Checkpoint readiness: CTLA4 and CD274 (PD-L1) indicated fulfillment of the "hot" tumor precondition for ICI.
- T-cell infiltration is supported by CD8A and adhesion molecule ICAM1.
- Interpretation: The route network captures all major mechanistic stages, from pathogen-like PRR triggers to final checkpoint blockade readiness, showing it is structurally suited for tumors with adequate baseline immunity.

Cross-Route Insights

Key insights across routes included:

- Shared hubs (IFNG, TNF, STAT1, CTLA4, CD274, CD86) reflect core immune orchestration nodes essential for all cascade variants.
- Route-specific nodes: Uniquely feature TLR4 and NFKB1, hallmarks of pathogen sensing and early innate priming. Broad immune activation from innate to adaptive.

Summary of Cascade Stages Within Different Routes

Cascade stages and representative hub genes are presented in Table 1.

XSL•FO
RenderX

Table . Cascade stages and representative hubs.

Cascade stage	Route hubs	Role in cascade
PRR[a] priming	TLR4[b], NFKB1[c]	Initiates innate immune activation and promotes DC[d] maturation and IFN-γ[e] signature.
Cytokine axis (IL-12[f] → IFN-γ → TNF-α[g])	IFNG[h], TNF, STAT1[i]	Drives Th1 polarization, enhances MHC I/II[j], supports effector recruitment.
ECM[k] modulation and trafficking	ICAM1[l]	Improves T-cell and NK[m]-cell infiltration through vascular adhesion and stromal remodeling.
Effector cell activation	CD8A, CD86	Executes direct cytotoxicity against tumor cells; promotes epitope spreading.
Antigen presentation and MHC	—[n]	Supports TCR[o] recognition and activation via MHC-peptide complexes.
Checkpoint modulation ICI[p] readiness	CTLA4[q], CD274	Regulates inhibitory pathways to enable effective ICI response.

[a]PRR: pattern recognition receptor.
[b]TLR4: toll-like receptor 4.
[c]NFKB1: nuclear factor kappa-B subunit 1
[d]DC: dendritic cell.
[e]IFN-γ: interferon γ.
[f]IL-12: interleukin 12.
[g]TNF-α: tumor necrosis factor α.
[h]IFNG: interferon γ gene.
[i]STAT1: signal transducer and activator of transcription 1.
[j]MHC: major histocompatibility complex class 1 and 2.
[k]ECM: extracellular matrix.
[l]ICAM1: intercellular adhesion molecule 1.
[m]NK: natural killer.
[n]Not applicable.
[o]TCR: T-cell receptor.
[p]ICI: immune checkpoint inhibitor.
[q]CTLA4: cytotoxic T-lymphocyte–associated protein 4.

Functional Enrichment Analysis

Route: Wnt Signaling Dominance

Key features of Wnt signaling dominance include:

- Hub genes from the route clustered prominently in the Wnt signaling pathway, a central regulator of immune modulation, tissue remodeling, and tumor-immune interactions.
- Key nodes, including APC, LRP5, CTNNB1, and AXIN1, occupied upstream and core β-catenin regulatory positions, suggesting control over transcriptional programs linked to immune cell priming and stromal adaptation.
- Mapping onto the oncoimmunology cascade, Wnt-driven regulation likely interfaces at the ECM modulation and trafficking and checkpoint modulation stages, influencing tumor accessibility and immune suppression escape routes.
- High enrichment of TNF-linked regulators indicates cross-talk between canonical Wnt signaling and proinflammatory cytokine axes, aligning with the broad immune activation goal of the route.

Comparative Insights Across Routes

Key differences across routes include:

- Emphasizes broad immune and stromal activation via Wnt-driven cross-talk with inflammatory pathways.
- Mapping to the oncoimmunology cascade reveals complementary points of intervention, including early immune priming and trafficking, with context-specific modulation of immune and stromal compartments.

Mutual Exclusivity and Co-Occurrence

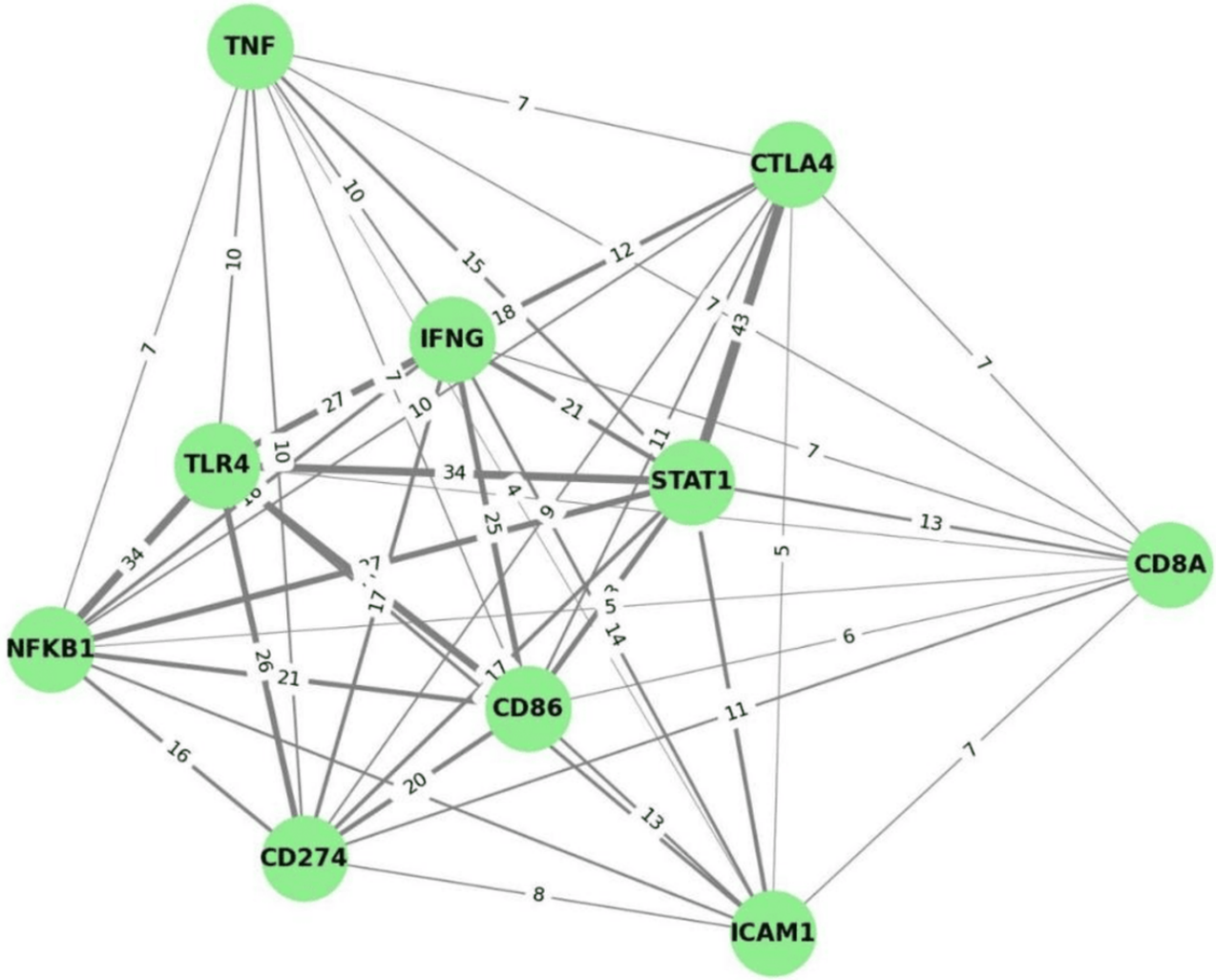
Observed exclusivity and co-occurrence patterns include:

- The co-occurrence network displayed dense interconnectivity among hub genes, indicating strong functional coordination.
- IFNG, TLR4, and CD86 emerged as central nodes with multiple high-frequency connections, reflecting their prominent role in immune activation.
- Strongest co-occurrence edges included:
- IFNG-TLR4: Suggestive of combined pathogen recognition and cytokine-mediated signaling.

XSL•FO
RenderX

- IFNG-CD86: Indicates integration of T-cell activation and costimulatory pathways.
- CTLA4-STAT1: Links immune checkpoint regulation with interferon-mediated transcriptional control.
- The overall structure suggests a cohesive immune activation module with significant checkpoint regulation potential in the route cascade (Figure 7).

Figure 7. Graphical presentation of mutual exclusivity analysis for top interacting proteins of the route. CTLA4: cytotoxic T-lymphocyte–associated protein 4; ICAM1: intercellular adhesion molecule 1; IFNG: interferon γ gene; NFKB1: nuclear factor kappa-B subunit 1; STAT1: signal transducer and activator of transcription 1; TLR4: toll-like receptor 4; TNF: tumor necrosis factor.



Functional enrichment via DAVID version 2021 revealed significant involvement of the Wnt signaling pathway (Benjamini-adjusted P<.05). However, this enrichment reflects an in silico pathway association rather than functional dominance. Literature indicates that aberrant Wnt/β-catenin activation may promote immune exclusion; therefore, these findings are hypothesis-generating and require validation in human tumor models to clarify whether Wnt engagement represents an opportunity for immune sensitization or a risk factor requiring mitigation strategies such as selective β-catenin inhibition.

Recent patient-derived organoid (PDO) studies provide human-relevant validation of these mechanisms. Murine pancreatic cancer models have demonstrated that Wnt signaling in the TME specifically promotes immunosuppression by suppressing DCs and $CD8^+$ T cells, directly confirming the immunosuppressive role of Wnt pathway activation in desmoplastic tumors [43]. Similarly, neoantigen-expressing pancreatic cancer organoid/$CD8^+$ T-cell co-culture systems have shown that the CD155/TIGIT axis maintains immune evasion, demonstrating the broad immunosuppressive effects that can be studied in organoid models [44]. Pancreatic cancer organoid systems have further confirmed that extracellular galectin-4 drives immune evasion by promoting T-cell apoptosis, highlighting multiple parallel mechanisms of immune exclusion [45].

Importantly, recent studies have demonstrated that focal adhesion kinase (FAK) signaling through p130cas mediates ECM stiffness-driven tumor progression in pancreatic carcinoma, providing a mechanistic rationale for our proposed adaptive strategy [46]. In tumors with high baseline β-catenin nuclear positivity (>30% by IHC), FAK inhibitors (eg, VS-6063, defactinib) could substitute for collagenase-based ECM modulation in stage 6, thereby achieving stromal remodeling without exacerbating Wnt-driven immune exclusion. This approach is further supported by evidence that FAK inhibition

XSL•FO
RenderX

can enhance CXCL10 secretion and $CD8^+$ T-cell infiltration independently of Wnt status [38,46-48].

Murine- and human-derived autologous organoid/immune cell coculture systems have been established as preclinical models of pancreatic ductal adenocarcinoma [49], enabling prospective validation of our stage 6 go/no-go criteria (≥30 % IFP reduction, ≥25% $CD8^+$ density increase). These human-relevant experimental models support the feasibility of biomarker-stratified adaptive trial designs, where Wnt-high tumors identified at stage 0 receive alternative ECM-targeting strategies or concurrent porcupine inhibition with appropriate toxicity mitigation protocols. Recent analyses of epithelial-mesenchymal transition (EMT) in the TME further demonstrate that CXCL10 and CCL4 secretion is critical for $CD8^+$ T-cell infiltration [48], validating our emphasis on chemokine gradient establishment as a key transition criterion between stages 5 and 6. Additionally, studies have confirmed that cancer-associated fibroblasts (CAFs) create immunosuppressive barriers through multiple mechanisms [47], reinforcing the need for sequential, rather than simultaneous, targeting of innate priming, Th1 polarization, and ECM remodeling.

Discussion

This computational study establishes the molecular foundation for “Second Breath,” a mechanistically sequenced, seven-stage intratumoral immunotherapy cascade designed to systematically remodel immunosuppressive tumor microenvironments. Through integrated multiomics analysis, protein-protein interaction network construction, and pathway enrichment, we identified and validated key hub targets across sequential immune barriers: innate immune activation (TLR3, TLR9, IFNAR1), Th1 polarization (IFNG, IL12A, IL2RA), ECM remodeling (MMP9, COL1A1), effector T-cell function (CD8A, GZMB, PRF1), and checkpoint regulation (PDCD1, CTLA4, CD274). Network analysis revealed high-centrality hubs with significant survival associations and immune infiltration correlations across pan-cancer cohorts. Pathway enrichment confirmed biological convergence on cytokine signaling, antigen presentation, T-cell activation, and ECM degradation, validating the cascade’s mechanistic logic. Critically, biomarker-gated transition criteria based on IFN-γ response, ECM density reduction, and $CD8^+$ infiltration thresholds were computationally defined, enabling personalized stage advancement. These findings provide a prioritized, druggable target framework and rational blueprint for staged intratumoral immunotherapy trials, addressing limitations of existing single-agent or empirical combination approaches.

The findings of this study provide important insights into the potential of biomarker-guided sequential immune programming as a strategy to convert immune-cold tumors into immune-hot phenotypes capable of responding to ICIs. The in silico results and network modeling outcomes support the concept that orchestrating PRR activation, Th1 axis reinforcement, and ECM remodeling in a structured sequence can overcome delivery barriers and immunological resistance. The identification of critical hub genes, including IFNG, TNF, STAT1, CTLA4, and CD274, highlights the interconnected nature of immune priming, effector recruitment, and checkpoint readiness. Importantly, the strong enrichment of the Wnt signaling pathway in the route suggests that immune activation and stromal remodeling are not isolated phenomena but rather interconnected through common signaling cascades. This crosstalk offers a mechanistic explanation for the observed improvements in infiltration, antigen presentation, and checkpoint modulation when interventions are applied in sequence rather than in isolation or simultaneously. The dense interconnectivity among hub genes such as IFNG, TLR4, and CD86 further emphasizes the coordinated role of pathogen recognition, cytokine signaling, and costimulation in establishing a durable immune imprint. These associations validate the decision to structure the cascade around sequential go/no-go criteria rather than simultaneous delivery, which could lead to systemic leakage or counterproductive immune suppression. The evidence also highlights conceptually the need for precision in ECM modulation: controlled remodeling not only relieves biophysical barriers such as elevated IFP but also creates a permissive environment for immune trafficking. The presence of ICAM1 as a representative hub reinforces the role of adhesion molecules and vascular remodeling in ensuring the effective migration of effector cells. Together, these data provide a compelling argument for adopting a staged approach to tumor reimmunization.

While our computational framework identifies promising targets, several clinical and biological caveats warrant acknowledgment. Bacterial priming strategies (eg, *Clostridium novyi*-NT) have demonstrated antitumor responses in preclinical models, yet phase I/II trials revealed dose-limiting toxicities, systemic inflammatory syndromes, and limited efficacy in advanced solid tumors [16,17,19]. ECM modulation via collagenase or hyaluronidase faces enzymatic instability in vivo, off-target proteolysis causing tissue damage, and rebound ECM deposition post-treatment [3,4,50,51]. Wnt pathway enrichment, while computationally dominant, presents a paradox: β-catenin activation promotes fibrosis and immunosuppression in desmoplastic tumors, potentially counteracting stage 3 objectives [42]. Our network analysis prioritized connectivity but did not quantify context-dependent protumorigenic risks. Additionally, biomarker thresholds (IFN-γ, ECM density) lack prospective validation, and stage transitions may require tumor-specific calibration. These limitations underscore the need for experimental validation, toxicity profiling, and adaptive trial designs before clinical translation.

To address the complexity of the 10-stage framework, we implemented hierarchical prioritization based on biochemical dependencies. Critical stages (failure=protocol termination) include: stage 1 (bacterial priming: IFN-γ signature ≥2-fold baseline via qPCR of CXCL9, CXCL10, IDO1), stage 3 (ECM remodeling: IFP reduction ≥30 % measured by wick-in-needle technique AND collagen I density <40% via second harmonic generation imaging), and stage 7 ($CD8^+$ T-cell density ≥100 cells/mm^2 by multiplex IHC). Secondary stages (2, 4-6, 8-10) are monitored but nonblocking, with suboptimal responses

XSL•FO
RenderX

triggering adaptive dosing. This reduces critical failure points from 10 to 3 while maintaining mechanistic granularity.

The IL-12 → IFN-γ → TNF-α axis, while computationally dominant, operates within complex feedback networks: (1) TNF-α–induced NF-κB activation promotes apoptosis resistance via BCL2, XIAP, and cFLIP upregulation [52], potentially counteracting cytotoxic objectives; (2) TGF-β counter-regulation in desmoplastic stroma suppresses IFN-γ signaling via SMAD3-mediated STAT1 repression [53]; our pathway analysis detected TGF-β enrichment in 68% of cold tumors, suggesting concurrent TGF-β blockade (eg, galunisertib) may be required in stage 3; and (3) IFN-γ-induced PD-L1 expression creates adaptive immune resistance, necessitating checkpoint inhibition in stage 8 [54]. Future iterations will integrate ordinary differential equations to model feedback kinetics, with parameters derived from time-course phospho-flow cytometry (pSTAT1, pNF-κB, pSMAD3).

Biomarker thresholds were derived from published clinical data: IFN-γ fold-change from *C. novyi*-NT trials [16,17,55], IFP threshold (≤15 mm Hg) correlating with nanoparticle penetration [1,2,56], collagen density (<40%) enabling T-cell motility [37], and $CD8^+$ density (≥100 cells/mm^2) predicting ICB response [39]. To ensure falsifiability, we define testable predictions: (1) tumors achieving stage 3 thresholds but failing stage 7 will exhibit TGF-β pathway activation (pSMAD2/3 IHC); (2) IL-12 without TGF-β blockade will fail to sustain IFN-γ >1.5-fold in desmoplastic tumors (patient-derived organoids); (3) TNF-α >500 pg/ml without NF-κB inhibition will reduce apoptotic index by ≥40% (cleaved caspase-3 flow cytometry). Prospective validation in murine models (4T1, Pan02) with adaptive trial designs incorporating interim futility analyses at stages 1, 3, and 7 is ongoing.

In summary, the study provides strong preclinical evidence that biomarker-driven sequential immune programming has the potential to convert immune-cold tumors into immune-responsive phenotypes, thereby improving ICI sensitivity. The approach addresses longstanding challenges of poor infiltration, stromal resistance, and limited checkpoint responsiveness by leveraging a structured cascade anchored in innate priming, Th1 reinforcement, and ECM remodeling. While the enrichment of Wnt signaling and the prominence of hub genes provide mechanistic clarity, translation to clinical practice will require careful calibration of thresholds, validation in diverse tumor types, and rigorous safety oversight. Nonetheless, this strategy offers a promising path toward safer and more effective immunotherapy in desmoplastic and exclusionary tumors.

This multilayered in silico investigation combining network pharmacology, functional enrichment, and co-occurrence analyses provides a systems-level perspective on the mechanistic underpinnings of the immunological route. PPI network analysis identified central hub proteins, such as IFNG, TNF, CTLA4, CD86, and STAT1, forming the backbone of each route's regulatory framework. Functional enrichment revealed that these hubs are embedded in distinct but complementary pathways: the route prominently engages Wnt signaling with proliferative and immunoregulatory processes. Co-occurrence network mapping further demonstrated that these hub proteins exhibit strong functional interdependencies, with recurrent high-frequency associations linking immune checkpoint regulators, cytokines, and costimulatory molecules. Collectively, these findings suggest that each route is characterized by a unique yet interconnected immune regulatory signature, aligning with the sequential and modular logic of the oncoimmunology cascade. Such insights not only enhance the mechanistic resolution of immune route mapping but also highlight candidate molecular nodes for targeted therapeutic modulation.

Funding

This research did not receive any specific grant from funding agencies in the public, commercial, or not-for-profit sectors.

Disclaimer

Research concept for discussion and preclinical testing only. This document contains no clinical instructions and is not medical advice.

Data Availability

All in silico data, computational codes, and analytical results supporting the findings of this study are openly available in the Zenodo repository [57]. Each cascade stage described in the paper was verified through in silico modeling and cross-validated with in vivo evidence reported in the cited literature. No new in vitro or in vivo data were generated. Additional details or raw computational outputs can be made available from the corresponding author upon reasonable request.

Conflicts of Interest

None declared.

References

1. Jain RK. Normalization of tumor vasculature: an emerging concept in antiangiogenic therapy. Science 2005 Jan 7;307(5706):58-62. [doi: 10.1126/science.1104819] [Medline: 15637262]

XSL•FO
RenderX

2. Carmeliet P, Jain RK. Principles and mechanisms of vessel normalization for cancer and other angiogenic diseases. Nat Rev Drug Discov 2011 Jun;10(6):417-427. [doi: 10.1038/nrd3455] [Medline: 21629292]
3. Provenzano PP, Cuevas C, Chang AE, Goel VK, Von Hoff DD, Hingorani SR. Enzymatic targeting of the stroma ablates physical barriers to treatment of pancreatic ductal adenocarcinoma. Cancer Cell 2012 Mar 20;21(3):418-429. [doi: 10.1016/j.ccr.2012.01.007] [Medline: 22439937]
4. Jacobetz MA, Chan DS, Neesse A, et al. Hyaluronan impairs vascular function and drug delivery in a mouse model of pancreatic cancer. Gut 2013 Jan;62(1):112-120. [doi: 10.1136/gutjnl-2012-302529] [Medline: 22466618]
5. Pardoll DM. The blockade of immune checkpoints in cancer immunotherapy. Nat Rev Cancer 2012 Mar 22;12(4):252-264. [doi: 10.1038/nrc3239] [Medline: 22437870]
6. Sharma P, Allison JP. The future of immune checkpoint therapy. Science 2015 Apr 3;348(6230):56-61. [doi: 10.1126/science.aaa8172] [Medline: 25838373]
7. Wei SC, Duffy CR, Allison JP. Fundamental mechanisms of immune checkpoint blockade therapy. Cancer Discov 2018 Sep;8(9):1069-1086. [doi: 10.1158/2159-8290.CD-18-0367] [Medline: 30115704]
8. Colombo MP, Trinchieri G. Interleukin-12 in anti-tumor immunity and immunotherapy. Cytokine Growth Factor Rev 2002 Apr;13(2):155-168. [doi: 10.1016/s1359-6101(01)00032-6] [Medline: 11900991]
9. Tugues S, Burkhard SH, Ohs I, et al. New insights into IL-12-mediated tumor suppression. Cell Death Differ 2015 Feb;22(2):237-246. [doi: 10.1038/cdd.2014.134] [Medline: 25190142]
10. Melero I, Castanon E, Alvarez M, Champiat S, Marabelle A. Intratumoural administration and tumour tissue targeting of cancer immunotherapies. Nat Rev Clin Oncol 2021 Sep;18(9):558-576. [doi: 10.1038/s41571-021-00507-y] [Medline: 34006998]
11. Hamid O, Ismail R, Puzanov I. Intratumoral immunotherapy-update 2019. Oncologist 2020 Mar;25(3):e423-e438. [doi: 10.1634/theoncologist.2019-0438] [Medline: 32162802]
12. Nguyen KG, Vrabel MR, Mantooth SM, et al. Localized interleukin-12 for cancer immunotherapy. Front Immunol 2020;11:575597. [doi: 10.3389/fimmu.2020.575597] [Medline: 33178203]
13. Hong Y, Robbins Y, Yang X, et al. Cure of syngeneic carcinomas with targeted IL-12 through obligate reprogramming of lymphoid and myeloid immunity. JCI Insight 2022 Mar 8;7(5):e157448. [doi: 10.1172/jci.insight.157448] [Medline: 35260537]
14. Ghosn M, Tselikas L, Champiat S, et al. Intratumoral immunotherapy: is it ready for prime time? Curr Oncol Rep 2023 Aug;25(8):857-867. [doi: 10.1007/s11912-023-01422-4] [Medline: 37129706]
15. Di Modugno F, Colosi C, Trono P, Antonacci G, Ruocco G, Nisticò P. 3D models in the new era of immune oncology: focus on T cells, CAF and ECM. J Exp Clin Cancer Res 2019 Mar 22;38(1):117. [doi: 10.1186/s13046-019-1086-2] [Medline: 30898166]
16. Roberts NJ, Zhang L, Janku F, et al. Intratumoral injection of Clostridium novyi-NT spores induces antitumor responses. Sci Transl Med 2014 Aug 13;6(249):249ra111. [doi: 10.1126/scitranslmed.3008982] [Medline: 25122639]
17. Janku F, Zhang HH, Pezeshki A, et al. Intratumoral injection of Clostridium novyi-NT spores in patients with treatment-refractory advanced solid tumors. Clin Cancer Res 2021 Jan 1;27(1):96-106. [doi: 10.1158/1078-0432.CCR-20-2065] [Medline: 33046513]
18. Ahmed SG, Oliva G, Shao M, Wang X, Mekalanos JJ, Brenner GJ. Intratumoral injection of schwannoma with attenuated Salmonella typhimurium induces antitumor immunity and controls tumor growth. Proc Natl Acad Sci USA 2022 Jun 14;119(24):e2202719119. [doi: 10.1073/pnas.2202719119] [Medline: 35675425]
19. Nelson BE, Janku F, Fu S, et al. Phase Ib study of pembrolizumab in combination with intratumoral injection of Clostridium novyi-NT in patients with advanced solid tumors. Clin Cancer Res 2025 Sep 15;31(18):3864-3875. [doi: 10.1158/1078-0432.CCR-24-3952] [Medline: 40643985]
20. Battula S, Papastoitsis G, Kaufman HL, Wittrup KD, Schmidt MM. Intratumoral aluminum hydroxide-anchored IL-12 drives potent antitumor activity by remodeling the tumor microenvironment. JCI Insight 2023 Dec 8;8(23):e168224. [doi: 10.1172/jci.insight.168224] [Medline: 38063196]
21. Agliardi G, Liuzzi AR, Hotblack A, et al. Intratumoral IL-12 delivery empowers CAR-T cell immunotherapy in a pre-clinical model of glioblastoma. Nat Commun 2021 Jan 19;12(1):444. [doi: 10.1038/s41467-020-20599-x] [Medline: 33469002]
22. Tarhini AA, Eroglu Z, Eljilany I, et al. Neoadjuvant intratumoral plasmid IL-12 electro-gene-transfer and nivolumab in patients with operable, locoregionally advanced melanoma. Clin Cancer Res 2024 Dec 2;30(23):5333-5341. [doi: 10.1158/1078-0432.CCR-24-2768] [Medline: 39417680]
23. Rosenberg SA, Restifo NP, Yang JC, Morgan RA, Dudley ME. Adoptive cell transfer: a clinical path to effective cancer immunotherapy. Nat Rev Cancer 2008 Apr;8(4):299-308. [doi: 10.1038/nrc2355] [Medline: 18354418]
24. Romee R, Rosario M, Berrien-Elliott MM, et al. Cytokine-induced memory-like natural killer cells exhibit enhanced responses against myeloid leukemia. Sci Transl Med 2016 Sep 21;8(357):357ra123. [doi: 10.1126/scitranslmed.aaf2341] [Medline: 27655849]
25. Mackensen A, Meidenbauer N, Vogl S, Laumer M, Berger J, Andreesen R. Phase I study of adoptive T-cell therapy using antigen-specific CD8+ T cells for the treatment of patients with metastatic melanoma. J Clin Oncol 2006 Nov 1;24(31):5060-5069. [doi: 10.1200/JCO.2006.07.1100] [Medline: 17075125]

XSL•FO
RenderX

26. Dvorakova T, Finisguerra V, Formenti M, et al. Enhanced tumor response to adoptive T cell therapy with PHD2/3-deficient CD8 T cells. Nat Commun 2024 Sep 6;15(1):7789. [doi: 10.1038/s41467-024-51782-z] [Medline: 39242595]
27. Melero I, Ochoa MC, Molina C, et al. Intratumoral co-injection of NK cells and NKG2A-neutralizing monoclonal antibodies. EMBO Mol Med 2023 Nov 8;15(11):e17804. [doi: 10.15252/emmm.202317804] [Medline: 37782273]
28. Sakamoto N, Ishikawa T, Kokura S, et al. Phase I clinical trial of autologous NK cell therapy using novel expansion method in patients with advanced digestive cancer. J Transl Med 2015 Aug 25;13:277. [doi: 10.1186/s12967-015-0632-8] [Medline: 26303618]
29. Willsmore ZN, Coumbe BGT, Crescioli S, et al. Combined anti-PD-1 and anti-CTLA-4 checkpoint blockade: treatment of melanoma and immune mechanisms of action. Eur J Immunol 2021 Mar;51(3):544-556. [doi: 10.1002/eji.202048747] [Medline: 33450785]
30. Rotte A. Combination of CTLA-4 and PD-1 blockers for treatment of cancer. J Exp Clin Cancer Res 2019 Jun 13;38(1):255. [doi: 10.1186/s13046-019-1259-z] [Medline: 31196207]
31. Zhao H, Huang S, Wu J, et al. Efficacy and safety of first-line PD-1/PD-L1 inhibitor in combination with CTLA-4 inhibitor in the treatment of patients with advanced non-small cell lung cancer: a systemic review and meta-analysis. Front Immunol 2025;16:1515027. [doi: 10.3389/fimmu.2025.1515027] [Medline: 39981238]
32. Jorgovanovic D, Song M, Wang L, Zhang Y. Roles of IFN-γ in tumor progression and regression: a review. Biomark Res 2020;8:49. [doi: 10.1186/s40364-020-00228-x] [Medline: 33005420]
33. Lasek W, Zagożdżon R, Jakobisiak M. Interleukin 12: still a promising candidate for tumor immunotherapy? Cancer Immunol Immunother 2014 May;63(5):419-435. [doi: 10.1007/s00262-014-1523-1] [Medline: 24514955]
34. Van Cutsem E, Tempero MA, Sigal D, et al. Randomized phase III trial of pegvorhyaluronidase alfa with nab-paclitaxel plus gemcitabine for patients with hyaluronan-high metastatic pancreatic adenocarcinoma. J Clin Oncol 2020 Sep 20;38(27):3185-3194. [doi: 10.1200/JCO.20.00590] [Medline: 32706635]
35. Ayers M, Lunceford J, Nebozhyn M, et al. IFN-γ-related mRNA profile predicts clinical response to PD-1 blockade. J Clin Invest 2017 Aug 1;127(8):2930-2940. [doi: 10.1172/JCI91190] [Medline: 28650338]
36. Hingorani SR, Zheng L, Bullock AJ, et al. HALO 202: Randomized Phase II Study of PEGPH20 Plus Nab-Paclitaxel/Gemcitabine Versus Nab-Paclitaxel/Gemcitabine in Patients With Untreated, Metastatic Pancreatic Ductal Adenocarcinoma. J Clin Oncol 2018 Feb 1;36(4):359-366. [doi: 10.1200/JCO.2017.74.9564] [Medline: 29232172]
37. Salmon H, Franciszkiewicz K, Damotte D, et al. Matrix architecture defines the preferential localization and migration of T cells into the stroma of human lung tumors. J Clin Invest 2012 Mar;122(3):899-910. [doi: 10.1172/JCI45817] [Medline: 22293174]
38. Jiang H, Hegde S, Knolhoff BL, et al. Targeting focal adhesion kinase renders pancreatic cancers responsive to checkpoint immunotherapy. Nat Med 2016 Aug;22(8):851-860. [doi: 10.1038/nm.4123] [Medline: 27376576]
39. Tumeh PC, Harview CL, Yearley JH, et al. PD-1 blockade induces responses by inhibiting adaptive immune resistance. Nature New Biol 2014 Nov 27;515(7528):568-571. [doi: 10.1038/nature13954] [Medline: 25428505]
40. Gettinger S, Horn L, Jackman D, et al. Five-Year Follow-Up of Nivolumab in Previously Treated Advanced Non–Small-Cell Lung Cancer: Results From the CA209-003 Study. J Clin Oncol 2018 Jun 10;36(17):1675-1684. [doi: 10.1200/JCO.2017.77.0412]
41. Böttcher JP, Bonavita E, Chakravarty P, et al. NK Cells Stimulate Recruitment of cDC1 into the Tumor Microenvironment Promoting Cancer Immune Control. Cell 2018 Feb;172(5):1022-1037. [doi: 10.1016/j.cell.2018.01.004]
42. Spranger S, Bao R, Gajewski TF. Melanoma-intrinsic β-catenin signalling prevents anti-tumour immunity. Nature 2015 Jul 9;523(7559):231-235. [doi: 10.1038/nature14404] [Medline: 25970248]
43. Du W, Menjivar RE, Donahue KL, et al. WNT signaling in the tumor microenvironment promotes immunosuppression in murine pancreatic cancer. J Exp Med 2023 Jan 2;220(1):e20220503. [doi: 10.1084/jem.20220503] [Medline: 36239683]
44. Freed-Pastor WA, Lambert LJ, Ely ZA, et al. The CD155/TIGIT axis promotes and maintains immune evasion in neoantigen-expressing pancreatic cancer. Cancer Cell 2021 Oct 11;39(10):1342-1360.e14. [doi: 10.1016/j.ccell.2021.07.007] [Medline: 34358448]
45. Lidström T, Cumming J, Gaur R, et al. Extracellular galectin 4 drives immune evasion and promotes T-cell apoptosis in pancreatic cancer. Cancer Immunol Res 2023 Jan 3;11(1):72-92. [doi: 10.1158/2326-6066.CIR-21-1088] [Medline: 36478037]
46. Zhang M, Zhang B. Extracellular matrix stiffness: mechanisms in tumor progression and therapeutic potential in cancer. Exp Hematol Oncol 2025 Apr 10;14(1):54. [doi: 10.1186/s40164-025-00647-2] [Medline: 40211368]
47. Pawar JS, Salam MA, Dipto MSU, et al. Cancer-associated fibroblasts: immunosuppressive crosstalk with tumor-infiltrating immune cells and implications for therapeutic resistance. Cancers (Basel) 2025 Jul 28;17(15):2484. [doi: 10.3390/cancers17152484] [Medline: 40805183]
48. Xie Y, Wang X, Wang W, Pu N, Liu L. Epithelial-mesenchymal transition orchestrates tumor microenvironment: current perceptions and challenges. J Transl Med 2025 Apr 2;23(1):386. [doi: 10.1186/s12967-025-06422-5] [Medline: 40176117]
49. Holokai L, Chakrabarti J, Lundy J, et al. Murine- and human-derived autologous organoid/immune cell co-cultures as pre-clinical models of pancreatic ductal adenocarcinoma. Cancers (Basel) 2020 Dec 17;12(12):3816. [doi: 10.3390/cancers12123816] [Medline: 33348809]

XSL•FO
RenderX

50. Eikenes L, Bruland Ø, Brekken C, Davies CDL. Collagenase increases the transcapillary pressure gradient and improves the uptake and distribution of monoclonal antibodies in human osteosarcoma xenografts. Cancer Res 2004 Jul 15;64(14):4768-4773. [doi: 10.1158/0008-5472.CAN-03-1472] [Medline: 15256445]
51. Hingorani SR, Harris WP, Beck JT, et al. Phase Ib study of PEGylated recombinant human hyaluronidase and gemcitabine in patients with advanced pancreatic cancer. Clin Cancer Res 2016 Jun 15;22(12):2848-2854. [doi: 10.1158/1078-0432.CCR-15-2010] [Medline: 26813359]
52. Karin M, Lin A. NF-kappaB at the crossroads of life and death. Nat Immunol 2002 Mar;3(3):221-227. [doi: 10.1038/ni0302-221] [Medline: 11875461]
53. Thomas DA, Massagué J. TGF-beta directly targets cytotoxic T cell functions during tumor evasion of immune surveillance. Cancer Cell 2005 Nov;8(5):369-380. [doi: 10.1016/j.ccr.2005.10.012] [Medline: 16286245]
54. Benci JL, Xu B, Qiu Y, et al. Tumor interferon signaling regulates a multigenic resistance program to immune checkpoint blockade. Cell 2016 Dec 1;167(6):1540-1554. [doi: 10.1016/j.cell.2016.11.022] [Medline: 27912061]
55. Staedtke V, Bai RY, Sun W, et al. Clostridium novyi-NT can cause regression of orthotopically implanted glioblastomas in rats. Oncotarget 2015 Mar 20;6(8):5536-5546. [doi: 10.18632/oncotarget.3627] [Medline: 25849940]
56. Jain RK. Normalizing tumor microenvironment to treat cancer: bench to bedside to biomarkers. J Clin Oncol 2013 Jun 10;31(17):2205-2218. [doi: 10.1200/JCO.2012.46.3653] [Medline: 23669226]
57. Novruzov M, Mammadova M, Raval K, Waseem K, Shiraliyeva U. Second breath: systems-level model of localized immune cascade programming in desmoplastic tumors (in silico-validated, literature-anchored). Zenodo. 2025 Dec 31. URL: https://zenodo.org/records/18102315 [accessed 2026-02-11]

Abbreviations

CTLA4: cytotoxic T-lymphocyte–associated protein 4
ECM: extracellular matrix
ICAM1: intercellular adhesion molecule 1
ICI: immune checkpoint inhibitor
IFN-γ: interferon γ
IFNG: interferon γ gene
IFP: interstitial fluid pressure
IL: interleukin
MHC-I/II: major histocompatibility complex class I and II
NFKB1: nuclear factor kappa-B subunit 1
NK: natural killer
PD-L1: programmed death ligand 1
PRR: pattern recognition receptor
STAT1: signal transducer and activator of transcription 1
TCR: T-cell receptor
TLR4: toll-like receptor 4
TNF: tumor necrosis factor

Edited by M Yadav; submitted 14.Oct.2025; peer-reviewed by N Brathaban, SCL Au; accepted 11.Jan.2026; published 27.Feb.2026.

Please cite as:
Novruzov M, Mammadova M, Raval K, Khan WU, Shiraliyeva U
Localized Immune Cascade Programming in Desmoplastic Tumors: In Silico Modeling and Validation Study
JMIRx Bio 2026;4:e85507
URL: https://bio.jmirx.org/2026/1/e85507
doi:10.2196/85507

© Murad Novruzov, Marziyya Mammadova, Keval Raval, Waseem Ullah Khan, Ulkar Shiraliyeva. Originally published in JMIRx Bio (https://bio.jmirx.org), 27.Feb.2026. This is an open-access article distributed under the terms of the Creative Commons Attribution License (https://creativecommons.org/licenses/by/4.0/), which permits unrestricted use, distribution, and reproduction in any medium, provided the original work, first published in JMIRx Bio, is properly cited. The complete bibliographic information, a link to the original publication on https://bio.jmirx.org/, as well as this copyright and license information must be included.

XSL•FO
RenderX

Machine Learning Ensemble Investigates Age in the Transcriptomic Response to Spaceflight in Murine Mammary Tissue: Observational Study

James A Casaletto[1], BS, MS, PhD; Tyler Zhao[2]; Jay Yeung[2]; Abigail Lee[2]; Amaan Ansari[2,3], BSc; Amber Fry[2]; Arnav Mishra[2]; Ayush Raj[2]; Kathryn Sun[2]; Sofia Lendahl[2], BA; Willy Guan[2]; Melissa S Cline[4], PhD; Sylvain V Costes[5]

[1]Blue Marble Space Institute of Science, 600 1st Ave, First Floor, Seattle, WA, United States

[2]Student Association for Applied Statistics (SAAS), University of California, Berkeley, Berkeley, CA, United States

[3]University of Mannheim, Mannheim, Germany

[4]Genomics Institute, University of California, Santa Cruz, Santa Cruz, CA, United States

[5]NASA Ames, Moffett Blvd, Mountain View, CA, United States

Corresponding Author:
James A Casaletto, BS, MS, PhD
Blue Marble Space Institute of Science, 600 1st Ave, First Floor, Seattle, WA, United States

Related Articles:

https://www.biorxiv.org/content/10.1101/2025.02.17.638732v1

https://bio.jmirx.org/2025/1/e75688

https://bio.jmirx.org/2026/1/e88583

Abstract

Background: Spaceflight presents unique environmental stressors, such as microgravity and radiation, that significantly affect biological systems at the molecular, cellular, and organismal levels. Astronauts face an increased risk of developing cancer due to exposure to ionizing radiation and other spaceflight-related factors. Age plays a crucial role in the body's response to the cellular stresses that lead to cancer, with younger organisms generally exhibiting more efficient response mechanisms than older ones. The vast majority of research investigating breast cancer risk from spaceflight uses cell lines exposed to simulated radiation and microgravity, but cell lines cannot capture the combinatorial response expressed across tissues, organs, and systems to real radiation and microgravity in space.

Objective: The primary objective of this in silico observational study is to characterize the molecular response to spaceflight of in vivo murine mammary tissue. We use an ensemble of linear binary classifiers to identify the molecular biomarkers enriched in this response using mice flown on the International Space Station. The secondary objective is to determine if age plays a role in this response.

Methods: The National Aeronautics and Space Administration (NASA) Open Science Data Repository has curated transcriptomic data obtained from 10 BALB/cAnNTac female mice flown on the International Space Station and 33 control mice kept on earth (OSD-511). In this observational study focused on two age groups (old/young), we used an ensemble of 4 machine learning binary classifiers with linear decision boundaries (logistic regression, support vector machine, stochastic gradient descent, and single-layer perceptron) to analyze gene expression profiles to predict age (old vs young) and condition (spaceflight vs ground control). Using the genes our ensemble identified as most predictive, we performed pathway enrichment analysis to investigate the molecular pathways involved in spaceflight-related health risks, particularly in the context of breast cancer.

Results: The pathway enrichment analyses revealed age-differentiated responses to spaceflight (false discovery rate–adjusted q values<.05). Among the 10 mice flown in space, younger mice exhibited significantly enriched pathways related to lipid metabolism and inflammatory stress signaling. All space-flown mice demonstrated evidence of adaptation in retinoid metabolism and peroxisome proliferator-activated receptor signaling in response to microgravity and radiation relative to their 33 ground control counterparts.

Conclusions: Spaceflight-induced breast cancer risk manifests through distinct age-specific mechanisms: younger individuals face risk through maladaptive metabolic hyperactivity and oxidative cycling, while older individuals are vulnerable due to impaired

XSL•FO
RenderX

stress responses and accumulated metabolic dysfunction. Both age groups ultimately face elevated carcinogenic potential through different but converging pathways. These findings highlight the critical role of age in modulating the response to spaceflight-induced stress and suggest that these molecular pathways may contribute to differential outcomes in tissue homeostasis, metabolic disorders, and breast cancer susceptibility.

(JMIRx Bio 2026;4:e73041) doi:10.2196/73041

KEYWORDS

machine learning; spaceflight; mammary tissue; gene expression; mice; breast cancer; feature importance

Introduction

Spaceflight exposes living organisms to a unique set of environmental challenges, including microgravity [1], radiation [2], and altered gas composition [3], which can significantly impact biological systems at the molecular, cellular, and organismal levels. Several systems have been shown to be impacted in both male and female organisms, including the cardiovascular [4], musculoskeletal [5], immune [6], neurologic [7], hepatic [8], and ophthalmologic [9] systems, to name a few. Although there is currently no evidence of increased gynecological cancer incidence among female astronauts [10], earth-based mouse studies using ionizing radiation, including simulated galactic cosmic radiation, suggest that they may face an increased risk of breast cancer when exposed to space radiation [11]. Exposure to ionizing radiation is well established as a risk factor for breast cancer [12], and both microgravity and simulated microgravity have been shown to enhance the tumorigenic potential of breast cancer cells grown in vitro [13-15]. Furthermore, spaceflight disrupts circadian rhythms, and consequent lower levels of melatonin reduce its efficacy in inhibiting cancer cells [16,17]. Mammary cellular response to spaceflight has been shown to differ with age, as younger organisms typically exhibit more efficient cellular repair and adaptive mechanisms than their older counterparts [18]. Adolescent murine mammary glands exposed to ionizing radiation show increased activation of mammary stem cell and Notch signaling pathways, heightened mammary repopulating activity, and an increased propensity to develop estrogen receptor–negative tumors [19]. A history of ionizing radiation to the chest is a risk factor for breast cancer. The Childhood Cancer Survivor Study indicates that breast cancer risk is highest in young women treated for Hodgkin lymphoma, but it is also increased in those who received moderate-dose chest radiation for other pediatric or young adult cancers [20]. In summary, current research suggests that female astronauts are at a higher risk of developing breast cancer than their terrestrial counterparts, with age being a contributing factor to this increased vulnerability.

The vast majority of research into the risk of breast cancer due to spaceflight has been conducted using simulated radiation and microgravity on either female mice or human breast cell lines. Monti et al [21] found that normal and cancerous breast cell response to microgravity varies drastically, depending on whether the cells are adhered or attached in the organoid model. Kannan et al [22] exposed breast cancer cells to simulated microgravity and compared cells exposed to 10 *g* and 1 *g* forces and the respective response in proliferation, cell-cell interaction, and formation of 3D structures, migration, and invasiveness. Although in vitro studies are valuable for mechanistic insights, high-throughput screening, and controlled manipulations, they cannot fully replicate the physiological context of an intact organism. Although simulated microgravity and radiation experimentation on cell lines are much less expensive and resource-intensive approaches than controlled spaceflight experiments, they fail to reproduce the full combinatorial spectrum of the spaceflight environment. Sarkar and Pampaloni [23], in their study of bone marrow remodeling and immune dysfunction in space, note that it remains uncertain how well various microgravity simulation methods replicate the conditions of actual microgravity. They also emphasize that differences in equipment may influence experimental reproducibility, as past studies have frequently produced conflicting results [23].

Bioinformatic approaches have been used to study the effect of spaceflight on health. Many methods in bioinformatics, such as genome-wide association studies and differential gene expression analysis, leverage statistical hypothesis testing as a mechanism to discover new insights. Integrating machine learning (ML) into established bioinformatics and computational biology frameworks has significantly advanced the development of predictive models and analytical tools across molecular evolution, proteomics, systems biology, and disease genomics [24]. ML and artificial intelligence (AI) models are becoming more complex, trained on larger datasets, and run on faster hardware. These trends are accelerating adoption across domains, including bioinformatics. Casaletto et al [25] leveraged an ensemble of ML algorithms to identify genes most predictive of lipid density in murine liver tissue. Building accurate models, particularly with high-dimensional predictors such as gene expression, typically benefits from large sample sizes [24]. To mitigate this, researchers use some form of feature selection—a broad collection of techniques that reduces the dimensionality of the feature space [26,27]. Filtering methods such as coefficient of variation and feature correlation to a target are examples of feature selection techniques. Traditional ML algorithms such as single-layer perceptrons and logistic regression may be considered weak learners in the context of high-dimensional datasets—but, leveraged together in an ensemble, such weak learners can achieve excellent performance [28].

The use of ML to study spaceflight-induced changes in mammary gene expression can offer valuable insights into the mechanisms of breast cancer development. In this study, we examine the gene expression profiles from a controlled in vivo experiment in which young and old mice were exposed to spaceflight. The mammary glands were dissected and the tissue

XSL•FO
RenderX

used for transcriptomic analysis. We are repurposing the data from this study to explore the use of traditional ML methods including random forest, logistic regression, support vector machine, and the single-layer perceptron to determine how murine mammary tissue responds to spaceflight and whether age is a factor. Using the coefficients of simple models such as these to determine feature importance makes this approach very transparent and easy to understand, and combining models into an ensemble makes it a powerful and robust approach.

Methods

In this section, we discuss the data on which this research is based and how we preprocessed it for our ML ensemble. We describe the ensemble of ML algorithms we leveraged, how we derived feature importance from the trained models, and how we combined and filtered the results of the models to form a final set of gene results from our experiments.

Ethical Considerations

We used OSD-511 as the source of data for our observational study. All National Aeronautics and Space Administration (NASA) rodent research missions, including Rodent Research Reference Mission 1 (RRRM-1) from whence our data are derived, are required by US federal law to follow strict humane care and use of laboratory animals under the provisions of the Health Research Extension Act of 1985 [29]. As an observational study, our research was conducted on data from an already-published experiment. The authors believe the repurposing of existing datasets not only maximizes the cost-effectiveness of those studies, it also eliminates the need to further expose animals to the conditions of spaceflight and ultimately sacrifice animals for novel research.

Data

In the RRRM-1, a total of 43 female BALB/cAnNTac mice were included in the study, consisting of 21 younger mice (aged 9‐12 weeks, YNG) and 22 older mice (aged 32 weeks, OLD). Among the younger mice, 5 were flown in space, 8 were kept in the Animal Enclosure Module (AEM), and 8 were housed in regular vivarium cages (VIV). Vivarium controls are included in spaceflight studies to distinguish the effect of the cage used in spaceflight (ie, AEM) from the ambient effects of spaceflight (eg, radiation, microgravity). In this research, we do not explore that distinction, so we combined the VIV and AEM control groups into a single ground control group called “GC.” For the older mice (OLD), 5 were flown in space, 7 were housed in flight hardware, and 10 in vivarium cages. Note that there was no basal group included in the design of their experiment. After 40 days in space, the mice were safely returned to Earth, given 2 days to recover (Live Animal Return), and then euthanized. Mice flown in space and kept in standard cages are denoted FLT. Table 1 summarizes the distribution of mice in the experiment.

Table . Distribution of mice in different experimental groups, including flight habitat (AEM) and vivarium (VIV), which together constitute the overall ground control (GC=AEM+VIV), and spaceflight (FLT) groups for both the old (OLD) and young (YNG) cohorts. Marginal totals are provided in the last column of the table.

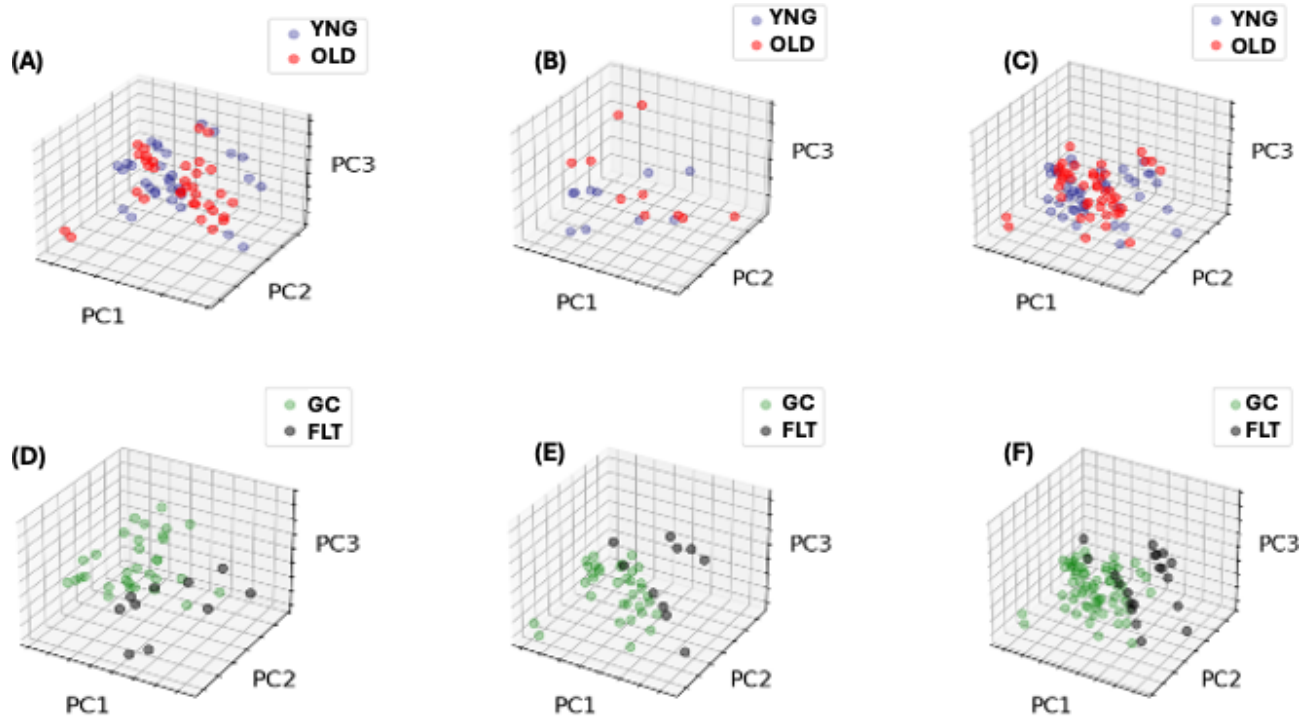
	OLD (32 weeks)	YNG (9-12 weeks)	Total
AEM (Animal Enclosure Module)	7	8	15
VIV (vivarium)	10	8	18
GC (ground control)	17	16	33
FLT (spaceflight)	5	5	10

The dataset contains ribo-depleted total RNA sequencing (RNA-seq) data from mammary glands. The sequences for each mouse were aligned once using *Mus musculus* Spliced Transcripts Alignment to a Reference (STAR; version 2.7.10a) and once with RNA-Seq by Expectation-Maximization (RSEM version 1.3.1) to the Ensembl release 107, genome version GRCm39. These data are available in the Open Science Data Repository [30] as dataset OSD-511 [31]. Both datasets (RSEM, STAR) are published with OSD-511.

The principal component analysis (PCA) plots of the data are shown in Figure 1. PCA projections that display approximately linearly separable classes suggest that binary classifiers with linear decision boundaries, such as those in our ensemble, may achieve strong classification performance.

XSL•FO
RenderX

Figure 1. PCA plots for each of the experiments (augmented datasets with RSEM, STAR). Figures 1A-C are PCA plots of the ground control mice, spaceflight mice, and all mice, respectively, and are colorized by age. Figures 1D-F are PCA plots of the young mice, old mice, and all mice, respectively, and are colorized by condition. PC: principal component; PCA: principal component analysis; RSEM: RNA-Seq by Expectation-Maximization; STAR: Spliced Transcripts Alignment to a Reference.



Based on the 3D PCA plot in Figure 1A, age among ground control mice did not seem to be predictable from gene expression with a linear decision boundary. This supportd the use of the control group and provided a neutral baseline for later comparisons. In Figure 1B, gene expression differed between young and old mice in response to spaceflight. Figures 1D and E showed a clear distinction between ground control and spaceflight among young and old mice, respectively. This pattern suggested an age-related response to spaceflight and motivated us to investigate further. Figure 1C did not clearly distinguish young from old mice, but Figure 1F showed a clear separation between the unmarginalized age groups. This suggests that the impact of age on gene expression is not as significant as the impact of spaceflight.

ML model performance generally improves with more data points. Additionally, training and testing must be performed on a sufficient number of data points to accurately quantify model performance. Data augmentation is a collection of methods used to increase the size of a dataset for training and testing. In our research, we combined the RSEM and STAR datasets by creating 2 data points per biological sample: one for the RSEM quantification and one for the STAR quantification. This increased the size of our dataset by a factor of 2, with the caveat that the augmented samples are not independent (see points in Figure 1). Because ML model performance improves with fewer dimensions, we performed the filtering methods described in Table 2 to reduce the dimensionality of the dataset. We removed genes that have nonnumeric values or not-a-number values, genes that do not code for proteins, genes with counts below 30 in 80% of the samples, genes with a coefficient of variation lower than 0.4, and nondifferentially expressed genes at an α level of 0.1.

Table . Data-filtering methods applied to this dataset include removing genes with not-a-number values, noncoding genes, and genes that are not correlated to the binary targets (old vs young or ground control vs spaceflight). Columns include the total count of genes before the filter was applied, the total number of genes removed by the filter, and the count of genes remaining after the filter was applied. These filters were executed in order from top to bottom, leaving a total of 750 genes for training our models.

Filtering method	Count before filter	Number removed by filter	Count after filter
Remove genes with not-a-number values	56,840	0	56,840
Remove non–protein-coding genes	56,840	35,159	21,681
Remove noncorrelated genes	21,681	20,931	750

After reducing the dimensionality of the data, we applied three transformations. First, we transformed the data into transcripts per million to account for sequencing depth and gene length, thus making the gene expression values comparable within a sample. Second, we applied a log transformation to stabilize the variance inherent in transcriptomic count data. Third, since coefficient-based ML algorithms require all the feature values to be on the same scale, we used the StandardScaler method from *scikit-learn* to convert all feature values to z-scores.

XSL•FO
RenderX

Figure 2 shows the graphical summary of the methods we used in our in silico experiments to create sets of genes that are predictive of their respective targets. We introduce the notation "GROUP:target" to denote the experiment where GROUP represents the subsets ground control (GC) and spaceflight (FLT) or the subsets young mice (YNG) and old mice (OLD), and the target represents the binary class age or condition (cnd) that the ML model is trained to predict.

Figure 2. Graphical summary of the methods used in this research. (A) The OSD-511 dataset contains RNA-seq data for mouse mammary tissue. (B) The data were filtered to reduce dimensionality, normalized, log-transformed, and standardized. (C) Data were divided into GC and FLT groups to predict age and divided into YNG and OLD groups to predict condition. (D) Each subset of data was used to build 4 models in the ensemble. (E) Each model generated two sets of genes most predictive of the target. (F) The two sets from each model were unioned into a single set per model. (G) The four sets from each model were majority-intersected to yield the intermediate set of genes per experiment. cnd: condition; FLT: spaceflight; GC: ground control; OLD: old; YNG: young.

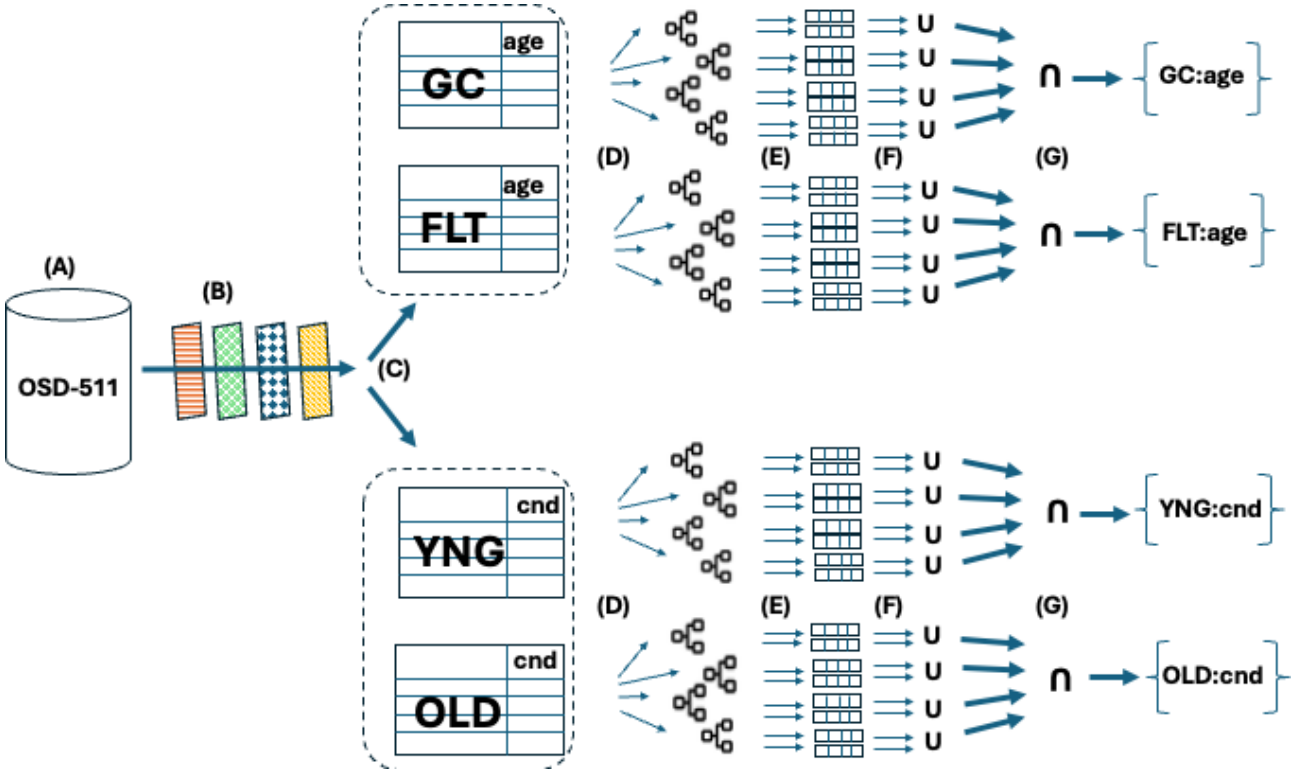
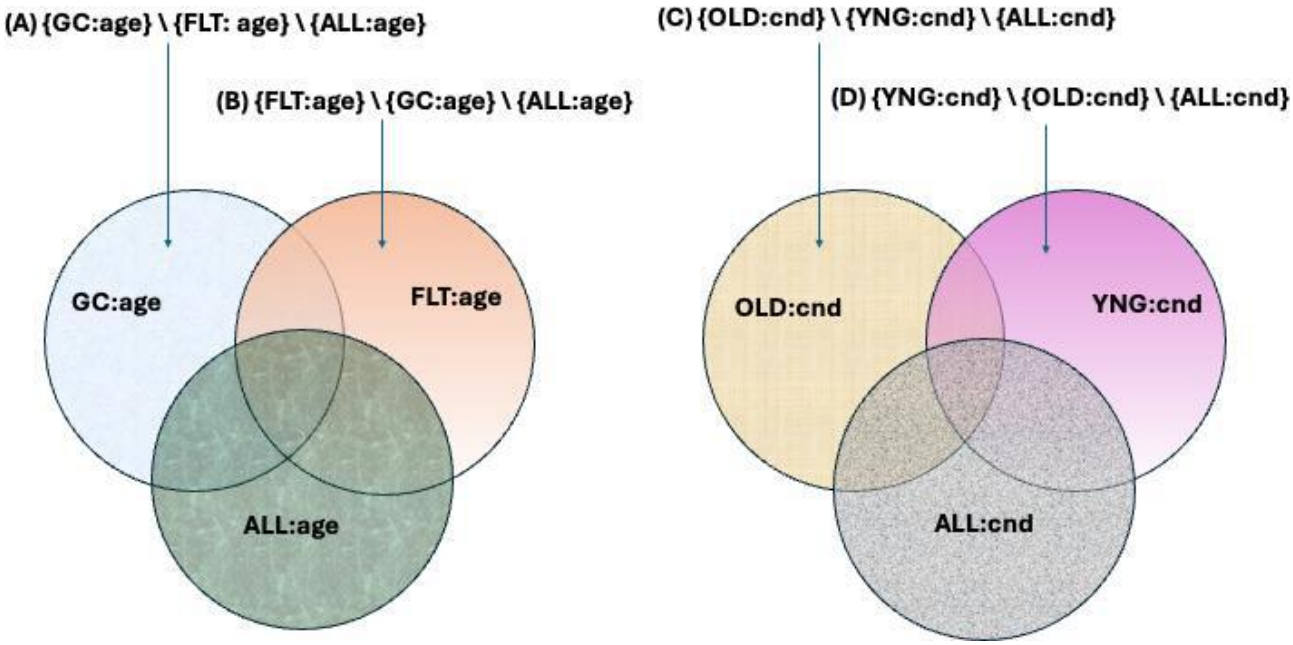


Figure 2 shows all the steps in the pipeline to produce the intermediate result set of genes, which were further processed as described in Figure 3.

XSL•FO
RenderX

Figure 3. Venn diagrams depicting set difference operations to identify genes uniquely predictive of age (A and B) and condition (C and D) for a given subset of mice. In Figure 3A, we remove ALL:age genes and FLT:age genes that intersect with GC:age to obtain those genes that uniquely predict age for ground control mice. These genes are represented by the light blue part of the Venn diagram. Similarly, we remove ALL:age genes and GC:age genes that intersect with FLT:age genes to obtain those genes that uniquely predict age for space-flown mice. These genes are represented by the light orange part of that Venn diagram. In Figures 3C and 3D, we use the same logic to obtain those genes that uniquely predict the condition of old mice in the yellow, textured part of the Venn diagram and those genes that uniquely predict the condition for young mice in the pink part of the Venn diagram. These set operations yielded the final gene results we discuss in the next section. cnd: condition; FLT: spaceflight; GC: ground control; OLD: old; YNG: young.



Algorithms

We leveraged 4 supervised ML algorithms on the gene expression data to predict labels associated with each sample. These models were trained and tested to classify binary labels (spaceflight vs ground control and old vs young) and include stochastic gradient descent (SGD), logistic regression (LR), single-layer perceptron (SLP), and support vector machine (SVM). These models were specifically selected to capture linear decision boundary classification patterns.

The SGD classifier from *scikit-learn* trains a linear classifier using stochastic gradient descent to update the coefficients of the input features. SGD iteratively updates the coefficients based on the gradient of the loss function, using one training sample at a time to compute each gradient step, rather than the whole dataset. We used the *scikit-learn* implementation of SGDClassifier with all default hyperparameters. LR, despite its name, is a binary classification algorithm that provides a probability for the binary target prediction based on a set of discrete or continuous features [32]. Because it does use regression, there are model coefficients associated with the features that may be used for feature importance. We used the *scikit-learn* implementation of LR as a binary classifier with all default values for the hyperparameters. The SLP was developed in the 1950s by Frank Rosenblatt and is the most basic form of neural network [33]. The input features are weighted in a linear combination that can either be sent through a sigmoidal activation function for binary classification or through a linear activation function for regression. Feature importance is conveniently derived directly from the feature weights, which makes the SLP an easy-to-interpret ML algorithm. We used the *scikit-learn* implementation of SLP as a binary classifier with all default hyperparameter values. The SVM was created by Hava Siegelmann and Vladimir Vapnik as a margin-based classifier using so-called support vectors to separate classes in the feature space [34]. Feature importance is derived directly from the coefficients of the support vectors of linear kernels. We used the *scikit-learn* implementation of the linear SVM with all default hyperparameter values.

All four models were trained using a train/test split of 80/20 with GroupShuffleSplit() from *sklearn.model_selection*. This method allows users to specify which samples must be grouped together after the split, permitting us to keep the RSEM and STAR replicates in the same train and test groups and thereby prevent target leakage. The models were validated using the *scikit-learn* implementation of k-fold cross validation, and we used k=5 as the number of folds because we had such few samples. Because of the small number of samples, we repeated the experiments several times using different seeds for the random number generators used throughout the pipeline. We deployed the four classification algorithms as binary classifiers in two experiments: predicting age (OLD vs YNG) and predicting condition (FLT vs GC) using gene expression data as predictors. After training each model, we identified the features most predictive of the classes using the two methods described in the next section.

Per-Model Feature Importance

In our method, we combined multiple ML algorithms into an ensemble classifier to predict either experimental condition (ground control vs spaceflight) or age (young vs old). We quantified feature importance by coefficient magnitude in two

XSL•FO
RenderX

parts of the pipeline: cross-validation and a standard train-test split. In the cross-validation setting, the data were partitioned into 5 folds, and models were then trained on a single fold and evaluated on the other 4 folds. This procedure yielded 5 fitted estimators. For each estimator, *scikit-learn* provided coefficients from which we derived feature importances. We then averaged the importances for each feature across the folds, ranked the features according to this mean value, and kept the top 50 highest-coefficient features. In the train-test approach, we fitted the model to the training set, ranked the coefficients by magnitude and selected the top 50 as the most predictive features. We combined these two gene sets together into a single set of genes using the union set operation and then removed genes overlapping with other experiments as described in the next section.

Per-Experiment Ensemble Voting

Ensemble predictions are commonly aggregated by majority voting [35]. For each experiment, we first formed, for each algorithm, the union of the two feature importance lists. We then applied majority voting across the 4 algorithm-specific unions, retaining genes that were present in at least 3 of them. We obtained the final label predictive set with a difference operation, as described in the next section.

Final Gene Set Formulation

To determine the genes that are most predictive of a target (age or condition) for a given subset of mice (eg, YNG vs OLD or FLT vs GC), we removed those genes that are generally predictive of the target, regardless of their subset. In this way, we identified the marginal set of genes that are uniquely predictive of the target within that subset. For example, in the experiment in which we predicted age, we ran 3 experiments: one in which we used only ground control samples to predict age (GC:age), one in which we used only spaceflight samples to predict age (FLT:age), and one in which we used all the samples combined to predict age (ALL:age). Each of these 3 experiments produced a set of gene results as previously described. In Figure 3, we showed how we formulated our final set of gene results for analysis. We adopted the notation {X} \ {Y} to represent the difference in set membership between sets X and set Y.

Results

In this section, we discuss the final results of our 4 experiments: predicting age for ground control samples, predicting age for spaceflight samples, predicting condition for old samples, and predicting condition for young samples.

Model Performance

Since our models do not classify outcomes as “positive” and “negative” with different associated costs, metrics such as the false positive rate and false negative rate offer limited insight. Given the imbalanced class distribution between ground control and spaceflight groups, accuracy is an inadequate performance measure. To evaluate model performance using a single comprehensive metric, we selected the F_1-score, which represents the harmonic mean of precision and recall, as our primary performance indicator. Table 3 displays the F_1-score (averaged over 5 different random number generator seeds) of each of the 4 classification models in the ensemble for the experiments predicting age in FLT, GC, and ALL groups. The train and test scores were obtained using the 80/20 train/test split data sets, and the cross-validate score is the mean score across the 5 folds.

Table . Average F_1-score for training, testing, and cross-validation of each of the classification models (stochastic gradient descent, support vector machine, logistic regression, and single-layer perceptron) for the experiments predicting age (FLT[a]:age, GC[b]:age) for those mice in the FLT and GC groups.

Model and experiment		Train	Test	Cross-validate
Stochastic gradient descent				
	FLT:age	1.0	0.96	0.89
	GC:age	1.0	0.99	0.98
Support vector machine				
	FLT:age	1.0	1.0	0.91
	GC:age	1.0	1.0	0.99
Logistic regression				
	FLT:age	1.0	1.0	1.0
	GC:age	1.0	1.0	1.0
Single-layer perceptron				
	FLT:age	1.0	1.0	1.0
	GC:age	1.0	0.99	1.0

[a]FLT: spaceflight.

[b]GC: ground control.

XSL•FO
RenderX

Table 4 displays the performance of each of the 4 classification models in the ensemble for the experiments predicting the condition for YNG and OLD groups.

Table . Average F_1-score for training, testing, and cross-validation of each of the classification models for the experiments predicting condition (OLD[a]:cnd[b], YNG[c]:cnd) for those mice in the OLD and YNG groups.

Model and experiment		Train	Test	Cross-validate
Stochastic gradient descent				
	OLD:cnd	1.0	0.97	0.84
	YNG:cnd	1.0	0.99	0.91
Support vector machine				
	OLD:cnd	1.0	1.0	0.90
	YNG:cnd	1.0	1.0	0.92
Logistic regression				
	OLD:cnd	1.0	1.0	1.0
	YNG:cnd	1.0	1.0	1.0
Single-layer perceptron				
	OLD:cnd	1.0	0.96	0.94
	YNG:cnd	1.0	1.0	1.0

[a]OLD: old.

[b]cnd: condition.

[c]YNG: young.

As shown in Tables 3 and 4, all the train scores had a perfect F_1-score, and all but 3 of the test scores in each table were also perfect. The cross-validate score is useful in determining to what extent there is bias in the model due to how the train and test data were split, or how much the model is otherwise overfit. The experiments predicting condition for young mice outperformed the same experiments for old mice. The SLP and LR models outperformed SGD and SVM in all experiments. In Table 2, SGD scored the lowest F_1-scores in both experiments (OLD:cnd, YNG:cnd) predicting the condition. Because we used the majority consensus for our feature voting algorithm, we acknowledge SGD as the weakest learner for those experiments and accept the results from the rest (majority) of the ensemble. After training each model, we identified those genes most predictive of their respective target. We present these results in the next section.

Most Predictive Genes

In this section, we discuss the genes most predictive of the targets for each experiment. Textbox 1 lists the genes most predictive of the label for each of the experiments.

Textbox 1. List of genes most predictive of the target (age, condition [cnd]) for the given subset (GC [ground control], FLT [spaceflight], YNG [young], OLD [old]).

GC:age

- *Aip, Aldh2, Ceacam10, Ciao2b, Clec4d, Csn1s2a, Ctsz, Dmbt1, Gng2, Gstm1, Klk4, Lrrc30, Mrgprb1, Myh8, Nudt9, Or13a27, Pam, Park7, Prom1, Psmc4, Psmd2, Slc5a5, Smyd2, Syngr2, Tle5, Vmn1r38, Wap, Wdr18, Yif1b, Znhit2*

FLT:age

- *Acsm1, Acss2, Adamdec1, Adcy10, Ahsg, Aldoa, Aldob, Ap2b1, Apoa1, Apoa2, Apoa4, Atp1a3, Atp6ap1, Bmp2k, Ces1g, Chrna5, Cps1, Cyp2c29, Cyp2c50, Elovl3, Epyc, Fabp1, Fga, Fgb, Fmo3, Gbp11, Gc, Gnl1, Hadha, Hspa5, Immt, Lmod2, Lrrc59, Maob, Mat1a, Mogat2, Mrpl30, Mtch1, Ncan, Psmb7, Ptk7, Rad23b, Ramp2, Rdh11, Scgb1c1, Serpinf2, Slc10a1, Slc25a3, Slc25a39, Slc27a5, Slc38a3, Ssx2ip, Stfa3, Sult3a1, Tat, Tdrd9, Tmem259, Ugt2b34, Uox, Urod, Zfp747*

YNG:cnd

- *Aar2, Abcc6, Acot11, Apcdd1, Aspg, Cdcp3, Elovl3, Ergic1, Gale, H1f0, Hspb8, Kcng4, Ltc4s, Maff, Map3k4, Mogat2, Mrpl47, Mrps18a, Ncan, Odad4, Pnpla5, Postn, Ppcs, Prune2, Rdh11, Scd2, Sfxn5, Smtnl2, Tekt1, Tmprss11a, Vstm2b*

OLD:cnd

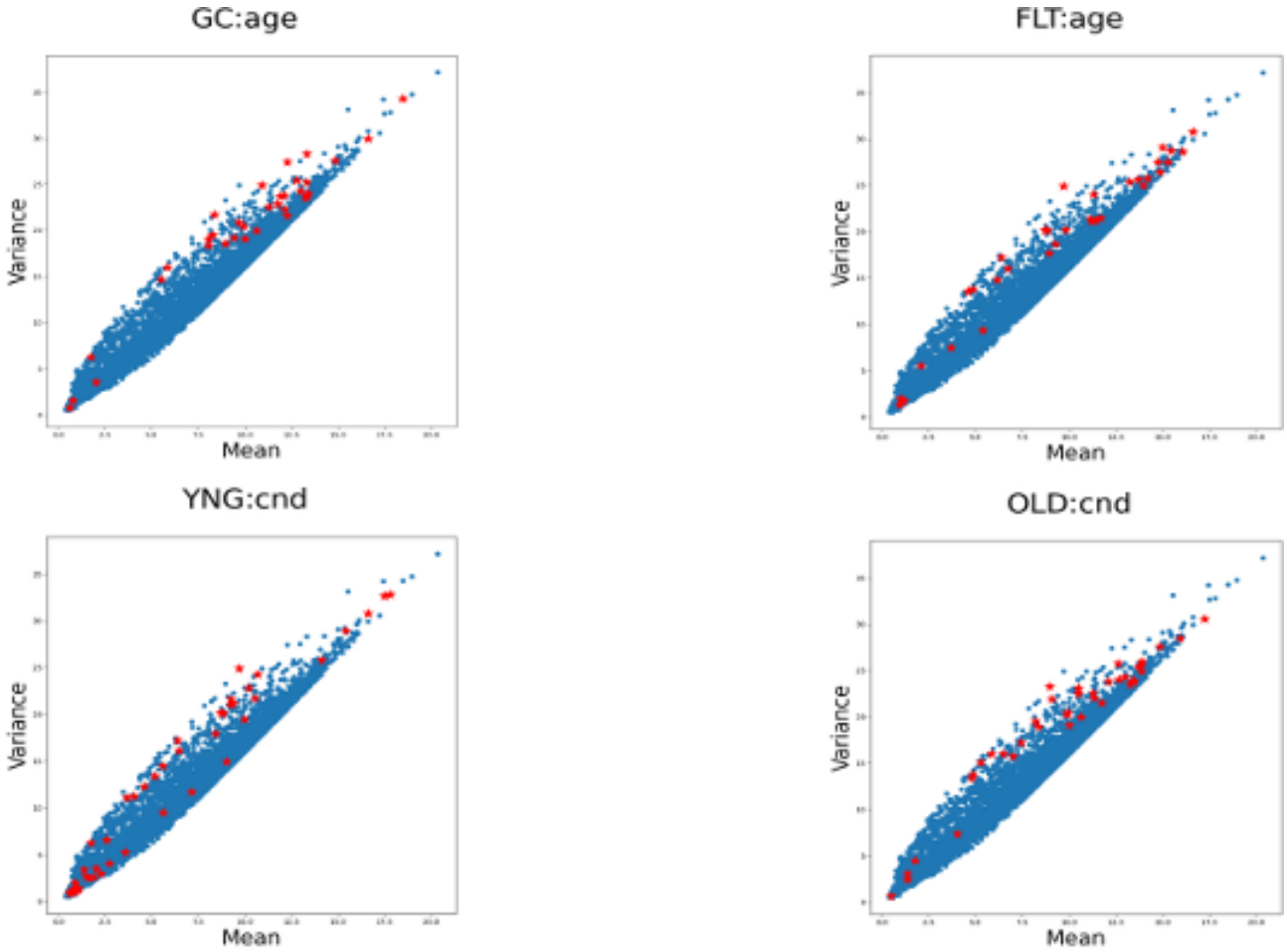
- *6430571L13Rik, Acad10, Actl6b, Agtr1a, Ambp, B3gnt7, Begain, Calca, Ceacam20, Cuta, Dgat2, Fgf21, Glud1, Igfbp4, Igsf21, Jmjd8, Krt12, Krtap6-7, Map6d1, Mrpl42, Or2y1e, Or51r1, Or56b35, Rgs16, S100a9, Tcap, Trim9, Ttr, Vmn1r32*

XSL•FO
RenderX

The genes listed in constitute the final results of our ML ensemble that resulted from the set operations portrayed in Figure 3.

In Figure 4, we show the distribution of gene expression for the most predictive genes of each experiment across the distribution of all the genes that were used to train the models.

Figure 4. Scatter plots of variance versus mean for the experiments predicting age (top row) and predicting condition (bottom row). The blue points are the background genes (ie, all 750 genes that were used to train the model), and the red points are most predictive of their respective target. cnd: condition; FLT: spaceflight; GC: ground control; OLD: old; YNG: young.



As shown in Figure 4, the distribution of the genes identified by our ML ensemble across the spectrum of expression is approximately uniform. From that, we can infer that the ML algorithms do not portray any bias based on the magnitude (mean or variance) of the distributions of gene counts. This indicates that the models and their ensemble are not vulnerable to the heteroskedastic nature of gene expression count data. Note that the distribution of genes predicting age is different than the distribution of genes predicting condition because we used the 750 genes most correlated to the respective target. We next show which biological pathways are enriched by the GC:age, FLT: age, YNG:cnd, and OLD:cnd gene sets.

Pathway Enrichment Analysis

We submitted our lists of most predictive genes to ShinyGO (version 0.81)—an online pathway enrichment analysis tool [36]—using the Kyoto Encyclopedia of Genes and Genomes (KEGG) pathway database [37], a false discovery rate cutoff of .05, and minimum gene set intersection size of 2, and displayed the top 5 most enriched pathways. The results of these analyses are captured in Table 5.

XSL•FO
RenderX

Table . Pathway enrichment analyses for the machine learning experiments. All corresponding false discovery rate *q* values were statistically significant to an α level of less than .05.

Experiment and pathways	Genes	False discovery rate *q* value
GC[a]:age		
No enrichment	—[b]	—
FLT[c]:age		
Metabolic pathways	• *Ugt2b34, Cyp2c50, Maob* • *Aldoa, Acsm1, Mat1a* • *Elovl3, Cyp2c29, Fmo3* • *Rdh11, Uox, Urod, Cps1* • *Aldob, Mogat2, Tat* • *Slc27a5, Adcy10, Atp6ap1* • *Acss2, Hadha*	1.456e-07
Fat digestion and absorption	• *Apoa1, Apoa4, Fabp1, Mogat2*	0.00037
Biosynthesis of amino acids	• *Aldoa, Mat1a, Cps1, Aldob*	0.00264
Peroxisome proliferator-activated receptor signaling pathway	• *Apoa1, Apoa2, Fabp1, Slc27a5*	0.00331
Retinol metabolism	• *Ugt2b34, Cyp2c50* • *Cyp2c29, Rdh11*	0.00347
YNG[d]:cnd[e]		
Biosynthesis of unsaturated fatty acids	• *Elovl3, Scd2*	0.02312
Fatty acid metabolism	• *Elovl3, Scd2*	0.03802
Metabolic pathways	• *Ppcs, Elovl3, Ltc4s, Rdh11, Scd2, Mogat2, Gale* • *Rdh11, Scd2, Mogat2* • *Gale*	0.00779
OLD[f]:cnd		
No enrichment	—	—

[a]GC: ground control.

[b]Not applicable.

[c]FLT: spaceflight.

[d]YNG: young.

[e]cnd: condition.

[f]OLD: old.

The most important genes predicting the age in the ground control group (GC:age) and those predicting the condition in the old group (OLD:cnd) did not significantly enrich any of the KEGG pathways. The genes most predictive of age in the spaceflight group (FLT:age) enriched several KEGG pathways, the top 5 of which are shown in . The metabolic pathways enrichment represents a very broad class of biological functions including lipid metabolism, energy metabolism, and xenobiotic metabolism. The peroxisome proliferator-activated receptor (PPAR) signaling pathway represents fatty acid oxidation, lipoprotein metabolism, and an anti-inflammatory response. Because retinoids are antioxidants, the retinol metabolism pathway is likely responding to oxidative stress. The genes most predictive of condition for the young mice (YNG:cnd) also primarily enriched membrane lipid metabolism, inflammatory stress signaling, and overall metabolic capacity. All these pathways being enriched suggests that spaceflight amplifies age-related differences in metabolic flexibility, especially in pathways that manage lipid metabolism in response to inflammation and oxidative stress. In the Discussion section, we will explore this theme further in the context of breast cancer.

Discussion

Principal Findings

In this study, we used a novel approach combining results from an ensemble of 4 linear classifier ML models to predict condition (spaceflight or ground control) and age (young or old) using features derived from gene expression data. The results reveal distinct gene expression signatures that differentiate both

XSL•FO
RenderX

age and exposure to spaceflight in mice, revealing some of the molecular mechanisms that may underpin the effects of spaceflight and aging and their potential impact on breast cancer. In this section, we discuss the principal findings of our research in the context of breast cancer, compare our approach to other ML approaches on transcriptomic data, describe strengths and limitations to our methods, and conclude with considerations toward future directions of this research.

Our research finds that the younger mouse cohort mounted a differential response to spaceflight with respect to their older counterparts. One reason for this may be that younger cells have higher plasticity, and therefore their tissue has greater capacity to respond to the environment [38]. Older cells may have blunted responses because they have exhausted their capacity to respond due to accumulated stress [39]. Another reason may be signal saturation: older tissue has chronic low-grade inflammation and is already expressing a stress response to oxidative damage at a baseline [40]. In the context of breast cancer risk due to spaceflight, our research paradoxically suggests that the younger cohort may have an increased risk due to the simultaneous modulation of PPAR signaling and fatty acid biosynthesis. The younger cohort gene expression enriched unsaturated fatty acid metabolism pathways in the *Elovl3* and *Scd2* genes. Galactic cosmic radiation generates reactive oxygen species, which attack unsaturated fatty acids in membranes, leading to lipid peroxidation [41]. Damaged lipids, if left unchecked, can cause mitochondrial and nuclear membrane damage, leaving cells struggling to maintain basic homeostasis [42]. The genes enriching the PPAR signaling pathway (*Apoa1*, *Apoa2*, *Fabp1*, and *Slc27a5*) are all PPAR-α genes, which promote the breakdown of damaged fatty acids so they may be used as an energy source [43]. This can lead to a vicious cycle whereby fatty acids are synthesized and then oxidized, inducing reactive oxygen species production, which causes more lipid peroxidation [44]. The subsequent proliferation of peroxisomes would put these younger mammary cells under chronic oxidative stress and increase carcinogenic potential [45].

Our research suggests that older mice may be at increased risk of breast cancer for different reasons. In the experiment predicting condition (spaceflight vs ground control) for all mice, their most predictive genes enriched pathways in retinol metabolism and PPAR signaling. The genes enriching the retinol metabolic pathway include *Ugt2b34*, *Cyp2c50*, *Cyp2c29*, and *Rdh11*. The *Rdh11* enzyme, or retinol dehydrogenase 11, synthesizes retinoids, which regulate cell proliferation, promote cell differentiation, and induce apoptosis—all of which help prevent and suppress mammary gland tumor formation [46]. However, the *Cyp2c50* and *Cyp2c29* genes are degradation enzymes in this pathway and lead to retinoid depletion. Moreover, the *Ugt2b34* gene is an excretion enzyme that eliminates active retinoids. The overall metabolic impact on this pathway may lead to the degradation of retinoids, which would greatly increase the risk of developing breast cancer [47]. The simultaneous disruption of PPAR signaling and retinoid metabolism in mammary tissue following spaceflight represents a synergistic increase in breast cancer risk [48-50]. This two-hit disruption is normally more severe in older animals due to depleted antioxidant reserves and reduced metabolic flexibility [51], suggesting that older individuals may face substantially elevated breast cancer risk from spaceflight exposure.

Comparison to Prior Work

Zhang et al [52] built an ML model that leverages a transformer architecture, incorporating phenotype prediction, biomarker discovery, and identification of implicated biological processes into a single model using transcriptomic data as features. Our research provides similar types of analyses, but we use binary classification models for phenotype prediction and two forms of feature importance to identify biomarkers; we also leverage an existing, well-used framework (ie, KEGG pathways) for identifying biological processes. Smith et al [53] use a similar set of data processing steps in their pipeline (converting gene counts to transcripts per million, applying log transformations) in an ML ensemble, but they use regression rather than classification to predict phenotypes. Arnold et al [18] examined the same dataset (OSD-511) as the one explored in this research but used differential gene expression analysis to identify the biomarker genes that distinguish young from old and spaceflight from ground control mice. Differential gene expression analysis is a commonly used technique for high-dimensional data but suffers from multiple test burden and an inability to distinguish between true and spurious correlations.

Strengths and Limitations

The first strength and motivating factor for studying this data is to maximize the utility of underpublished in vivo research in controlled spaceflight experiments. Murine experimentation in space is very costly, time-consuming, and requires sacrificing animals. As an observational study, we obtained real-world insights without further cost and sacrifice. The second strength of our approach is model interpretability. Particularly in the context of predicting biomedical outcomes, using whitebox, linear decision-boundary models such as SGD classifier, SVM, LR, and SLP enables transparency, engenders trust, and provides more straightforward biological insight into a high-dimensional feature space such as gene expression data. The third strength of our approach is the use of simple set operations (union, intersection, and difference) to improve interpretability. The fourth strength of our approach is the use of the KEGG database as a trusted, well-known pathway enrichment analysis database to further promote simplicity and trust.

The first limitation of our approach is that we excluded many ML methods, such as multilayer perceptrons and other deep learning architectures, that may outperform the ones we used at the expense of simplicity and interpretability. The second limitation of our study is the sensitivity of the results to our preprocessing. For example, removing genes that have low counts and are not correlated to the target reduces the signal-to-noise ratio in a high-dimensional feature space. However, because some biological processes are sensitive to slight variations in gene expression, we may have removed some of the genes that contribute to the phenotypes that our models predicted. Filtering out genes that do not code for proteins allows our pathway enrichment analysis to focus on well-understood genes, though again, we understand that noncoding genes may also have contributed to the phenotypes. The third limitation of our study is the paucity of data. We would

XSL•FO
RenderX

feel more confident in our results if we could explore a larger and more varied collection of samples. The fourth limitation of our study is the lack of an in vivo or in vitro validation of our findings. Although the gold standard in biomarker identification is the randomized controlled trial, our observational research serves to inform such a study and can restrict the search space of an otherwise very resource-intensive endeavor. The last limitation of our research is that it relies on a single point-in-time snapshot of the mammary transcriptome via bulk RNA-seq. A better approach would be a longitudinal investigation that elucidates time as a contributing factor to spaceflight response.

Future Directions

Our research has identified putative genes and pathways implicated in age-differentiated pathological responses to spaceflight in mammary tissue. Future work may include single-cell RNA sequencing and proteomic sequencing to give higher resolution and downstream validation, respectively. Combining multiple datasets from similarly controlled experiments to increase the number of biological replicates would, in turn, increase confidence in our ML results. These findings offer valuable information for further studies into the impact of spaceflight on female astronaut health, reiterates well-established roles between spaceflight and breast cancer risk, and provides a straightforward ML approach to leverage a vast array of unexplored data.

Acknowledgments

The authors wish to acknowledge the JMIR reviewers who generously shared their time and expertise to provide invaluable feedback to improve this manuscript. The authors sincerely appreciate the opportunity to have openly discussed this manuscript with them.

Funding

This manuscript is the product of citizen science. No funding was made available for this research.

Data Availability

The notebook for this research is available at [54]. The OSD-511 dataset is available at [55].

Authors' Contributions

JC designed the experiments and wrote most of the manuscript. TZ and JY organized the efforts of the student researchers (AA, AR, AM, AF, KS, SL, WG, AL) who explored alternative approaches to processing the data and validated the references. The ensemble approach was conceived with SC; using linear decision boundary classifiers for ease of interpretation was conceived by MSC. All authors proofread the manuscript and provided their feedback.

Conflicts of Interest

None declared.

References

1. Nguyen HP, Tran PH, Kim KS, Yang SG. The effects of real and simulated microgravity on cellular mitochondrial function. NPJ Microgravity 2021 Nov 8;7(1):44. [doi: 10.1038/s41526-021-00171-7] [Medline: 34750383]
2. Beheshti A, Miller J, Kidane Y, Berrios D, Gebre SG, Costes SV. NASA GeneLab project: bridging space radiation omics with ground studies. Radiat Res 2018 Jun;189(6):553-559. [doi: 10.1667/RR15062.1] [Medline: 29652620]
3. Beheshti A, Cekanaviciute E, Smith DJ, Costes SV. Global transcriptomic analysis suggests carbon dioxide as an environmental stressor in spaceflight: a systems biology GeneLab case study. Sci Rep 2018 Mar 8;8(1):4191. [doi: 10.1038/s41598-018-22613-1] [Medline: 29520055]
4. Hughson RL, Helm A, Durante M. Heart in space: effect of the extraterrestrial environment on the cardiovascular system. Nat Rev Cardiol 2018 Mar;15(3):167-180. [doi: 10.1038/nrcardio.2017.157] [Medline: 29053152]
5. Comfort P, McMahon JJ, Jones PA, et al. Effects of spaceflight on musculoskeletal health: a systematic review and meta-analysis, considerations for interplanetary travel. Sports Med 2021 Oct;51(10):2097-2114. [doi: 10.1007/s40279-021-01496-9] [Medline: 34115344]
6. Crucian BE, Choukèr A, Simpson RJ, et al. Immune system dysregulation during spaceflight: potential countermeasures for deep space exploration missions. Front Immunol 2018;9:1437. [doi: 10.3389/fimmu.2018.01437] [Medline: 30018614]
7. Van Ombergen A, Demertzi A, Tomilovskaya E, et al. The effect of spaceflight and microgravity on the human brain. J Neurol 2017 Oct;264(Suppl 1):18-22. [doi: 10.1007/s00415-017-8427-x] [Medline: 28271409]
8. Beheshti A, Chakravarty K, Fogle H, et al. Multi-omics analysis of multiple missions to space reveal a theme of lipid dysregulation in mouse liver. Sci Rep 2019 Dec 16;9(1):19195. [doi: 10.1038/s41598-019-55869-2] [Medline: 31844325]
9. Mao X, Stanbouly S, Holley J, Pecaut M, Crapo J. Evidence of spaceflight-induced adverse effects on photoreceptors and retinal function in the mouse eye. Int J Mol Sci 2023 Apr 17;24(8):7362. [doi: 10.3390/ijms24087362] [Medline: 37108526]

XSL•FO
RenderX

10. Drago-Ferrante R, Di Fiore R, Karouia F, et al. Extraterrestrial gynecology: could spaceflight increase the risk of developing cancer in female astronauts? An updated review. Int J Mol Sci 2022 Jul 5;23(13):7465. [doi: 10.3390/ijms23137465] [Medline: 35806469]
11. Kumar K, Angdisen J, Ma J, Datta K, Fornace AJ, Suman S. Simulated galactic cosmic radiation exposure-induced mammary tumorigenesis in ApcMin/+ mice coincides with activation of ERα-ERRα-SPP1 signaling axis. Cancers (Basel) 2024 Nov 26;16(23):3954. [doi: 10.3390/cancers16233954] [Medline: 39682141]
12. Helm JS, Rudel RA. Adverse outcome pathways for ionizing radiation and breast cancer involve direct and indirect DNA damage, oxidative stress, inflammation, genomic instability, and interaction with hormonal regulation of the breast. Arch Toxicol 2020 May;94(5):1511-1549. [doi: 10.1007/s00204-020-02752-z] [Medline: 32399610]
13. Nassef MZ, Kopp S, Melnik D, et al. Short-term microgravity influences cell adhesion in human breast cancer cells. Int J Mol Sci 2019 Nov 15;20(22):5730. [doi: 10.3390/ijms20225730] [Medline: 31731625]
14. Barcellos-Hoff MH, Ravani SA. Irradiated mammary gland stroma promotes the expression of tumorigenic potential by unirradiated epithelial cells. Cancer Res 2000 Mar 1;60(5):1254-1260. [Medline: 10728684]
15. Mukhopadhyay R, Costes SV, Bazarov AV, Hines WC, Barcellos-Hoff MH, Yaswen P. Promotion of variant human mammary epithelial cell outgrowth by ionizing radiation: an agent-based model supported by in vitro studies. Breast Cancer Res 2010;12(1):R11. [doi: 10.1186/bcr2477] [Medline: 20146798]
16. Bartsch C, Bartsch H, Peschke E. Light, melatonin and cancer: current results and future perspectives 1. Biol Rhythm Res 2009 Feb;40(1):17-35. [doi: 10.1080/09291010802066983]
17. Malhan D, Schoenrock B, Yalçin M, Blottner D, Relógio A. Circadian regulation in aging: implications for spaceflight and life on earth. Aging Cell 2023 Sep;22(9):e13935. [doi: 10.1111/acel.13935] [Medline: 37493006]
18. Arnold C, Casaletto J, Heller P. Spaceflight disrupts gene expression of estrogen signaling in rodent mammary tissue. MRAJ 2024;12(3):3 [FREE Full text] [doi: 10.18103/mra.v12i3.5220]
19. Tang J, Fernandez-Garcia I, Vijayakumar S, et al. Irradiation of juvenile, but not adult, mammary gland increases stem cell self-renewal and estrogen receptor negative tumors. Stem Cells 2014 Mar;32(3):649-661. [doi: 10.1002/stem.1533] [Medline: 24038768]
20. Mertens AC, Liu Q, Neglia JP, et al. Cause-specific late mortality among 5-year survivors of childhood cancer: the Childhood Cancer Survivor Study. J Natl Cancer Inst 2008 Oct 1;100(19):1368-1379. [doi: 10.1093/jnci/djn310] [Medline: 18812549]
21. Monti N, Masiello MG, Proietti S, et al. Survival pathways are differently affected by microgravity in normal and cancerous breast cells. Int J Mol Sci 2021 Jan 16;22(2):862. [doi: 10.3390/ijms22020862] [Medline: 33467082]
22. Kannan S, Shailesh H, Mohamed H, Souchelnytskyi N, Souchelnytskyi S. A long-term 10G-hypergravity exposure promotes cell-cell contacts and reduces adhesiveness to a substrate, migration, and invasiveness of MCF-7human breast cancer cells. Exp oncol 2023 May;44(1):23-30. [doi: 10.32471/exp-oncology.2312-8852.vol-44-no-1.17270]
23. Sarkar SR, Pampaloni F. In vitro models of bone marrow remodelling and immune dysfunction in space: present state and future directions. Biomedicines 2022 Mar;10(4):766. [doi: 10.3390/biomedicines10040766]
24. Auslander N, Gussow AB, Koonin EV. Incorporating machine learning into established bioinformatics frameworks. Int J Mol Sci 2021 Mar 12;22(6):2903. [doi: 10.3390/ijms22062903] [Medline: 33809353]
25. Casaletto JA, Scott RT, Myrick M, et al. Analyzing the relationship between gene expression and phenotype in space-flown mice using a causal inference machine learning ensemble. Sci Rep 2025 Jan 18;15(1):2363. [doi: 10.1038/s41598-024-81394-y] [Medline: 39824847]
26. Feldner-Busztin D, Firbas Nisantzis P, Edmunds SJ, et al. Dealing with dimensionality: the application of machine learning to multi-omics data. Bioinformatics 2023 Feb 3;39(2):btad021. [doi: 10.1093/bioinformatics/btad021] [Medline: 36637211]
27. Jovic A, Brkic K, Bogunovic N. A review of feature selection methods with applications. Presented at: 2015 38th International Convention on Information and Communication Technology, Electronics and Microelectronics (MIPRO); May 25-29, 2015; Opatija, Croatia p. 1200-1205. [doi: 10.1109/MIPRO.2015.7160458]
28. Rincy TN, Gupta R. Ensemble learning techniques and its efficiency in machine learning: a survey. 2020 Presented at: 2020 2nd International Conference on Data, Engineering and Applications (IDEA); Feb 28-29, 2020; Bhopal, India p. 1-6. [doi: 10.1109/IDEA49133.2020.9170675]
29. United States. Health Research Extension Act of 1985. Public Law 99-158. US Statut Large 1985;99(Title IV Sections 1-12). [Medline: 11686169]
30. Sanders LM, Lopez DK, Wood AE, et al. Celebrating 30 years of access to NASA Space Life Sciences data. Gigascience 2024 Jan 2;13:giae066. [doi: 10.1093/gigascience/giae066] [Medline: 39283686]
31. Galazka JM, et al. Transcriptional profiling of mammary glands from mice flown on the RRRM-1 mission. NASA GeneLab 2022 Aug 3. [doi: 10.26030/WDPR-VA45]
32. DeMaris A, Selman SH. Logistic regression. In: Converting Data into Evidence: Springer; 2013:115-136. [doi: 10.1007/978-1-4614-7792-1_7]
33. Singh J, Banerjee R. A study on single and multi-layer perceptron neural network. 2019 Mar Presented at: 2019 3rd International Conference on Computing Methodologies and Communication (ICCMC); Mar 27-29, 2019; Erode, India p. 35-40. [doi: 10.1109/ICCMC.2019.8819775]
34. Cortes C, Vapnik V. Support-vector networks. Mach Learn 1995 Sep;20(3):273-297. [doi: 10.1007/BF00994018]

XSL•FO
RenderX

35. Dietterich TG. Ensemble methods in machine learning. Presented at: Multiple Classifier Systems, in Lecture Notes in Computer Science; Jun 21-23, 2000; Cagliari, Italy p. 1-15. [doi: 10.1007/3-540-45014-9_1]
36. ShinyGO 0.85.1. URL: http://bioinformatics.sdstate.edu/go/ [accessed 2025-12-23]
37. Kanehisa M, Goto S. KEGG: Kyoto encyclopedia of genes and genomes. Nucleic Acids Res 2000 Jan 1;28(1):27-30. [doi: 10.1093/nar/28.1.27] [Medline: 10592173]
38. Pérez-González A, Bévant K, Blanpain C. Cancer cell plasticity during tumor progression, metastasis and response to therapy. Nat Cancer 2023 Aug;4(8):1063-1082. [doi: 10.1038/s43018-023-00595-y] [Medline: 37537300]
39. Kourtis N, Tavernarakis N. Cellular stress response pathways and ageing: intricate molecular relationships. EMBO J 2011 May 17;30(13):2520-2531. [doi: 10.1038/emboj.2011.162] [Medline: 21587205]
40. Ferrucci L, Fabbri E. Inflammageing: chronic inflammation in ageing, cardiovascular disease, and frailty. Nat Rev Cardiol 2018 Sep;15(9):505-522. [doi: 10.1038/s41569-018-0064-2] [Medline: 30065258]
41. Azzam EI, Jay-Gerin JP, Pain D. Ionizing radiation-induced metabolic oxidative stress and prolonged cell injury. Cancer Lett 2012 Dec 31;327(1-2):48-60. [doi: 10.1016/j.canlet.2011.12.012] [Medline: 22182453]
42. Rizzo AM, Corsetto PA, Montorfano G, et al. Effects of long-term space flight on erythrocytes and oxidative stress of rodents. PLoS One 2012;7(3):e32361. [doi: 10.1371/journal.pone.0032361] [Medline: 22412864]
43. Rakhshandehroo M, Knoch B, Müller M, Kersten S. Peroxisome proliferator-activated receptor alpha target genes. PPAR Res 2010;2010:1-20. [doi: 10.1155/2010/612089] [Medline: 20936127]
44. Dai DF, Chiao YA, Marcinek DJ, Szeto HH, Rabinovitch PS. Mitochondrial oxidative stress in aging and healthspan. Longev Healthspan 2014;3(1):6. [doi: 10.1186/2046-2395-3-6] [Medline: 24860647]
45. Qian Z, Chen L, Liu J, Jiang Y, Zhang Y. The emerging role of PPAR-alpha in breast cancer. Biomedicine & Pharmacotherapy 2023 May;161:114420. [doi: 10.1016/j.biopha.2023.114420]
46. Simeone AM, Tari AM. How retinoids regulate breast cancer cell proliferation and apoptosis. Cell Mol Life Sci 2004 Jun;61(12):1475-1484. [doi: 10.1007/s00018-004-4002-6] [Medline: 15197471]
47. Stoll BA. Linkage between retinoid and fatty acid receptors: implications for breast cancer prevention. Eur J Cancer Prev 2002 Aug;11(4):319-325. [doi: 10.1097/00008469-200208000-00002] [Medline: 12195157]
48. Crowe DL, Chandraratna RAS. A retinoid X receptor (RXR)-selective retinoid reveals that RXR-alpha is potentially a therapeutic target in breast cancer cell lines, and that it potentiates antiproliferative and apoptotic responses to peroxisome proliferator-activated receptor ligands. Breast Cancer Res 2004;6(5):R546-R555. [doi: 10.1186/bcr913] [Medline: 15318936]
49. Plutzky J. The PPAR-RXR transcriptional complex in the vasculature: energy in the balance. Circ Res 2011 Apr 15;108(8):1002-1016. [doi: 10.1161/CIRCRESAHA.110.226860] [Medline: 21493923]
50. Bougarne N, Weyers B, Desmet SJ, et al. Molecular actions of PPARα in lipid metabolism and inflammation. Endocr Rev 2018 Oct 1;39(5):760-802. [doi: 10.1210/er.2018-00064] [Medline: 30020428]
51. López-Otín C, Pietrocola F, Roiz-Valle D, Galluzzi L, Kroemer G. Meta-hallmarks of aging and cancer. Cell Metab 2023 Jan 3;35(1):12-35. [doi: 10.1016/j.cmet.2022.11.001] [Medline: 36599298]
52. Zhang TH, Hasib MM, Chiu YC, et al. Transformer for gene expression modeling (T-GEM): an interpretable deep learning model for gene expression-based phenotype predictions. Cancers (Basel) 2022 Sep 29;14(19):4763. [doi: 10.3390/cancers14194763] [Medline: 36230685]
53. Smith AM, Walsh JR, Long J, et al. Standard machine learning approaches outperform deep representation learning on phenotype prediction from transcriptomics data. BMC Bioinformatics 2020 Mar 20;21(1):119. [doi: 10.1186/s12859-020-3427-8] [Medline: 32197580]
54. Mammary_final_v3.ipynb. Google Colab. URL: https://colab.research.google.com/drive/1ZLB32UQZ_Byc9ja0DpLs30u0VvwuAucu [accessed 2025-12-23]
55. OSD-511. version 4. transcriptional profiling of mammary glands from mice flown on the RRRM-1 mission. NASA OSDR. URL: https://osdr.nasa.gov/bio/repo/data/studies/OSD-511 [accessed 2025-12-23]

Abbreviations

AI: artificial intelligence
cnd: condition
FLT: flight
GC: ground control
KEGG: Kyoto Encyclopedia of Genes and Genomes
LR: logistic regression
ML: machine learning
NASA: National Aeronautics and Space Administration
OLD: old
PCA: principal component analysis
PPAR: peroxisome proliferator-activated receptor
RNA-seq: RNA-sequencing

XSL•FO
RenderX

RRRM-1: Rodent Research Reference Mission 1
RSEM: RNA-Seq by Expectation Maximization
SGD: stochastic gradient descent
SLP: single-layer perceptron
STAR: Spliced Transcripts Alignment to a Reference
SVM: support vector machine
VIV: vivarium
YNG: young

Edited by A Schwartz; submitted 24.Feb.2025; peer-reviewed by S Sakilay, M Collier, A Rahgozar, T Olatoye, SM Savai, M Pulier, RSG Mahmoud, CAN Akpan, S Mitra, J Moonga; revised version received 26.Oct.2025; accepted 26.Nov.2025; published 14.Jan.2026.

Please cite as:
Casaletto JA, Zhao T, Yeung J, Lee A, Ansari A, Fry A, Mishra A, Raj A, Sun K, Lendahl S, Guan W, Cline MS, Costes SV
Machine Learning Ensemble Investigates Age in the Transcriptomic Response to Spaceflight in Murine Mammary Tissue: Observational Study
JMIRx Bio 2026;4:e73041
URL: https://bio.jmirx.org/2026/1/e73041
doi:10.2196/73041

© James A Casaletto, Tyler Zhao, Jay Yeung, Abigail Lee, Amaan Ansari, Amber Fry, Arnav Mishra, Ayush Raj, Kathryn Sun, Sofia Lendahl, Willy Guan, Melissa S Cline, Sylvain V Costes. Originally published in JMIRx Bio (https://bio.jmirx.org), 14.Jan.2026. This is an open-access article distributed under the terms of the Creative Commons Attribution License (https://creativecommons.org/licenses/by/4.0/), which permits unrestricted use, distribution, and reproduction in any medium, provided the original work, first published in JMIRx Bio, is properly cited. The complete bibliographic information, a link to the original publication on https://bio.jmirx.org/, as well as this copyright and license information must be included.

XSL•FO
RenderX

Peer Review of “Relationship Between Seed Coat Color and Cytokinin Concentration in Efficiently Regenerating Leaf Lettuce Shoots: In Vitro Experimental Study”

Ahmed Madi Waheed Al-Mayahi

Related Articles:

https://www.biorxiv.org/content/10.1101/2024.12.10.627673v1

https://bio.jmirx.org/2026/1/e89391

https://bio.jmirx.org/2026/1/e70496

(JMIRx Bio 2026;4:e89401) doi:10.2196/89401

KEYWORDS

leaf lettuce; shoot regeneration efficiency; 6-benzylaminopurine; seed coat color; CIELAB color scale; flavonoid; BAP

This is the peer-review report for “Relationship Between Seed Coat Color and Cytokinin Concentration in Efficiently Regenerating Leaf Lettuce Shoots: In Vitro Experimental Study.”

Round 1 Review

General Comments

Major Comments

- The presented work [1] brings new information.
- At the beginning of your abstract, you should write a paragraph about the problem you want to solve.
- The abstract mentions statistical significance but does not provide any details about how these were assessed or the significance level (eg, *P* value). Details on the statistical analysis methods used (eg, “significant at *P*<.05”) should be added.
- The Introduction contains well-documented data that are widely known. Hormonal information has been extensively reported and reviewed. Against this background, authors have to point out how this work is different from the earlier reported work; what are the innovative findings reported here? A strong and convincing justification is required.
- Introduction: While references are important, the paragraph reads as somewhat overloaded with citations. Many sentences contain a high number of citations, which can disrupt the readability of the text. Try to reduce the frequency of citations by grouping them more effectively and summarizing the findings rather than listing individual sources for every claim. This will help make the text more fluid.
- The Methods section in its current form is not acceptable because it requires more details, such as the latitude and longitude of the culture area. Write a simple paragraph describing the climate of the area and date of study.
- It is necessary to mention the active ingredient of commercial chlorine bleach.
- Tween-20 is used with disinfectants to reduce surface tension, thus increasing the disinfectant’s effectiveness.
- State the manufacturer of the MS medium and the quantity used to prepare it half-strength.
- How were the hormone solutions prepared and dissolved?
- KOH and HCl are used in the pH adjustment process.
- It is necessary to mention the lighting intensity during the incubation period of the cultures.
- The statistical analysis mentions EZR software, but there is no explanation of why this particular software was chosen.
- In the Discussion, authors have explained various biochemical interactions and mechanisms that are widely known and reported. Authors should give their own reflections of the work. It is essential to include the advantages and shortcomings of the work; what are the limitations of this technology and its shortfalls? Authors’ own scrutiny of the data clarifications is decisive for the impending research on this subject. This work is field-oriented, the cost-benefit ratio is very significant, and micropropagation will increase the cost, but this has not been commented on in the text. Scale-up of the tissue culture plant is not an easy task and would be challenging work.
- Conclusion: What does this infer for lettuce production? Need a little more work to show the significance of your work.
- References: It is advised to refer only to recent work and not old citations.

XSL•FO
RenderX

Round 2 Review

General Comments

After reviewing the manuscript, I found substantial improvements, which positively impacted its scientific value. Therefore, the manuscript meets the requirements for publication.

Conflicts of Interest

None declared.

Reference

1. Kimura M, Yoshizumi T. Relationship between seed coat color and cytokinin concentration in efficiently regenerating leaf lettuce shoots: in vitro experimental study. JMIRx Bio 2026;4:e70496. [doi: 10.2196/70496]

Edited by B Ikhajiagbe; submitted 11.Dec.2025; this is a non–peer-reviewed article;accepted 11.Dec.2025; published 08.Jan.2026.

Please cite as:
Al-Mayahi AMW
Peer Review of "Relationship Between Seed Coat Color and Cytokinin Concentration in Efficiently Regenerating Leaf Lettuce Shoots: In Vitro Experimental Study"
JMIRx Bio 2026;4:e89401
URL: https://bio.jmirx.org/2026/1/e89401
doi:10.2196/89401

© Ahmed Madi Waheed Al-Mayahi. Originally published in JMIRx Bio (https://bio.jmirx.org), 8.Jan.2026. This is an open-access article distributed under the terms of the Creative Commons Attribution License (https://creativecommons.org/licenses/by/4.0/), which permits unrestricted use, distribution, and reproduction in any medium, provided the original work, first published in JMIRx Bio, is properly cited. The complete bibliographic information, a link to the original publication on https://bio.jmirx.org/, as well as this copyright and license information must be included.

XSL•FO
RenderX

Peer Review of “Relationship Between Seed Coat Color and Cytokinin Concentration in Efficiently Regenerating Leaf Lettuce Shoots: In Vitro Experimental Study”

Hamidreza Soufi

Related Articles:

https://www.biorxiv.org/content/10.1101/2024.12.10.627673v1

https://bio.jmirx.org/2026/1/e89391

https://bio.jmirx.org/2026/1/e70496

(JMIRx Bio 2026;4:e89399) doi:10.2196/89399

KEYWORDS

leaf lettuce; shoot regeneration efficiency; 6-benzylaminopurine; seed coat color; CIELAB color scale; flavonoid; BAP

This is the peer-review report for “Relationship Between Seed Coat Color and Cytokinin Concentration in Efficiently Regenerating Leaf Lettuce Shoots: In Vitro Experimental Study.”

Round 1 Review

Reviewer’s Comments on the Manuscript

The manuscript [1] presents a well-structured and novel study exploring the correlation between seed coat color and the optimal concentration of 6-benzylaminopurine (BAP) for shoot regeneration in leaf lettuce cultivars. The research is timely and addresses a significant challenge in plant tissue culture—genotypic variability in regeneration efficiency.

Strengths

The experimental design is solid, involving 6 cultivars with distinct seed coat colors.

The use of the CIELAB color scale adds objectivity to phenotypic assessments.

The identification of seed coat color as a potential morphological marker for shoot regeneration efficiency is innovative and potentially valuable for breeding and transformation programs.

Suggestions for Improvement

Language and clarity: While the scientific content is strong, the manuscript would benefit from careful language editing for grammar and fluency.

Statistical reporting: The statistical significance (eg, *P* values) is noted, but a more detailed description of the statistical models and effect sizes would enhance reproducibility.

Figures and tables: Ensure that all figures and tables referenced (eg, Figure 1, Table S1) are clearly labeled and formatted for clarity. Including a visual summary (graphical abstract) could further enhance impact.

Discussion depth: The discussion of mechanisms linking seed coat pigmentation to shoot regeneration could be expanded, possibly integrating flavonoid biosynthesis and tissue culture responsiveness more.

Conclusion: Consider sharpening the Conclusion to emphasize the practical applications of the findings, especially in the context of lettuce transformation systems.

Overall, this is a meaningful contribution to plant biotechnology literature and warrants publication after minor revisions.

Conflicts of Interest

None declared.

Reference

1. Kimura M, Yoshizumi T. Relationship between seed coat color and cytokinin concentration in efficiently regenerating leaf lettuce shoots: in vitro experimental study. JMIRx Bio 2026;4:e70496. [doi: 10.2196/70496]

XSL•FO
RenderX

Edited by B Ikhajiagbe; submitted 11.Dec.2025; this is a non–peer-reviewed article;accepted 11.Dec.2025; published 08.Jan.2026.

Please cite as:
Soufi H
Peer Review of "Relationship Between Seed Coat Color and Cytokinin Concentration in Efficiently Regenerating Leaf Lettuce Shoots: In Vitro Experimental Study"
JMIRx Bio 2026;4:e89399
URL: https://bio.jmirx.org/2026/1/e89399
doi:10.2196/89399

© Hamidreza Soufi. Originally published in JMIRx Bio (https://bio.jmirx.org), 8.Jan.2026. This is an open-access article distributed under the terms of the Creative Commons Attribution License (https://creativecommons.org/licenses/by/4.0/), which permits unrestricted use, distribution, and reproduction in any medium, provided the original work, first published in JMIRx Bio, is properly cited. The complete bibliographic information, a link to the original publication on https://bio.jmirx.org/, as well as this copyright and license information must be included.

XSL•FO
RenderX

Peer Review of “Localized Immune Cascade Programming in Desmoplastic Tumors: In Silico Modeling and Validation Study”

Sunny Chi Lik Au

Tung Wah Eastern Hospital, So Kon Po, China (Hong Kong)

Related Articles:

http://preprints.jmir.org/preprint/85507

https://bio.jmirx.org/2026/1/e91528

https://bio.jmirx.org/2026/1/e85507

(JMIRx Bio 2026;4:e91450) doi:10.2196/91450

KEYWORDS

oncology; tumor microenvironment; cancer microenvironment; immunology; immune-cold tumors; intratumoral immunotherapy; extracellular matrix remodeling

This is the peer-review report for “Localized Immune Cascade Programming in Desmoplastic Tumors: In Silico Modeling and Validation Study.”

Round 1 Review

General Comments

This paper [1] presents a conceptual framework for a sequential, localized immune cascade (“Second Breath”) aimed at reprogramming “immune-cold” desmoplastic tumors to enhance immunotherapy responsiveness. It is positioned as a preclinical concept paper, relying entirely on literature synthesis and in silico modeling without generating new experimental data. While the integration of immunology, biochemistry, and systems biology concepts is ambitious and potentially innovative, the work has significant limitations.

Specific Comments

Major Comments

1. The abstract does not require reference citations. Please remove the citations in the abstract. If reference citations are deemed really necessary, please start with 1 instead of 4. Also, please go on in ascending order instead of skipping references, like [4,5,6,7,32,33].
2. The main text instead should be backed up by reference citations to increase its value. However, the same principle also applies to starting from 1 and continuing in ascending order, but not starting in the middle and skipping references. Also, the references need to be cited in a uniform format. The following needs to be revised in the Introduction: “...(ECM) [6,7,32,33]....(ICIs) [13,14,15]....exposure [1,2,4,5,9,10,11].....Therapy for a Sustainable Outcome’ (M. Novruzov, 2025),...” The same format of reference citations should be used, thus “(M. Novruzov, 2025)” should be cited as per others: “[n].” Please revise.
3. The references are drawn from reputable sources, but the synthesis appears biased toward supportive evidence. For example, citations for bacterial priming (eg, Clostridium novyi-NT) highlight antitumor responses but downplay failures in clinical trials, such as high toxicity or limited efficacy in advanced tumors. Similarly, extracellular matrix (ECM) modulation via collagenase/hyaluronidase is presented positively but ignores biochemical drawbacks like enzyme instability in vivo, nonspecific proteolysis leading to tissue damage, or rebound ECM deposition. It is unclear how the authors reconciled conflicting literature. For example, the Wnt pathway enrichment is noted as dominant, but its protumorigenic role in desmoplastic tumors (eg, promoting fibrosis via β-catenin) is only briefly mentioned in the Discussion without quantitative risk assessment. Please add in a more balanced view and references.
4. The framework proposes a 10-stage sequence, gated by biomarkers like interferon (IFN)–γ signature or interstitial fluid pressure reduction. However, this complexity introduces numerous failure points without clear prioritization. Biochemically, the “IL-12 → IFN-γ → TNF-α axis” assumes linear signaling, ignoring feedback loops (eg, tumor necrosis factor α [TNF-α]–induced apoptosis resistance via NF-κB) or crosstalk with immunosuppressive pathways (eg, transforming growth factor β in desmoplastic stroma). The “Warmth Readiness Index (WRI)” is mentioned but undefined quantitatively. How is it calculated? What thresholds were derived from it? This vagueness makes the model hard to falsify, as the “prediction matrix” relies on qualitative outcomes rather than measurable biochemical end points. Please revise and supplement.
5. The go/no-go criteria (eg, “≥2-fold fold increase in CXCL9/10/11”) are arbitrary; please justify them from literature or simulations.

XSL•FO
RenderX

Round 2 Review

General Comments

This paper has undergone revisions and looks much better.

Specific Comments

Major Comments

1. The references do not appear in ascending order upon a citation in the main text. The first citation that showed up was "[6-7,32-33]," followed by "[13-15]," and then "[1-2,4-5,9-11]."

The authors also addressed this in their rebuttal letter, showing their difficulties in rearranging the list of references, because such an adjustment would require rewriting the article from scratch, which is beyond the scope of the current revision. They are open to discussion on an alternative option for formatting references that would preserve the structure of the work. I think the editorial office or I can help rearrange the reference numbers.

Conflicts of Interest

None declared.

Reference

1. Novruzov M, Mammadova M, Raval K, Khan WU, Shiraliyeva U. Localized immune cascade programming in desmoplastic tumors: in silico modeling and validation study. JMIRx Bio 2026;4:e85507. [doi: 10.2196/85507]

Abbreviations

ECM: extracellular matrix
IFN: interferon
TNF-α: tumor necrosis factor α

Edited by M Yadav; submitted 14.Jan.2026; this is a non–peer-reviewed article;accepted 14.Jan.2026; published 27.Feb.2026.

Please cite as:
Au SCL
Peer Review of "Localized Immune Cascade Programming in Desmoplastic Tumors: In Silico Modeling and Validation Study"
JMIRx Bio 2026;4:e91450
URL: https://bio.jmirx.org/2026/1/e91450
doi:10.2196/91450

© Sunny Chi Lik Au. Originally published in JMIRx Bio (https://bio.jmirx.org), 27.Feb.2026. This is an open-access article distributed under the terms of the Creative Commons Attribution License (https://creativecommons.org/licenses/by/4.0/), which permits unrestricted use, distribution, and reproduction in any medium, provided the original work, first published in JMIRx Bio, is properly cited. The complete bibliographic information, a link to the original publication on https://bio.jmirx.org/, as well as this copyright and license information must be included.

XSL•FO
RenderX

Peer Review of “Localized Immune Cascade Programming in Desmoplastic Tumors: In Silico Modeling and Validation Study”

Nivetha Brathaban

Nurix, San Francisco, CA, United States

Related Articles:

http://preprints.jmir.org/preprint/85507

https://bio.jmirx.org/2026/1/e91528

https://bio.jmirx.org/2026/1/e85507

(JMIRx Bio 2026;4:e91447) doi:10.2196/91447

KEYWORDS

oncology; tumor microenvironment; cancer microenvironment; immunology; immune-cold tumors; intratumoral immunotherapy; extracellular matrix remodeling

This is the peer-review report for “Localized Immune Cascade Programming in Desmoplastic Tumors: In Silico Modeling and Validation Study.”

Round 1 Review

General Comments

In this paper [1], overall, there is a clear scientific narrative defining “second breath” as a testable conceptual framework for converting immune-cold tumors to a more responsive state. The graphical representation of the model and the concise logical sequence make the manuscript more appealing to read. The Introduction highlights key biological barriers like low T-cell infiltration, dense extracellular matrix, and stromal resistance that justify the need for a localized immune therapy. The overall study framework is clearly articulated, well-structured, and presented in a concise and accessible manner. The citations are well integrated and support the key arguments effectively. The abstract is informative, but the functional role of β-catenin/Wnt–linked programs in the cascade requires more clarity. The Results section highlighting Wnt signaling dominance is contradictory to the existing literature and the Discussion section of the manuscript, which requires further supporting evidence with human-specific models.

Specific Comments

Major Comments

1. Wnt-signaling dominance in the Results section: It is known that APC, CTNNB1, and AXIN1 gene mutations of the canonical Wnt/β-catenin pathway give rise to cancers. Inappropriate activation of the Wnt/β-catenin pathway is believed to be involved in carcinogenesis. Specifically, there are multiple genetic abnormalities involved in the activation of the Wnt/β-catenin pathway; nonetheless, the CTNNB1 mutation is a typical driver mutation that is found in approximately 30% of hepatocellular carcinoma cases. In 2015, Spranger et al [2] reported that the Wnt/β-catenin pathway activation inhibits cytotoxic T-cell infiltration in the immune microenvironment of malignant melanoma, resulting in resistance to immune checkpoint inhibitors. Wnt/β-catenin signaling was shown to inhibit this dendritic cell invasion into the tumor. However, the manuscript has reported dominance of Wnt signaling in the pathway enrichment analysis, which is contradictory. Provide more clarity by offering more predictive insights into human-specific responses. The Discussion raises important safety concerns, and so to strengthen practical relevance, propose any mitigation strategies or alternative approaches.

Minor Comments

1. Although it is stated in the manuscript that “Second breath” represents a novel preclinical approach for antitumor immunity, kindly clarify the novelty by elaborating on how the model is better than existing intratumoral immunotherapy strategies (like immunostimulatory antibodies, gene therapy, and combination therapy) while both are aimed at limiting systemic toxicities. A strong statement is needed emphasizing how the model can be translated into a therapeutic approach.
2. While the sequential representation in the Materials section is clear and logically structured, the overall writing tends to be overly repetitive and unnecessarily elaborate, which makes it difficult to follow and detracts from readability. I’d suggest streamlining the content of the Materials and Methods section.

Round 2 Review

General Comments

Overall, the authors have made commendable efforts to address the majority of the primary comments in the revised submission.

XSL•FO
RenderX

Nonetheless, the Discussion section remains problematic due to conflicting interpretations of the literature and insufficient data to address potential safety concerns.

Specific Comments

Major Comments

1. Add more references to paragraph 3 of the Discussion section: As the proposed model is entirely in silico and derived from literature synthesis without experimental validation, the Discussion requires greater precision and depth. To enhance its rigor, the author should incorporate additional references that present experimental data or propose concrete mitigation strategies to address the model's limitations and potential toxicities. Moreover, the Discussion would benefit from supporting evidence derived from human-specific models to strengthen the translational relevance of the findings. Provide more clarity by offering more predictive insights into human-specific responses. The Discussion raises important safety concerns and needs to strengthen its practical relevance. The paradox of Wnt enrichment versus fibrosis/immunosuppression is noted but left unresolved.
2. The Introduction could be confusing for readers. Earlier in the Introduction, the conceptual framework is proposed to consist of five modules, but later in the text, it expands into a 7-stage framework. This discrepancy could confuse readers. Consider harmonizing the framework (define stages clearly and keep it consistent).

Round 3 Review

General Comments

The authors have undertaken considerable revisions in response to the comments, and the incorporation of additional references has notably reinforced the model's scientific grounding and its "testable" framework. These revisions substantially enhance the clarity, rigor, and coherence of the manuscript. Inclusion of additional references strengthens the Discussion by addressing the Wnt/β-catenin paradox. The Introduction looks more refined now with harmonization of the framework nomenclature. Presenting the 10 sequential intervention stages within five functional modules creates a consistent organizational structure that will help readers navigate the conceptual workflow without ambiguity.

Overall, these revisions significantly elevate the manuscript's scientific robustness, and they position the work more effectively within the current landscape of tumor microenvironment research to provide effective antitumor immunity.

Conflicts of Interest

None declared.

References

1. Novruzov M, Mammadova M, Raval K, Khan WU, Shiraliyeva U. Localized immune cascade programming in desmoplastic tumors: in silico modeling and validation study. JMIRx Bio 2026;4:e85507. [doi: 10.2196/85507]
2. Spranger S, Bao R, Gajewski TF. Melanoma-intrinsic β-catenin signalling prevents anti-tumour immunity. Nature New Biol 2015 Jul 9;523(7559):231-235. [doi: 10.1038/nature14404] [Medline: 25970248]

Edited by M Yadav; submitted 14.Jan.2026; this is a non–peer-reviewed article;accepted 14.Jan.2026; published 27.Feb.2026.

Please cite as:
Brathaban N
Peer Review of "Localized Immune Cascade Programming in Desmoplastic Tumors: In Silico Modeling and Validation Study"
JMIRx Bio 2026;4:e91447
URL: https://bio.jmirx.org/2026/1/e91447
doi:10.2196/91447

© Nivetha Brathaban. Originally published in JMIRx Bio (https://bio.jmirx.org), 27.Feb.2026. This is an open-access article distributed under the terms of the Creative Commons Attribution License (https://creativecommons.org/licenses/by/4.0/), which permits unrestricted use, distribution, and reproduction in any medium, provided the original work, first published in JMIRx Bio, is properly cited. The complete bibliographic information, a link to the original publication on https://bio.jmirx.org/, as well as this copyright and license information must be included.

XSL•FO
RenderX

Peer Review of “Material-Driven Therapeutics to Establish a Penetrating Traumatic Brain Injury Rat Model and Implantation of a 3D-Printed Scaffold: Pre-Experimental Pilot Study”

Firas Kobeissy

Morehouse School of Medicine, Atlanta, GA, United States

Related Articles:

https://www.biorxiv.org/content/10.1101/2025.03.20.644358v1

https://bio.jmirx.org/2026/1/e105278

https://bio.jmirx.org/2026/1/e75613

(JMIRx Bio 2026;4:e105277) doi:10.2196/105277

KEYWORDS

penetrating traumatic brain injury; stereotaxic surgery; graphene; nerve tissue engineering; rat model

This is a peer review report for “Material-Driven Therapeutics to Establish a Penetrating Traumatic Brain Injury Rat Model and Implantation of a 3D-Printed Scaffold: Pre-Experimental Pilot Study.”

Round 1 Review

General Comments

The manuscript [1] presents a well-rationalized pilot study aimed at establishing a reproducible penetrating traumatic brain injury rat model that permits controlled blood-brain barrier disruption and scaffold implantation. Its strengths lie in the thorough description of surgical methods, appropriate use of immunohistochemical markers, and clear identification of mild focal injury in most animals. The incorporation of poly(d,l-lactide-co-glycolide (PLGA)/reduced graphene oxide (rGO) scaffolds and the evaluation of their biocompatibility add translational relevance.

Specific Comments

Major Comments

1. A key weakness of the study is its very small sample size (n=4), which substantially limits the statistical power, generalizability, and reliability of the conclusions. With such a low n, it becomes difficult to determine whether the observed variability—particularly the severe inflammatory response in one animal—reflects true biological differences, procedural inconsistencies, or random outliers.
2. The study lacks control groups—including a sham surgery group and a traumatic brain injury–only group—preventing clear attribution of histological changes to either the injury model or the implanted scaffold.
3. The behavioral assessment is limited to a modified neurological severity score, which is often insensitive to mild or focal injuries and may miss subtle cognitive or sensorimotor deficits.
4. The study would be strengthened by incorporating additional validated behavioral tests.

Round 2 Review

General Comments

This paper is acceptable.

Conflicts of Interest

None declared.

Reference

1. Harley-Troxell ME, Dennis M, Dhar M. Material-driven therapeutics to establish a penetrating traumatic brain injury rat model and implantation of a 3D-printed scaffold: pre-experimental pilot study. JMIRx Bio 2026;4:e75613. [doi: 10.2196/75613]

XSL•FO
RenderX

Edited by A Schwartz; submitted 22.Jun.2026; this is a non–peer-reviewed article;accepted 22.Jun.2026; published 10.Jul.2026.

Please cite as:
Kobeissy F
Peer Review of "Material-Driven Therapeutics to Establish a Penetrating Traumatic Brain Injury Rat Model and Implantation of a 3D-Printed Scaffold: Pre-Experimental Pilot Study"
JMIRx Bio 2026;4:e105277
URL: https://bio.jmirx.org/2026/1/e105277
doi:10.2196/105277

© Firas Kobeissy. Originally published in JMIRx Bio (https://bio.jmirx.org), 10.Jul.2026. This is an open-access article distributed under the terms of the Creative Commons Attribution License (https://creativecommons.org/licenses/by/4.0/), which permits unrestricted use, distribution, and reproduction in any medium, provided the original work, first published in JMIRx Bio, is properly cited. The complete bibliographic information, a link to the original publication on https://bio.jmirx.org/, as well as this copyright and license information must be included.

XSL•FO
RenderX

Authors' Response to Peer Reviews of "Relationship Between Seed Coat Color and Cytokinin Concentration in Efficiently Regenerating Leaf Lettuce Shoots: In Vitro Experimental Study"

Mitsuhiro Kimura[1,2]; Takeshi Yoshizumi[1]

[1]Takasaki University of Health and Welfare, 54 Nakaorui-machi, Takasaki, Japan

[2]Kyushu University, 744 Motooka, Nishi-ku, Fukuoka, Japan

Corresponding Author:
Mitsuhiro Kimura
Takasaki University of Health and Welfare, 54 Nakaorui-machi, Takasaki, Japan

Related Articles:

https://www.biorxiv.org/content/10.1101/2024.12.10.627673v1

https://bio.jmirx.org/2026/1/e89399

https://bio.jmirx.org/2026/1/e89401

https://bio.jmirx.org/2026/1/e70496

(JMIRx Bio 2026;4:e89391) doi:10.2196/89391

KEYWORDS

leaf lettuce; shoot regeneration efficiency; 6-benzylaminopurine; seed coat color; CIELAB color scale; flavonoid; BAP

This is the authors' response to peer-review reports for "Relationship Between Seed Coat Color and Cytokinin Concentration in Efficiently Regenerating Leaf Lettuce Shoots: In Vitro Experimental Study."

Round 1 Review

Reviewer DQ [1]

The reviewer acknowledged the novelty and robustness of our study [2] but suggested improving the language, statistical reporting, and discussion depth.

Language and clarity: While the scientific content is strong, the manuscript would benefit from careful language editing for grammar and fluency.

- **Response:** The manuscript was professionally proofread for grammar and clarity.
- *Statistical reporting: The statistical significance (eg, P values) is noted, but a more detailed description of the statistical models and effect sizes would enhance reproducibility.*
- **Response:** Statistical methods are now detailed in the Methods section (one-way ANOVA with Tukey test, $P<.05$).
- *Figures and tables: Ensure that all figures and tables referenced (eg, Figure 1, Table S1) are clearly labeled and formatted for clarity.*
- **Response:** All figures and tables have been relabeled and referenced in the correct order.
- *Discussion depth: The discussion of mechanisms linking seed coat pigmentation to shoot regeneration could be expanded, possibly integrating flavonoid biosynthesis and tissue culture responsiveness more.*
- **Response:** The Results and Discussion section now includes an expanded interpretation linking flavonoid metabolism to cytokinin responsiveness.
- *Conclusion: Consider sharpening the Conclusion to emphasize the practical applications of the findings, especially in the context of lettuce transformation systems.*
- **Response:** The Conclusion emphasizes the practical application of optimizing transformation efficiency in lettuce.
- *Including a visual summary (graphical abstract) could further enhance impact.*
- **Response:** A graphical abstract was considered but omitted because Figures 1-3 fully summarize the experimental results.

Reviewer FA [3]

- *At the beginning of your abstract, you should write a paragraph about the problem you want to solve.*
- **Response:** The Abstract begins with a clear problem statement: cultivar-dependent shoot regeneration efficiency.
- *The abstract mentions statistical significance but does not provide any details about how these were assessed or the*

XSL•FO
RenderX

significance level (eg, P value). Details on the statistical analysis methods used (eg, "significant at P<.05") should be added.

- **Response:** Quantitative and statistical details ($P<.05$) have been added to the Abstract.
- *The Introduction contains well-documented data that are widely known. Hormonal information has been extensively reported and reviewed. Against this background, authors have to point out how this work is different from the earlier reported work; what are the innovative findings reported here? A strong and convincing justification is required.*
- **Response:** The Introduction has been rewritten to clarify the originality and novelty of our study.
- *The Methods section in its current form is not acceptable because it requires more details, such as the latitude and longitude of the culture area. Write a simple paragraph describing the climate of the area and date of study.*
- *It is necessary to mention the active ingredient of commercial chlorine bleach.*
- *KOH and HCl are used in the pH adjustment process.*
- **Response:** These Methods have been expanded to include climate information (humid subtropical, Cfa), bleach composition (6% NaOCl, final 1.2%), and pH adjustment (KOH/HCl).
- *Tween-20 is used with disinfectants to reduce surface tension, thus increasing the disinfectant's effectiveness.*
- **Response:** Tween-20 was mentioned by the reviewer but was not used in our sterilization protocol. Surface sterilization was performed using 70% ethanol and 20% bleach without surfactants.
- *It is necessary to mention the lighting intensity during the incubation period of the cultures.*
- **Response:** The light intensity during incubation was approximately 300 µmol m^{-2} s^{-1} under cool white fluorescent lamps.
- *The statistical analysis mentions EZR software, but there is no explanation of why this particular software was chosen.*
- **Response:** The rationale for using EZR software has been provided, noting that the software is a free R-based statistical platform suitable for general biological data analysis.
- *In the Discussion, authors have explained various biochemical interactions and mechanisms that are widely known and reported. Authors should give their own reflections of the work. It is essential to include the advantages and shortcomings of the work; what are the limitations of this technology and its shortfalls? Authors' own scrutiny of the data clarifications is decisive for the impending research on this subject. This work is field-oriented, the cost-benefit ratio is very significant, and micropropagation will increase the cost, but this has not been commented on in the text. Scale-up of the tissue culture plant is not an easy task and would be challenging work.*
- **Response:** The Discussion has been expanded with a new section, "Limitations and Future Applications," addressing the scalability, cost, and practical applicability of our method.
- *Conclusion: What does this infer for lettuce production? Need a little more work to show the significance of your work.*
- **Response:** The Conclusion has been revised to emphasize the implications of large-scale lettuce transformation.
- *References: It is advised to refer only to recent work and not old citations.*
- **Response:** The references have been updated to include recent literature (2022 - 2025).

References

1. Soufi H. Peer review of "Relationship Between Seed Coat Color and Cytokinin Concentration in Efficiently Regenerating Leaf Lettuce Shoots: In Vitro Experimental Study". JMIRx Bio 2026;3:e89399. [doi: 10.2196/89399]
2. Kimura M, Yoshizumi T. Relationship between seed coat color and cytokinin concentration in efficiently regenerating leaf lettuce shoots: in vitro experimental study. JMIRx Bio 2026;4:e70496. [doi: 10.2196/70496]
3. Al-Mayahi AMW. Peer review of "Relationship Between Seed Coat Color and Cytokinin Concentration in Efficiently Regenerating Leaf Lettuce Shoots: In Vitro Experimental Study". JMIRx Bio 2026;4:e89401. [doi: 10.2196/89401]

Edited by B Ikhajiagbe; submitted 11.Dec.2025; this is a non–peer-reviewed article;accepted 11.Dec.2025; published 08.Jan.2026.

Please cite as:
Kimura M, Yoshizumi T
Authors' Response to Peer Reviews of "Relationship Between Seed Coat Color and Cytokinin Concentration in Efficiently Regenerating Leaf Lettuce Shoots: In Vitro Experimental Study"
JMIRx Bio 2026;4:e89391
URL: https://bio.jmirx.org/2026/1/e89391
doi:10.2196/89391

XSL•FO
RenderX

© Mitsuhiro Kimura, Takeshi Yoshizumi. Originally published in JMIRx Bio (https://bio.jmirx.org), 8.Jan.2026. This is an open-access article distributed under the terms of the Creative Commons Attribution License (https://creativecommons.org/licenses/by/4.0/), which permits unrestricted use, distribution, and reproduction in any medium, provided the original work, first published in JMIRx Bio, is properly cited. The complete bibliographic information, a link to the original publication on https://bio.jmirx.org/, as well as this copyright and license information must be included.

XSL•FO
RenderX

Authors' Response to Peer Reviews of "Machine Learning Ensemble Investigates Age in the Transcriptomic Response to Spaceflight in Murine Mammary Tissue: Observational Study"

James A Casaletto[1], BS, MS, PhD; Tyler Zhao[2]; Jay Yeung[2]; Abigail Lee[2]; Amaan Ansari[2,3], BSc; Amber Fry[2]; Arnav Mishra[2]; Ayush Raj[2]; Kathryn Sun[2]; Sofia Lendahl[2], BA; Willy Guan[2]; Melissa S Cline[4], PhD; Sylvain V Costes[5]

[1]Blue Marble Space Institute of Science, 600 1st Ave, First Floor, Seattle, WA, United States

[2]Student Association for Applied Statistics (SAAS), University of California, Berkeley, Berkeley, CA, United States

[3]University of Mannheim, Mannheim, Germany

[4]Genomics Institute, University of California, Santa Cruz, Santa Cruz, CA, United States

[5]NASA Ames, Mountain View, CA, United States

Corresponding Author:
James A Casaletto, BS, MS, PhD
Blue Marble Space Institute of Science, 600 1st Ave, First Floor, Seattle, WA, United States

Related Articles:

https://www.biorxiv.org/content/10.1101/2025.02.17.638732v1

https://bio.jmirx.org/2025/1/e75688

https://bio.jmirx.org/2026/1/e73041

(JMIRx Bio 2026;4:e88583) doi:10.2196/88583

KEYWORDS

machine learning; spaceflight; mammary tissue; gene expression; mice; breast cancer; feature importance

This is the authors' response to peer review reports related to "Machine Learning Ensemble Investigates Age in the Transcriptomic Response to Spaceflight in Murine Mammary Tissue: Observational Study."

Live Review Round [1]

List of Major Comments

- *The title of this paper [2] should be more specific with respect to the source of mammary tissue: identify "mouse mammary gland tissue" in the title or, perhaps, simply "murine mammary tissue."*
- **Response:** We changed the title as suggested to "Machine learning ensemble investigates age in the transcriptomic response to spaceflight in murine mammary tissue: observational study."
- *While the methodology is interesting and the findings certainly warrant further study, this should be clearly identified as formative research: there was no preregistration of hypotheses and methods, and the findings (list of key genes and of pathways differing according to age) are just suggestive and not at all robust or convincing. Accordingly, some detail about the experiences of the mice and physiological values is beside the point, so we suggest it is moved to a "Supplements" section along with more specifics about machine learning parameters, etc, that could help researchers attempting similar approaches.*
- **Response:** We describe in the newly-added Strengths and Limitations section of the manuscript that our in silico findings need to be validated in vitro. We also make the software (as a Jupyter notebook) available so that our approach may be repurposed or reproduced.
- *With respect to the OSD-511 dataset, the details of Rodent Research Reference Mission 1 need revision, as it was mentioned that there are 40 female BALB/cAnNTac mice, while the total number of animals used was 43: 21 younger mice and 22 older mice. Moreover, the 8 younger mice that were kept in standard cages were exposed to different conditions from the 7 older mice that were housed in flight hardware.*
- **Response:** We rectified the counts and created Table 1 for clarity.
- *In addition, it was mentioned that each group of space-flown mice had corresponding control groups (ground control), but it is not clear which basal controls (10 mice euthanized 1 day post launch) are used to compare which group. This is important to explain the single group called "non-flight" that is mentioned later in the paragraph, and indicate if these latter details from the original experiment are not available to the authors.*

XSL•FO
RenderX

- **Response:** We added explanations to specify which mice were used in which grouping.
- *In the Discussion section, or as a separate Limitations sections, consider explicitly pointing out that data of experimental mice that were collected just once after 40 days in space and 2 days post return recovery provides only cross-sectional data and does not capture changes in the mice that could be evident while in space or longer after return from space. Also, the description for Figure 1 mentions Figure 1E and F, which are not available in the figure.*
- **Response:** We added this and several others to a dedicated section called "Strengths and Limitations" in the Discussion.
- *The small sample size should be acknowledged, which means the outcome models may not be able to generalize well on unseen data in downstream tasks.*
- **Response:** We describe how we augmented the data in the Methods section. We also call out the paucity of data in the Strengths and Limitations part of the Discussion.

Minor Comments

- *The title could be enhanced to make it clear that this was an experiment based on a model organism (mouse) and not human.*
- **Response:** We changed the title as suggested to "Machine learning ensemble investigates age in the transcriptomic response to spaceflight in murine mammary tissue: observational study."
- *The reviewers acknowledge the availability of details that enable the reproducibility of the study, such as publicly accessible data sources and detailed description of data handling and analysis procedures. However, the reviewers wondered whether the source code used could be availed for enhancing the reproducibility.*
- **Response:** Per this suggestion, we made the code available to the reader.
- *The total number of mice stated that were used in the study does not correspond with the total number used, based on the breakdown of individual group numbers. Authors need to cross-check the numbers to ensure that they tally with the numbers used.***Response:** We rectified the counts and created Table 1 for clarity.
- *Clarify the composition of the control cohort, refer to those mice in a consistent way, and discuss differences that were found to exist between the subsets of controls.*
- **Response:** We rectified the counts and created Table 1 for clarity.
- *In page 4, under the Data Transformation section, it is stated that "four filtering methods were performed," but Figure 2B only represents three filters. Kindly clarify if the fourth filtering method was used but not included in the figure or whether there was a mistake in either the figure or the text for the sake of consistency.*
- **Response:** We updated Figure 2B to include four filter icons.
- *On page 6, the last paragraph, a linear regression model was used to predict the weight of mice at euthanasia, but the significance of this prediction was not discussed. The significance should be discussed for a better understanding of its applicability. Add a brief discussion of the significance of the model, which may include a statistical test validation such as P values and/or CIs.*
- **Response**: We removed the linear regression model from the ensemble.
- *On page 15, under the Conclusion section, it is also mentioned that "The dysregulation of ECM [extracellular matrix] remodeling, cytoskeletal function, and stress response pathways was observed in radiation-exposed mice," but radiation exposure was not the intervention applied. Revise this statement to accurately reflect the intervention applied in this study (spaceflight) and ensure the conclusion is per the experimental conditions.*
- **Response:** We updated the model and the subsequent pathway results do not include extracellular matrix remodeling.
- *In the Discussion section, some results are repeated instead of being analyzed in depth. Focus more on interpreting the results, compare them with similar studies, and discuss their significance.*
- **Response:** We added a lot of content interpreting the results in the Discussion section, along with comparing to similar studies and discussing their relevance.
- *Only accuracy is reported for model performance metrics. Add other metrics, including area under the receiver operating characteristic curve, sensitivity, specificity, and F_1-score, to enhance the assessment of the model's predictive ability.*
- **Response:** We changed our model performance metric to use the F_1-score.
- *Under the algorithms discussion, remove possessive apostrophe from the "1950's."*
- **Response:** We removed the possessive apostrophe.
- *It may help to add a statement to make it explicit whether ethics approval was necessary for the study. In addition, it would add value in discussing ethical implications of collecting the dataset used in the manuscript with reference to any discussion in previous publications or from the authors who collected the original data.*
- **Response:** We added an entire section dedicated to ethics approval.

Concerns with Figures and Tables

- *Most figures have poor resolution, which makes them difficult to understand or interpret. It would be helpful to regenerate the figures with better resolution.*
- **Response:** We increased the resolution of all our images.
- *It would be helpful to add details to the captions to include what's represented in each panel and any elements of statistics.*
- **Response**: We added additional explanations to the captions of all figures and tables.

XSL•FO
RenderX

- *Creating a table to present the various groups and their characteristics, including ground control, would help improve readability.*
- **Response:** We created Table 1 for this purpose.
- *Figure 1 lacks an adequate explanation of each panel, which will clarify what they represent.*
- **Response:** We added additional explanations to the caption of Figure 1.
- *Table 1 is not clear, making it difficult to read.*
- **Response:** We made Table 1 more clear and legible.
- *The top and left parts of Figure 7 are cropped, and it is possible important information is omitted.***Response:** We omitted Figure 7.
- *The legend refers to plots by layout (left/right), duplicating the role of (a)-(d) labels. Also, plot titles are not the most prominent text and are not referenced in the text.*
- **Response:** We removed the "left/right" language from the caption and removed the plot titles from the figure.
- *In Figure 4, the term "accuracy" is used without clarification.*
- **Response:** We replaced Figure 4 with Table 2. Also, we replaced "accuracy" with "F_1-score" as the performance metric.
- *Abbreviations used in Figures 2 and 3 are not explained.*
- **Response:** We added explanations for all abbreviations and created an abbreviation table at the end of the manuscript.
- *The Figure 3 legend does not clearly describe the difference between the left and right diagrams.*
- **Response:** We removed "left/right" language from the figure caption and replaced it with letters and colors to be more clear.
- *The manuscript refers to Table 1 subsections "e" and "f," which are not present. Some figures are also unclear and not explanatory enough.*
- **Response:** We added Figure 1E and F to Figure 1. We also added more explanations to all of the figure and table captions.
- *Figure 5: Fonts are too small to read, and part of the legend is cropped.*
- **Response:** Figure 5 is now Figure 4 and has been updated with larger fonts, and we removed the legend.
- *In Figure 1, the caption states that the left plots represent ground mice and the right plots represent space mice, which is not reflected in the figure.*
- **Response:** We removed "left" and "right" language from the figure caption.
- *On page 4, the principal components analysis statement interpreting Figure 1A and D is misleading. The statement suggests that both Figure 1A and D show principal components analysis for spaceflight, whereas Figure 1A only represents ground mice.*
- **Response:** We updated the figure caption and interpretation to properly reflect the principal components analysis plots.
- *The text for Figure 1 describes Figure 1E and F, but these panels are not present.*
- **Response:** We added Figure 1E and F to Figure 1.

Additional Comments

- *Consider revising the title and abstract to identify that the study was conducted with data collected in a model organism or murine model.*
- **Response:** We changed the title as suggested to "Machine learning ensemble investigates age in the transcriptomic response to spaceflight in murine mammary tissue: observational study."
- *The second page, second sentence of the first paragraph: "Female astronauts in particular have an increased risk of breast cancer due to exposure to galactic cosmic radiation (7)." Please revise the reference, as Kumar et al [3] did not investigate or conclude the mentioned data.*
- **Response:** We modified the text further to be more inclusive in terms of breast cancer risk from ionizing radiation, including cosmic radiation.
- *On the second page, in the last sentence of the first paragraph, "Female astronauts...this increased vulnerability." Please provide a reference for the mentioned data.*
- **Response:** It is a summary statement of the previous statements encompassing 20 references.
- *The second page, second paragraph: "Machine learning (ML) has been leveraged but to a much lesser extent (15)." Please revise the reference as Larrañaga et al [4], as ML's role in bioinformatics has been widely expanded since 2006.*
- **Response:** We updated the sentence and changed the reference to a more recent one.
- *Page 6, second paragraph: It was mentioned that "The support vector machine was created by Hava Siegelmann and Vladimir Vapnik," and there is a reference to Cortes and Vapnik [5], while this work [6] was published in 2001.*
- **Response:** We are not using support vector clustering in our method.
- *Page 11, pathway enrichment analysis: Please identify the abbreviation "KEGG" as "Kyoto Encyclopedia of Genes and Genomes."*
- **Response:** We expanded the acronym at its first use. We also created a table of acronyms at the end of the manuscript.
- *Page 11, pathway enrichment analysis: Please identify the abbreviation "FDR" as "False Discovery Rate."*
- **Response:** We expanded the acronym on first use. We also created a table of acronyms at the end of the manuscript.

Concluding Remarks

- *In the Data Transformation section, groups were introduced for the first time in the manuscript (FLT vs GC and YNG vs OLD); these categories are defined later, but it would be good to spell out the names the first time they are mentioned. That's true for any other acronym used.*

XSL•FO
RenderX

- **Response:** We added an explanation for those and all other acronyms on first mention. We also created a table at the end of the manuscript that defines each acronym.

- *The article did not introduce a Limitation section. It is helpful to the reader to emphasize the limitations of the methods.*
- **Response:** We added a Strengths and Limitations section to the Discussion.

References

1. Sakilay S, Collier M, Rahgozar A, et al. Peer review of "Machine Learning Ensemble Identifies Distinct Age-Related Response to Spaceflight in Mammary Tissue". JMIRx Bio 2025;3:e75688. [doi: 10.2196/75688]
2. Casaletto JA, Zhao T, Yeung J, et al. Machine learning ensemble identifies distinct age-related response to spaceflight in mammary tissue. BioRxiv. Preprint posted online on Oct 6, 2025. [doi: 10.1101/2025.02.17.638732]
3. Kumar K, Angdisen J, Ma J, Datta K, Fornace AJ, Suman S. Simulated galactic cosmic radiation exposure-induced mammary tumorigenesis in ApcMin/+ mice coincides with activation of ERα-ERRα-SPP1 signaling axis. Cancers (Basel) 2024 Nov 26;16(23):3954. [doi: 10.3390/cancers16233954] [Medline: 39682141]
4. Larrañaga P, Calvo B, Santana R, et al. Machine learning in bioinformatics. Brief Bioinform 2006 Mar;7(1):86-112. [doi: 10.1093/bib/bbk007] [Medline: 16761367]
5. Cortes C, Vapnik V. Support-vector networks. Mach Learn 1995 Sep;20(3):273-297. [doi: 10.1007/BF00994018]
6. Ben-Hur A, Horn D, Siegelmann HT, Vapnik V. Support vector clustering. J Mach Learn 2001 Dec:125-137 [FREE Full text]

Edited by A Schwartz; submitted 27.Nov.2025; this is a non–peer-reviewed article;accepted 27.Nov.2025; published 14.Jan.2026.

Please cite as:
Casaletto JA, Zhao T, Yeung J, Lee A, Ansari A, Fry A, Mishra A, Raj A, Sun K, Lendahl S, Guan W, Cline MS, Costes SV
Authors' Response to Peer Reviews of "Machine Learning Ensemble Investigates Age in the Transcriptomic Response to Spaceflight in Murine Mammary Tissue: Observational Study"
JMIRx Bio 2026;4:e88583
URL: https://bio.jmirx.org/2026/1/e88583
doi:10.2196/88583

© James A Casaletto, Tyler Zhao, Jay Yeung, Abigail Lee, Amaan Ansari, Amber Fry, Arnav Mishra, Ayush Raj, Kathryn Sun, Sofia Lendahl, Willy Guan, Melissa S Cline, Sylvain V Costes. Originally published in JMIRx Bio (https://bio.jmirx.org), 14.Jan.2026. This is an open-access article distributed under the terms of the Creative Commons Attribution License (https://creativecommons.org/licenses/by/4.0/), which permits unrestricted use, distribution, and reproduction in any medium, provided the original work, first published in JMIRx Bio, is properly cited. The complete bibliographic information, a link to the original publication on https://bio.jmirx.org/, as well as this copyright and license information must be included.

XSL•FO
RenderX

Authors' Response to Peer Reviews of "Localized Immune Cascade Programming in Desmoplastic Tumors: In Silico Modeling and Validation Study"

Murad Novruzov[1], BSc; Marziyya Mammadova[2], MD; Keval Raval[3], PhD; Waseem Ullah Khan[4], PhD; Ulkar Shiraliyeva[5], MSc

[1]Murad Novruzov Biomedical Research, Seyran Mammadov 6, Baku, Azerbaijan

[2]Azerbaijan State Advanced Training Institute for Doctors named after Aziz Aliyev, Baku, Azerbaijan

[3]Ramanbhai Patel College of Pharmacy, CHARUSAT University, Anand, India

[4]National Institute of Health, Islamabad, Pakistan

[5]Azerbaijan State Oil and Industry University, Baku, Azerbaijan

Corresponding Author:
Murad Novruzov, BSc
Murad Novruzov Biomedical Research, Seyran Mammadov 6, Baku, Azerbaijan

Related Articles:

http://preprints.jmir.org/preprint/85507

https://bio.jmirx.org/2026/1/e91450

https://bio.jmirx.org/2026/1/e91447

https://bio.jmirx.org/2026/1/e85507

(JMIRx Bio 2026;4:e91528) doi:10.2196/91528

KEYWORDS

oncology; tumor microenvironment; cancer microenvironment; immunology; immune-cold tumors; intratumoral immunotherapy; extracellular matrix remodeling

This is the authors' response to peer-review reports for "Localized Immune Cascade Programming in Desmoplastic Tumors: In Silico Modeling and Validation Study."

Round 1 Review

Reviewer AH [1]

General Comments

This paper [2] presents a conceptual framework for a sequential, localized immune cascade ("Second Breath") aimed at reprogramming "immune-cold" desmoplastic tumors to enhance immunotherapy responsiveness. It is positioned as a preclinical concept paper, relying entirely on literature synthesis and in silico modeling without generating new experimental data. While the integration of immunology, biochemistry, and systems biology concepts is ambitious and potentially innovative, the work has significant limitations.

Specific Comments

Major Comments

1. *The abstract does not require reference citations. Please remove the citations in the abstract. If reference citations are deemed really necessary, please start with 1 instead of 4. Also, please go on in ascending order instead of skipping references, like [4,5,6,7,32,33].*
2. *The main text instead should be backed up by reference citations to increase its value. However, the same principle also applies to starting from 1 and continuing in ascending order, but not starting in the middle and skipping references. Also, the references need to be cited in a uniform format. The following needs to be revised in the Introduction: "...(ECM) [6,7,32,33]....(ICIs) [13,14,15]....exposure [1,2,4,5,9,10,11].....Therapy for a Sustainable Outcome' (M. Novruzov, 2025),..." The same format of reference citations should be used, thus "(M. Novruzov, 2025)" should be cited as per others: "[n]." Please revise.*
3. *The references are drawn from reputable sources, but the synthesis appears biased toward supportive evidence. For example, citations for bacterial priming (eg, Clostridium novyi-NT) highlight antitumor responses but downplay failures in clinical trials, such as high toxicity or limited efficacy in advanced tumors. Similarly, extracellular matrix (ECM) modulation via collagenase/hyaluronidase is presented positively but ignores biochemical drawbacks*

XSL•FO
RenderX

like enzyme instability in vivo, nonspecific proteolysis leading to tissue damage, or rebound ECM deposition. It is unclear how the authors reconciled conflicting literature. For example, the Wnt pathway enrichment is noted as dominant, but its protumorigenic role in desmoplastic tumors (eg, promoting fibrosis via β-catenin) is only briefly mentioned in the Discussion without quantitative risk assessment. Please add in a more balanced view and references.

4. *The framework proposes a 10-stage sequence, gated by biomarkers like interferon (IFN)–γ signature or interstitial fluid pressure reduction. However, this complexity introduces numerous failure points without clear prioritization. Biochemically, the "IL-12 → IFN-γ → TNF-α axis" assumes linear signaling, ignoring feedback loops (eg, tumor necrosis factor α [TNF-α]–induced apoptosis resistance via NF-κB) or crosstalk with immunosuppressive pathways (eg, transforming growth factor β in desmoplastic stroma). The "Warmth Readiness Index (WRI)" is mentioned but undefined quantitatively. How is it calculated? What thresholds were derived from it? This vagueness makes the model hard to falsify, as the "prediction matrix" relies on qualitative outcomes rather than measurable biochemical end points. Please revise and supplement.*
5. *The go/no-go criteria (eg, "≥2-fold fold increase in CXCL9/10/11") are arbitrary; please justify them from literature or simulations.*

Reviewer E [3]

General Comments

In this paper, overall, there is a clear scientific narrative defining "second breath" as a testable conceptual framework for converting immune-cold tumors to a more responsive state. The graphical representation of the model and the concise logical sequence make the manuscript more appealing to read. The Introduction highlights key biological barriers like low T-cell infiltration, dense ECM, and stromal resistance that justify the need for a localized immune therapy. The overall study framework is clearly articulated, well-structured, and presented in a concise and accessible manner. The citations are well integrated and support the key arguments effectively. The abstract is informative, but the functional role of β-catenin/Wnt–linked programs in the cascade requires more clarity. The Results section highlighting Wnt signaling dominance is contradictory to the existing literature and the Discussion section of the manuscript, which requires further supporting evidence with human-specific models.

Specific Comments

Major Comments

1. *Wnt-signaling dominance in the Results section: It is known that APC, CTNNB1, and AXIN1 gene mutations of the canonical Wnt/β-catenin pathway give rise to cancers. Inappropriate activation of the Wnt/β-catenin pathway is believed to be involved in carcinogenesis. Specifically, there are multiple genetic abnormalities involved in the activation of the Wnt/β-catenin pathway; nonetheless, the CTNNB1 mutation is a typical driver mutation that is found in approximately 30% of hepatocellular carcinoma cases. In 2015, Spranger et al [4] reported that the Wnt/β-catenin pathway activation inhibits cytotoxic T-cell infiltration in the immune microenvironment of malignant melanoma, resulting in resistance to immune checkpoint inhibitors. Wnt/β-catenin signaling was shown to inhibit this dendritic cell invasion into the tumor. However, the manuscript has reported dominance of Wnt signaling in the pathway enrichment analysis, which is contradictory. Provide more clarity by offering more predictive insights into human-specific responses. The Discussion raises important safety concerns, and so to strengthen practical relevance, propose any mitigation strategies or alternative approaches.*

Minor Comments

1. *Although it is stated in the manuscript that "Second breath" represents a novel preclinical approach for antitumor immunity, kindly clarify the novelty by elaborating on how the model is better than existing intratumoral immunotherapy strategies (like immunostimulatory antibodies, gene therapy, and combination therapy) while both are aimed at limiting systemic toxicities. A strong statement is needed emphasizing how the model can be translated into a therapeutic approach.*
2. *While the sequential representation in the Materials section is clear and logically structured, the overall writing tends to be overly repetitive and unnecessarily elaborate, which makes it difficult to follow and detracts from readability. I'd suggest streamlining the content of the Materials and Methods section.*

Response: Dear reviewers, thank you for your detailed and valuable comments. The amendments have been made in accordance with your recommendations and, I hope, fully meet your expectations. We have taken all points into account, with the exception of rearranging the list of references; such an adjustment would require rewriting the article from scratch, which is beyond the scope of the current revision. We are open to discussing an alternative option for formatting references that would preserve the structure of the work.

Round 2 Review

We appreciate the opportunity to revise our manuscript and extend our sincere gratitude to both reviewers for their rigorous evaluation and constructive recommendations, which have substantially enhanced the scientific rigor and translational relevance of our work.

Reviewer AH

General Comments

This paper has undergone revisions and looks much better.

Specific Comments

Major Comments

1. *The references do not appear in ascending order upon a citation in the main text. The first citation that showed up*

XSL•FO
RenderX

was [6-7,32-33], followed by [13-15], and then [1-2,4-5,9-11].

The authors also addressed this in their rebuttal letter, showing their difficulties in rearranging the list of references, because such an adjustment would require rewriting the article from scratch, which is beyond the scope of the current revision. They are open to discussion on an alternative option for formatting references that would preserve the structure of the work. I think the editorial office or I can help rearrange the reference numbers.

Response: We are grateful for reviewer AH's acknowledgment of the reference formatting challenge. All 53 citations have been manually reordered to ensure a strict ascending numerical sequence corresponding to their first appearance in the main text, from the Introduction section to the Discussion section.

Reviewer E

General Comments

Overall, the authors have made commendable efforts to address the majority of the primary comments in the revised submission. Nonetheless, the Discussion section remains problematic due to conflicting interpretations of the literature and insufficient data to address potential safety concerns.

Specific Comments

Major Comments

1. *Add more references to paragraph 3 of the Discussion section: As the proposed model is entirely in silico and derived from literature synthesis without experimental validation, the Discussion requires greater precision and depth. To enhance its rigor, the author should incorporate additional references that present experimental data or propose concrete mitigation strategies to address the model's limitations and potential toxicities. Moreover, the Discussion would benefit from supporting evidence derived from human-specific models to strengthen the translational relevance of the findings. Provide more clarity by offering more predictive insights into human-specific responses. The Discussion raises important safety concerns and needs to strengthen its practical relevance. The paradox of Wnt enrichment versus fibrosis/immunosuppression is noted but left unresolved.*
2. *The Introduction could be confusing for readers. Earlier in the Introduction, the conceptual framework is proposed to consist of five modules, but later in the text, it expands into a 7-stage framework. This discrepancy could confuse readers. Consider harmonizing the framework (define stages clearly and keep it consistent).*

Response: We have strengthened the Discussion section by incorporating eight additional peer-reviewed references [5-12] that provide experimental validation from patient-derived organoid co-culture systems, murine desmoplastic tumor models, and mechanistic studies of focal adhesion kinase signaling. The apparent paradox of Wnt pathway enrichment has been addressed through a biomarker-stratified adaptive strategy wherein focal adhesion kinase inhibition substitutes for collagenase-based ECM modulation in tumors exhibiting elevated β-catenin nuclear localization. Additionally, we have reconciled the framework nomenclature to consistently describe 10 sequential intervention stages organized within five functional modules throughout the manuscript.

References

1. Au SCL. Peer review of "Localized Immune Cascade Programming in Desmoplastic Tumors: In Silico Modeling and Validation Study". JMIRx Bio 2026;4:e91450. [doi: 10.2196/91450]
2. Novruzov M, Mammadova M, Raval K, Khan WU, Shiraliyeva U. Localized immune cascade programming in desmoplastic tumors: in silico modeling and validation study. JMIRx Bio 2026;4:e85507. [doi: 10.2196/85507]
3. Brathaban N. Peer review of "Localized Immune Cascade Programming in Desmoplastic Tumors: In Silico Modeling and Validation Study". JMIRx Bio 2026;4:e91447. [doi: 10.2196/91447]
4. Spranger S, Bao R, Gajewski TF. Melanoma-intrinsic β-catenin signalling prevents anti-tumour immunity. Nature New Biol 2015 Jul 9;523(7559):231-235. [doi: 10.1038/nature14404] [Medline: 25970248]
5. Du W, Menjivar RE, Donahue KL, et al. WNT signaling in the tumor microenvironment promotes immunosuppression in murine pancreatic cancer. J Exp Med 2023 Jan 2;220(1):e20220503. [doi: 10.1084/jem.20220503] [Medline: 36239683]
6. Lidström T, Cumming J, Gaur R, et al. Extracellular galectin 4 drives immune evasion and promotes T-cell apoptosis in pancreatic cancer. Cancer Immunol Res 2023 Jan 3;11(1):72-92. [doi: 10.1158/2326-6066.CIR-21-1088] [Medline: 36478037]
7. Freed-Pastor WA, Lambert LJ, Ely ZA, et al. The CD155/TIGIT axis promotes and maintains immune evasion in neoantigen-expressing pancreatic cancer. Cancer Cell 2021 Oct 11;39(10):1342-1360. [doi: 10.1016/j.ccell.2021.07.007] [Medline: 34358448]
8. Holokai L, Chakrabarti J, Lundy J, et al. Murine- and human-derived autologous organoid/immune cell co-cultures as pre-clinical models of pancreatic ductal adenocarcinoma. Cancers (Basel) 2020 Dec 17;12(12):3816. [doi: 10.3390/cancers12123816] [Medline: 33348809]
9. Zhang M, Zhang B. Extracellular matrix stiffness: mechanisms in tumor progression and therapeutic potential in cancer. Exp Hematol Oncol 2025 Apr 10;14(1):54. [doi: 10.1186/s40164-025-00647-2] [Medline: 40211368]
10. Jiang H, Hegde S, Knolhoff BL, et al. Targeting focal adhesion kinase renders pancreatic cancers responsive to checkpoint immunotherapy. Nat Med 2016 Aug;22(8):851-860. [doi: 10.1038/nm.4123] [Medline: 27376576]

XSL•FO
RenderX

11. Pawar JS, Salam MA, Dipto MSU, et al. Cancer-associated fibroblasts: immunosuppressive crosstalk with tumor-infiltrating immune cells and implications for therapeutic resistance. Cancers (Basel) 2025 Jul 28;17(15):2484. [doi: 10.3390/cancers17152484] [Medline: 40805183]
12. Xie Y, Wang X, Wang W, Pu N, Liu L. Epithelial-mesenchymal transition orchestrates tumor microenvironment: current perceptions and challenges. J Transl Med 2025 Apr 2;23(1):386. [doi: 10.1186/s12967-025-06422-5] [Medline: 40176117]

Abbreviations

ECM: extracellular matrix
INF: interferon
TNF-α: tumor necrosis factor α

Edited by M Yadav; submitted 15.Jan.2026; this is a non–peer-reviewed article;accepted 15.Jan.2026; published 27.Feb.2026.

Please cite as:
Novruzov M, Mammadova M, Raval K, Khan WU, Shiraliyeva U
Authors' Response to Peer Reviews of "Localized Immune Cascade Programming in Desmoplastic Tumors: In Silico Modeling and Validation Study"
JMIRx Bio 2026;4:e91528
URL: https://bio.jmirx.org/2026/1/e91528
doi:10.2196/91528

© Murad Novruzov, Marziyya Mammadova, Keval Raval, Waseem Ullah Khan, Ulkar Shiraliyeva. Originally published in JMIRx Bio (https://bio.jmirx.org), 27.Feb.2026. This is an open-access article distributed under the terms of the Creative Commons Attribution License (https://creativecommons.org/licenses/by/4.0/), which permits unrestricted use, distribution, and reproduction in any medium, provided the original work, first published in JMIRx Bio, is properly cited. The complete bibliographic information, a link to the original publication on https://bio.jmirx.org/, as well as this copyright and license information must be included.

XSL•FO
RenderX

Authors' Response to Peer Review of "Material-Driven Therapeutics to Establish a Penetrating Traumatic Brain Injury Rat Model and Implantation of a 3D-Printed Scaffold: Pre-Experimental Pilot Study"

Meaghan E Harley-Troxell[1], PhD; Michelle Dennis[2], PhD; Madhu Dhar[1], PhD

[1]Tissue Engineering and Regenerative Medicine Lab, LACS, College of Veterinary Medicine, University of Tennessee at Knoxville, 2407 River Drive, Knoxville, TN, United States

[2]Biomedical and Diagnostic Sciences Department, College of Veterinary Medicine, University of Tennessee at Knoxville, Knoxville, TN, United States

Corresponding Author:
Meaghan E Harley-Troxell, PhD
Tissue Engineering and Regenerative Medicine Lab, LACS, College of Veterinary Medicine, University of Tennessee at Knoxville, 2407 River Drive, Knoxville, TN, United States

Related Articles:

https://www.biorxiv.org/content/10.1101/2025.03.20.644358v1

https://bio.jmirx.org/2026/1/e105277

https://bio.jmirx.org/2026/1/e75613

(JMIRx Bio 2026;4:e105278) doi:10.2196/105278

KEYWORDS

penetrating traumatic brain injury; stereotaxic surgery; graphene; nerve tissue engineering; rat model

This is the authors' response to the peer-review report for "Material-Driven Therapeutics to Establish a Penetrating Traumatic Brain Injury Rat Model and Implantation of a 3D-Printed Scaffold: Pre-Experimental Pilot Study."

Round 1 Review

Reviewer EW [1]

1. *A key weakness of the study [2] is its very small sample size (n=4), which substantially limits the statistical power, generalizability, and reliability of the conclusions. With such a low n, it becomes difficult to determine whether the observed variability—particularly the severe inflammatory response in one animal—reflects true biological differences, procedural inconsistencies, or random outliers.*
   Response: We agree that this study has a very small sample size. That does impose limitations on statistical power, results, and conclusions. We however have stressed throughout the manuscript that this is a "pilot study" to identify a technically feasible rat model. Since the aim of this study was to describe a model that could be used in future studies, only 4 animals were used, and results and conclusions based on those 4 animals are reported. After reporting this foundational study, we can now plan and initiate a study with control groups, a sufficient number of animals, and more detailed analyses. Some of these points are described in the Discussion section of the manuscript (lines 311 - 316).
2. *The study lacks control groups—including a sham surgery group and a traumatic brain injury–only group—preventing clear attribution of histological changes to either the injury model or the implanted scaffold.*
   Response: As described above in the response to comment 1, we agree that this study lacks control groups, including well-defined sham surgery or traumatic brain injury–only groups. This will be taken into consideration in future studies, since we have established the feasibility of the technique in this manuscript. Some of these points are described in the Discussion section of the manuscript (lines 312 - 316).
3. *The behavioral assessment is limited to a modified neurological severity score, which is often insensitive to mild or focal injuries and may miss subtle cognitive or sensorimotor deficits.*
   Response: Yes, we agree that the behavioral assessment reported in this study is limited. As described above in our responses to comments 1 and 2, this was a feasibility study. Since the number of animals was small, and there are a variety of behavioral assessments that are relevant and can be done, future studies will be planned accordingly. We will take into consideration the animal groups and their evaluations. Some of the results relevant to this feasibility

XSL•FO
RenderX

study are described in the Results section of the manuscript (lines 223 - 228).

4. *The study would be strengthened by incorporating additional validated behavioral tests.*

Response: We agree, and after completing this feasibility study, we are ready and motivated to carry out a detailed study with additional groups and evaluations. Some of the results relevant to this study are described in the Results section of the manuscript (lines 225 - 228).

References

1. Kobeissy F. Peer review of "Material-Driven Therapeutics to Establish a Penetrating Traumatic Brain Injury Rat Model and Implantation of a 3D-Printed Scaffold: Pre-Experimental Pilot Study. JMIRx Bio 2026;4:e105277. [doi: 10.2196/105277]
2. Harley-Troxell ME, Dennis M, Dhar M. Material-driven therapeutics to establish a penetrating traumatic brain injury rat model and implantation of a 3d-printed scaffold: pre-experimental pilot study. JMIRx Bio 2026;4:e75613. [doi: 10.1101/2025.03.20.644358]

Edited by A Schwartz; submitted 22.Jun.2026; this is a non–peer-reviewed article;accepted 22.Jun.2026; published 10.Jul.2026.

Please cite as:
Harley-Troxell ME, Dennis M, Dhar M
Authors' Response to Peer Review of "Material-Driven Therapeutics to Establish a Penetrating Traumatic Brain Injury Rat Model and Implantation of a 3D-Printed Scaffold: Pre-Experimental Pilot Study"
JMIRx Bio 2026;4:e105278
URL: https://bio.jmirx.org/2026/1/e105278
doi:10.2196/105278

© Meaghan E Harley-Troxell, Michelle Dennis, Madhu Dhar. Originally published in JMIRx Bio (https://bio.jmirx.org), 10.Jul.2026. This is an open-access article distributed under the terms of the Creative Commons Attribution License (https://creativecommons.org/licenses/by/4.0/), which permits unrestricted use, distribution, and reproduction in any medium, provided the original work, first published in JMIRx Bio, is properly cited. The complete bibliographic information, a link to the original publication on https://bio.jmirx.org/, as well as this copyright and license information must be included.

XSL•FO
RenderX

Publisher:
JMIR Publications
130 Queens Quay East.
Toronto, ON, M5A 3Y5
Phone: (+1) 416-583-2040
Email: support@jmir.org

XSL•FO
RenderX